UNIVERSITY OF CALIFORNIA, SAN DIEGO

Control relevant identification of plant and disturbance dynamics with application to noise and vibration control

A dissertation submitted in partial satisfaction of the
requirements for the degree Doctor of Philosophy

in

Engineering Sciences (Mechanical Engineering)

by

Jie Zeng

Committee in charge:

Professor Raymond de Callafon, Chair
Professor Robert Bitmead, Co-Chair
Professor Kenneth Kreutz-Delgado
Professor William Helton
Professor William McEneaney

2006

The dissertation of Jie Zeng is approved, and it is acceptable in quality and form for publication on microfilm:

Co-Chair

Chair

University of California, San Diego

2006

TABLE OF CONTENTS

LIST OF FIGURES

ACKNOWLEDGEMENTS

I would like to thank my advisor Prof. Raymond de Callafon for his support, without his guidance this work could not have been accomplished.

I also would like to thank my wife Lu Jin and my family for their encouragement and support.

The text of Chapter 4, in part, is a reprint of the material as it appears in 13th IFAC Symposium on System Identification and in Proc. IEEE International Conference on Mechatronics, and in part, has been submitted for publication in Automatica. The dissertation author was the primary researcher and author in these works and the co-author listed in these publications directed and supervised the research which forms the basis for this chapter.

The text of Chapter 7, is a reprint of the material as it appears in the 42nd IEEE Conference on Decision and Control. The dissertation author was the primary researcher and author in these works and the co-author listed in these publications directed and supervised the research which forms the basis for this chapter.

The text of Chapter 8, is a reprint of the material as it appears in the 42nd IEEE Conference on Decision and Control, in part, it has been submitted for publication in Journal of Sound and Vibration. The dissertation author was the primary researcher and author in these works and the co-author listed in these publications directed and supervised the research which forms the basis for this chapter.

CURRICULUM VITAE

Jie Zeng

Education

1991-1995	Bachelor Degree in Mechanical Engineering Shenyang Polytechnic University, Shengyang, P.R.China
1997-2000	Master Degree in Engineering Mechanics Tsinghua University, Beijing, P.R.China
2001-2006	Doctor of Philosophy in Mechanical Engineering University of California, San Diego, U.S.A

Work Experience

1995-1997	Mechanical Engineer Automobile Industry Inc., Beijing, China
1997-2000	Research Assistant Tsinghua University, Beijing, China
2000-2001	Research Assistant Hongkong University, Hongkong, China
2001-2005	Research Assistant University of California, San Diego, U.S.A

Publications

R. A. de Callafon,J. Zeng, C. E. Kinney. *"Active noise control for the forced−air cooling system in a data projector."* To appear in Control Engineering Practice, 2006.

J. Zeng, R. A. de Callafon. *"Recursive least square feedforward estimation for active noise cancellation in the presence of acoustic coupling."* To appear in Journal of Sound and Vibration, 2006.

J. Zeng, R. A. de Callafon. *"Control relevant estimation of plant and noise dynamics-low order model approximation on the basis of closed-loop data."* To appear in Automatica, 2006.

J. Zeng, R. A. de Callafon. *"Filter parametrized by orthonormal basis functions for active noise control."* ASME IMECE, 2005.

J. Zeng, R. A. de Callafon. *"Feedforward estimation for active noise cancellation in the presence of acoustic coupling."* in Proc. 43nd IEEE Conference on Decision and Control, Paradise Island, Bahamas, 2004.

J. Zeng, R. A. de Callafon. *"Recursive least square generalized FIR filter estimation for active noise cancellation. "* in Proc. IFAC Workshop on Adaptation and Learning in Control and Signal Processing, Yokohama, Japan, 2004.

J. Zeng, R. A. de Callafon. *"Servo experiment for the estimation of models for windage and actuator dynamics in a hard disk drive."* in Proc. IEEE International Conference on Mechatronics, Istanbul, Turkey, 2004.

J. Zeng, R. A. de Callafon. *"Feedforward noise cancellation in an air-duct using generalized FIR filter estimation."* in Proc.42nd IEEE Conference on Decision and Control, Maui, Hawaii, USA, 2003,pp.6392-6397.

J. Zeng, R. A. de Callafon. *"Model approximation of plant and noise dynamics on the basis of closed-loop data."* Prepr.. 13th IFAC Symposium on System Identification, Rotterdam, the Netherlands, 2003, pp. 531-536.

ABSTRACT OF THE DISSERTATION

Control relevant identification of plant and disturbance dynamics with application to noise and vibration control

by

Jie Zeng

Doctor of Philosophy in Engineering Sciences (Mechanical Engineering)

University of California, San Diego, 2006

Professor Raymond A. de Callafon, Chair
Professor Robert Bitmead, Co-Chair

Estimation of models for both plant and disturbance dynamics is important in controller design applications which especially focus on the disturbance and vibration rejection. Several methods for low order model estimation on the basis of the closed-loop data exist in the literature, but fail to address the simultaneous estimation of low order models of both plant and disturbance dynamics. This dissertation contributes to the development of a new methodology to extend the results to low order disturbance model estimation, and apply these techniques to the control problems for disturbance rejection.

In addition to the control relevant estimation problem, this dissertation also provides new tools for feedforward based disturbance rejection found in Active Noise Control (ANC) systems. We focus on the feedforward control algorithms that are one of the most popular methods to cancel low frequency sound where passive methods are ineffective. This dissertation shows that the feedforward filter design can also be seen as a model matching problem with the system model

approximated on the basis of the expansion of orthonormal basis functions. Therefore, existing results on generalized FIR filters are exploited to provide feedforward compensation with the advantage of including the prior information of the system dynamics in the tapped delay line of the filter. It has the same linear parameter structure as FIR filter which is favorable for adaptation process. In the case that the acoustic coupling can not be neglected in the process of designing the feedforward filter, a dual-Youla parametrization is introduced and applied to estimate the possible perturbation of the feedforward filter and the robust stability of the closed loop system is enforced during the design of feedforward filter for active noise cancellation.

Chapter 1

Identification for Disturbance Modeling

1.1 Rational

Noise and vibration caused by traffic, industry, or recreational activities, is an ever increasing problem in the modern world. Noise comes from almost everywhere in our life such as automobile, jet planes, computer server, rotating fans, garbage trucks, construction equipment, manufacturing processes. Noise negatively affects human health and well-being. Problems related to noise include hearing loss, stress, high blood pressure, sleep loss, distraction and lost productivity, and a general reduction in the quality of life. Vibration can not only create unwanted noise, but also cause the mis-operation of a dynamical system. Because of the bad effect of noise and vibration on our life, we have to find a way to control the unwanted noise and vibration. Many researchers made their efforts to the fields of noise and vibration control in the past decades.

Traditionally, noise was reduced by passive ways like mufflers, damping plates, sound absorbing materials, double-glazing windows, noise barriers etc. All these passive methods are mostly effective for reducing high frequency sound compo-

nents. However, to reduce low frequency noise signals it will require large amounts of absorption materials which will make the cost expensive and also make the passive treatments bulky and heavy. In the last decade, active control of sound and vibration (at audio frequencies) has emerged as a viable technology to bridge the gap between desired active noise control using passive solutions and active solutions. The basic mechanism and idea behind active noise control is to cancel the offending sound (disturbance) by a controller emission of a secondary opposite (out-of-phase) sound signal.

In order to get the most effective active noise control in a dynamical system, the understanding of the dynamics of sound propagation within the ANC system becomes very important. Sound propagation, even in a simple air duct, is characterized by a dynamical system with many resonance mode due to sound reflection and standing waves of sound propagation. As such accurate modeling of the dynamics of sound and vibration propagation requires intricate models with accurate knowledge on the boundary conditions of the ANC system. An alternative approach would be to model dynamics of disturbances on the basis of actual experimental data and use so called identification techniques to model dynamics relevant for disturbance rejection. The basic idea behind the system identification technique is that the modeling of system dynamics can be characterized with the systematic relationship of measured input/output data by minimizing the 2-norm of prediction error. The schematic diagram of system identification is shown in Fig. 1.1. By measuring the control variable and observed variable, the physical noise and vibration system can be characterized with dynamics of control system G_θ and dynamics of disturbance H_θ with the use of Least Mean Square (LMS) technique. The motivation to use system identification technique in this dissertation is that the complexity of the system or incomplete knowledge of dynamic system limits the usage of modeling in many engineering application. Therefore it is desirable to formulate a model that is linear, and time invariant and has low complexity that can be used for optimal/robust control design which system

identification can be used to satisfy this requirement.

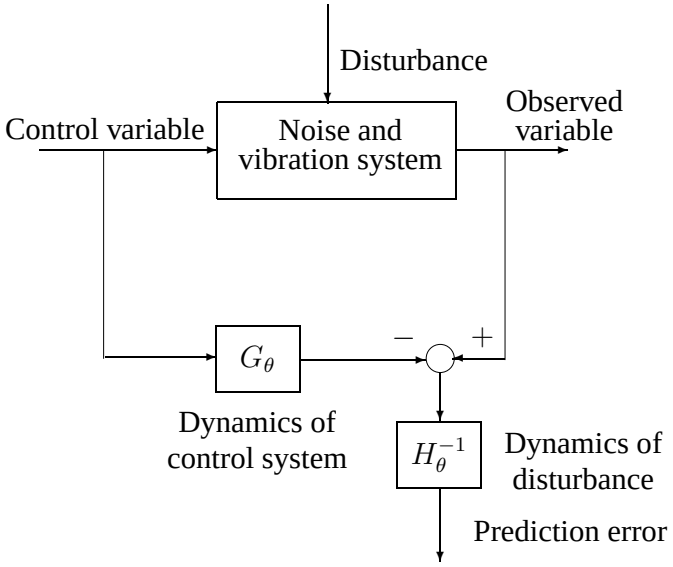

Figure 1.1. Schematic diagram of system identification

1.2 Contribution of dissertation

The goal of this dissertation is to find an efficient system identification technique to identify both models of deterministic system and disturbance, and find ways to provide techniques for designing feedback and feedforward algorithms for noise and vibration control. This dissertation mainly focuses on feedforward based techniques as adaptation of feedforward compensation is a very effective way for sound cancellation. The contribution of this research include:

- This dissertation will present a new extended new stage identification method to estimate control-relevant models for both plant and noise dynamics. These models are important for the control applications that focus on the noise and vibration rejection.

- Model approximation based on the expansion of the orthonormal basis functions. How to choose the set of the orthonormal basis will directly affect the approximation results.

- Apply the generalized (orthonormal) finite impulse response (FIR) filter in the feedforward active noise control application to provide better performance than simple FIR filter.

- Apply a recursive least square generalized FIR filter estimation to provide an on-line adaptive feedforward active noise control which is the most popular ANC application.

- Apply dual-Youla parametrization to estimate the possible perturbation of a feedforward filter in the active noise control in the presence of the acoustic coupling.

Chapter 2

Background and Problem Formulation

2.1 Identification of models for disturbance control

2.1.1 Identification and closed loop experiments

For the modeling purposes of a system with unknown or partially known dynamics, system identification techniques can be used to characterize the dynamic behavior of the system [59]. Models obtained by system identification techniques can be used for simulation, prediction or control purposes. Depending on the intended purpose of the model, different quality requirements on the modeling procedure need to be posed. These requirements differ especially in many practical situations where models are used to approximate signal and system dynamics behavior.

Models for simulation purposes focus mainly on system dynamics, whereas models for prediction purposes may require open-loop accurate models of both system and noise dynamics to provide reliable prediction of output signals [59].

On the other hand, models intended for control purposes may require high quality system dynamic representations of critical closed-loop behavior to design reliable robust servo controllers [83]. The difference between open-loop and closed-loop approximate modeling lies in the requirement of control-relevant approximate modeling and the ability to deal with data obtained from closed-loop experiments. Even though the correlation between the unmeasurable noise and the input is a fundamental problem in closed loop experiment, performing identification experiments under the closed loop environments is necessary because of the safety and economic reasons.

2.1.2 Approaches to closed-loop identification

The need for control oriented modeling has resulted in several methodologies that aim at iteratively improving closed-loop system behavior on the basis of closed-loop experiments [57, 66, 1, 41]. In most of the existing methods, the emphasis is placed on the control-relevant approximation of system dynamics only and ignore the approximate modeling of the noise (disturbance) dynamics that is relevant in noise (disturbance) control. For minimum variance and LQG control, successful modeling and control performance improvements have been shown in [26, 38], but these results assume consistent estimation of system and disturbance dynamics.

In dealing with closed-loop data, one of the problems in approximate closed-loop identification of plant and noise dynamics is the correlation of the disturbance with any of the signals in the closed-loop. As a result, a so-called direct identification using input and output of the plant will lead to bias approximation results for the system and disturbance dynamics [83, 11]. Possible ways to overcome this problem is by assuming low noise correlation condition [25, 91, 3] that might only be realistic in simulation studies.

A possible way to deal with closed-loop data is a reparametrization of the closed-loop identification problem. Reparametrization can be done by a direct parametrization of the closed-loop transfer function as done in [84] or in the recur-

sive algorithms for closed-loop identification of [51, 52, 53]. Although powerful for estimating control-relevant plant dynamics, bias approximation results similar to direct identification are obtained in case an approximate noise model is estimated [44].

An alternative parametrization of the closed-loop identification problem is built on the dual-Youla parametrization [58], coprime factor identification [12] or a two-stage identification [81]. In these methods, an auxiliary or previously estimated model is used for filtering purposes to recast the closed-loop identification problem in a standard open-loop estimation problem [83]. These methods have shown promising results for low order and control-relevant plant modeling, but do not address the low order model estimation of the disturbance dynamics. However, if we are interested in designing a controller that can be used for noise (disturbance) rejection, the noise model should have the same importance as the model of the system dynamics in order to obtain a good performance of noise (disturbance) control.

> Is it possible to develop a new identification method that can be used to identify low order control-relevant plant and disturbance modeling, and the estimated models can be directly applied for optimal/robust control design for noise (disturbance) rejection?

If the models estimated using the above described identification methods can capture the essential closed loop dynamical behavior of a physical system, then these approximated models can be used to design optimal feedback or feedforward controller for this physical system, and the control design process is so called model-based control design process. In this dissertation, we only focus on the feedfoward control design technique for active noise cancellation based on the models estimated with the corresponding identification method.

2.2 Active control of sound disturbance

2.2.1 Active noise control (ANC)

Acoustic noise has more and more negative effects to the human health as the rapid development of the modern technology. Many industrial machines and transportation equipments such as engines, fans, transformer, compressors, automobile, and airplane create high decibel noise that can influence the hearing of the population around their environment. Other than that, the mechanical vibration generated by the operation of the equipments is another related type of noise that deteriorate the environments.

The traditional way to suppress the acoustic noise applied mufflers, damping plates, sound absorbing materials, double-glazing windows, noise barriers to attenuate the undesired noise [32, 6], and this kind of methods are called passive noise control. All these passive methods are effective for reducing high frequency sound components. However, they are relatively heavy, bulky, and of course more expensive for a low frequency noise reduction.

In order to overcome these problems caused by the the passive methods, active noise control (ANC) has received considerable consideration and showed significant promise in the last decade. The basic idea of active noise control is that an additional secondary opposite (out-of-phase) sound signal generated by a controller is used to cancel the undesired sound (disturbance).

The design of active noise control utilizing a microphone and a speaker to generate a cancelling sound was first proposed in a 1936 patent by Lueg [60]. Even though the patent outlined the basic idea of active noise control, it did not have any real applications at that time. Fig. 2.1 illustrates how the unwanted sound disturbance measured with a microphone can be cancelled by a anti-phase sound created by a speaker.

Active noise control is developing rapidly because it permits improvements of the performance of noise control with potential benefits in size, weight, volume

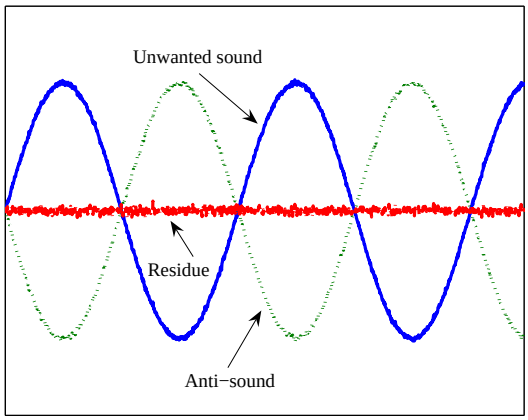

Figure 2.1. Illustration of active noise control

and cost. A historic reviews of the development of active noise control is presented in [87, 27, 28, 48].

2.2.2 Approaches to active noise control (ANC)

Control algorithms for noise cancellation are typically based on feedforward compensation, feedback control or a hybrid form of both [45, 21]. Feedback control is effective for disturbance attenuation in the case that the reference signal is not available to be measured. However, performance limiting aspects such as time delays, non-minimum phase behavior and requirements on fast adaptation pose different design constraints on creating stabilizing feedback control application for noise control system. Successful implementation of feedback noise control can be found in specific applications that have been optimized with respect to feedback performance limitation [90, 2, 62].

In the application of active noise control, feedforward filter algorithms have been widely used in active noise cancellation for broadband noise reduction. The basic principle of this algorithm is based on the fact that the feedforward signal,i.e,

the external noise source is an independent (or known) signal which has no correlation with the actuator output. Failure to reach this requirement implies that the overall system contains acoustic coupling, and then closed loop stability and robustness become more crucial and need to be considered.

In the case that the reference signal can be measured and has no correlation with the actuator output, a pure feedforward compensation algorithm based on the finite impulse response (FIR) filter can be obtained in the active noise control. The advantage of choosing the FIR filter as an adaptive filter is that the FIR filter only incorporates zeros, hence the filter is always stable, and can provide a linear phase response. However, when a more complex dynamical system is considered, a sufficient number of coefficient are needed to represent the related dynamical system, and it will increase the computational burden substantially, and also may cause a slow convergence. As a result, infinite impulse response (IIR) adaptive filter could be a good choice over the FIR filter with the advantage that the poles of an IIR filter can achieve the same performance (resonance, sharp cutoff, etc) as the FIR filter, but with a much lower order. Therefore, IIR filters may require less computation than FIR filters. The other important advantage is that IIR filters with sufficient order can insistently match poles as well as zeros of a physical system, whereas FIR filters can give only rough approximations to poles. Therefore, IIR filters can further minimize the mean-square error of an adaptive filter, which is very important for ANC applications.

Even though the potential saving in computation and further reduction of the residual error, these advantage come at certain costs, such as IIR filters are not unconditionally stable because of the possibility that some poles of the filter may move outside of the unit circle during the adaptive process, the adaptation may converge to a local minimum because the performance surface of adaptive IIR filters is generally non-quadratic and the convergence rate is relatively slower than FIR filters. These problems described above make adaptive IIR filters much more difficult to use in the practical applications.

> Is there a way we develop a filter that has the properties of the advantage of both FIR filters and IIR filters to maintain the new adaptive filters stable, and much lower order?

In the case that an independent reference signal is difficult to obtained in many practical situations, the most common way to obtain the feedforward signal it to use sensors located in the upstream locations to measure the feedforward signal. From a control point of view, the system is no longer a pure feedforward cone because a positive feedback (also called acoustic coupling) exists between the control speaker and input microphone which tends to destabilize an ANC system. Therefore, modifications to the control algorithm have to be made to stabilize the feedforward based ANC system. This problem has been extensively studied in the ANC literature, and several solving methods have been proposed, listed as follows.

- Directional microphones and loudspeakers [43, 79, 68, 17]. The main limitation of this method is that directional arrays are usually highly dependent on the spacing of the array elements and are only directional over a relatively narrow frequency range [20]. It means that it is difficult to obtain a good performance over a broad frequency range with this method.
- Adaptive neutralization filter in parallel with the feedback path [88].
- Adaptive IIR filter to compensate for acoustic feedback [20].
- Distributed parameter systems [39]. By using distributed parameter models, a unidirectional signal can be obtained as a feedforward signal to cancel the external noise using distributed parameter models.
- H_∞ theory to design a feedforward filter. H_∞ theory can automatically incorporate the acoustic coupling during the design process [5].

More details about the effect of acoustic coupling and the related solutions please refer to [47]. The methods described above have their own advantages and drawbacks in the system stability and ANC performance view.

Is there an alterative way to solve the acoustic coupling problem during the design of feedforward controller for ANC? Can the system stability be enforced and ANC performance be maintained with the proposed method?

2.2.3 Adaptive algorithms for ANC

Basically, active noise control can be divided into two categories: nonadaptive active control and adaptive active control. Nonadaptive active control has been developed using the standard control technique such as LQG, H_2 and H_∞ algorithms to compute an optimal controller. The drawback of nonadaptive active control is that it can not track and respond to any changes of the dynamical system. In order to overcome this, the ANC system has to be adaptive.

Adaptive filters have received much attention over last 20 years [16]. Adaptive filters adjust their coefficients to minimize an error signal by using the least-mean-square (LMS) algorithms, and it can be realized as finite impulse response (FIR) filter, infinite impulse response (IIR) filter, lattice and transform-domain filter.

A modified version of LMS algorithm named FxLMS algorithm is the most popular adaptation algorithms for practical applications. This FxLMS algorithm is computationally simple, but the relatively slow convergence speed is the main drawback. In order to improve the convergence properties, some different ANC algorithms have been proposed, namely., lattice-ANC systems [78, 46, 67]; Frequency-domain ANC systems [74, 75, 69, 49]; IIR-filter-based LMS algorithms [20, 10]; Recursive least square based algorithms [9, 47, 7, 33]; Kalman filtering [8]. The selection of a good adaptive algorithm is based on the requirements for the convergence rate, computation and performance. For example, if a fast convergence rate is needed in an ANC application, and if we do not care about the computation, then RLS algorithm or Kalman filtering should be chosen instead of LMS algorithm because RLS algorithm and Kalam filtering can provide much better convergence rate, but much more computation burden than LMS algorithm.

2.3 Problem formulation

As pointed out in the previous sections, most closed-loop identification methods [83, 23] have shown promising results for low order and control-relevant plant modeling, but do not address the low order model estimation of the disturbance dynamics. If we are interested in designing a controller that can be used for noise (disturbance) rejection, the estimate of the noise model should be given the same treatment as the modeling of the system dynamics in order to obtain a good performance of noise control. Using the models of system dynamics and noise dynamics, the next step would be to design optimal controllers for disturbance rejection. As part of the research effort, the emphasis is focused on active noise cancellation.

In active noise control techniques, feedforward ANC is the most popular and simplest method to be applied to cancel the undesired noise, and an adaptive filter must be considered in order to cope with the variations such as system dynamics and environment. Usually an adaptive filter is realized by FIR filter or IIR filter. However, FIR filter is not good enough to adapt a very complicated system because FIR filter incorporates only zeros and a much higher order FIR filter will be needed. Even though IIR filter can overcome the problem of FIR filter confronts, stability problem is the main limitation of IIR filter. We may find a way to develop a filter that can combine the advantages of both FIR filter and IIR filter and can be easily applied in the ANC application.

In ANC application, the acoustic coupling is an intricate problem. As indicated before, there are many methods trying to solve the effect of acoustic coupling in the ANC application. Many of these methods focus on cancelling the bad effect of acoustic coupling, and do not incorporate the acoustic coupling in the process of designing a feedforward filter. So, we are interested in designing an adaptive feedforward filter that can incorporate the acoustic coupling for ANC?

The overall problem formulation of this dissertation are described as follows

- Problem 1:
  - Given input/output data measurements obtained under closed-loop conditions, estimate models that approximate the plant and disturbance dynamics. The approximation is done in such a way that models can be used in control design applications that focus on the disturbance rejection.

- Problem 2:
  - In the feedforward ANC, design an adaptive filter to provide broad band frequency noise cancellation. This type of adaptive filter can be used to describe a more complicated system in a relatively lower order comparing with FIR filter.

- Problem 3:
  - In the feedforward ANC, find a method to design a feedforward filter in the presence of acoustic coupling. This method can incorporate the effect of acoustic coupling and the robust stability of the closed loop system can be enforced during the design of feedforward filter for ANC.

2.4 Overview of this dissertation

Following the proposed problem formulation, this dissertation is structured as follows. In Chapter 3, some closed loop approximate identification methods are discussed, and also their properties are presented. Chapter 4 presents a new identification method so called extended two stage method. The advantage of this method lies in the simultaneous estimation of low order of plant dynamics and disturbance dynamics. An application of using extended two stage method to estimate the low order plant dynamics and disturbance dynamics in a mechanical data storage application is given at the end of the chapter. Chapter 5 discusses the model approximation using orthonormal basis function. An analytical solution for model matching using orthonormal basis is also derived. In this chapter, the

advantage of including orthonormal basis in the tapped delay line is presented. In the end, a case study to illustrate the advantage of using orthonormal basis function is presented. in Chapter 6, general techniques used in the active noise control such as adaptive algorithm and adaptive filter structure are discussed. The problems it may face in the application of active noise control are also presented. Chapter 7 shows the application of a generalized (orthonormal) FIR filter to the active noise cancellation. Chapter 8 presents an application of dual-Youla parameterization to active noise control in the present of acoustic coupling. Chapter 9 summarizes the conclusions of this dissertation.

Chapter 3

Approximate Identification Under Closed Loop Conditions

3.1 Preliminaries

In order to analyze the problems that are associated to an identification based on closed-loop experiments, a linear time invariant finite dimensional feedback connection $\mathcal{T}(G_0, C)$ of a plant G_0 and a feedback controller C is considered. The feedback connection $\mathcal{T}(G_0, C)$ can be defined in the following definition.

Definition 3.1.1. *Consider a well-posed feedback connection $\mathcal{T}(G_0, C)$ where u and y indicate respectively the input and possibly disturbed output signal of G_0. Then $\mathcal{T}(G_0, C)$ is defined by*

$$\mathcal{T}(G_0, C) := \begin{bmatrix} G_0 \\ I \end{bmatrix} (I + CG_0)^{-1} \begin{bmatrix} C & I \end{bmatrix} \tag{3.1}$$

and maps the reference signals $col(r_2, r_1)$ to the signals $col(y, u)$

The feedback connection $\mathcal{T}(G_0, C)$ is called stable if and only if $\mathcal{T}(G_0, C) \in \mathcal{RH}_\infty$ where $\mathcal{RH}_\infty$ indicate the standard space of all proper, real rational and

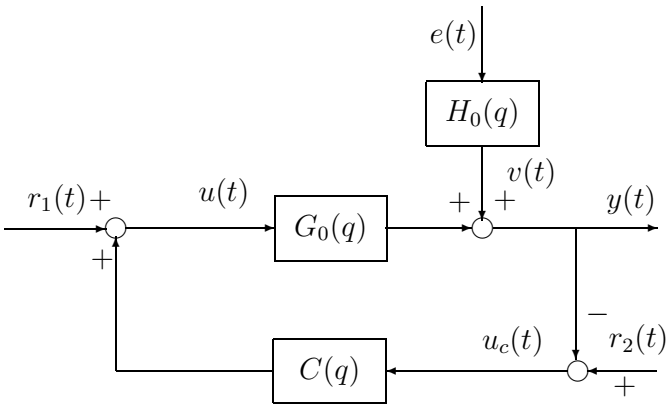

Figure 3.1. Closed-loop data generating system

stable transfer functions [24]. This feedback connection $\mathcal{T}(G_0, C)$ can be observed from the block diagram depicted in Fig. 3.1.

In Fig. 3.1, $G_0(q)$ denotes a finite dimensional, discrete time, linear and time invariant (FDLTI) unknown plant, $C(q)$ presents a causal, discrete time, finite dimensional, linear, time invariant feedback controller. For analysis purposes, both $G_0(q)$ and $C(q)$ are assumed to be stable.

The data set

$$Z^N = \Big\{u(1), y(1), \cdots, u(N), y(N)\Big\} \tag{3.2}$$

consisting of measured input and output signals $u(t)$ and $y(t)$, $t = 1, \cdots, N$ is the basis of system identification technique.

The output $y(t)$ of the plant $G_0(q)$ is feed back to the input $u(t)$ using a negative feedback

$$u(t) = r_1(t) - C(q)\big[y(t) - r_2\big] \tag{3.3}$$

and $r_1(t)$ and $r_2(t)$ are possible external reference signals for closed-loop excitation purposes. Additionally, an additive disturbance $v(t)$ acts on the output of the

plant

$$y(t) = G_0(q)u(t) + v(t),\ v(t) = H_0(q)e(t) \tag{3.4}$$

which is modelled as a monic stable and stably invertible disturbance filter $H_0(q)$ having a white noise input $e(t)$ with variance λ_0.

The z-transform shift-operator q is defined as

$$qu(t) := u(t+1),\ q^{-1}u(t) = u(t-1) \tag{3.5}$$

where q and q^{-1} denote the forward and backward shift operators, respectively.

In this dissertation, the argument q of the transfer function and the argument t of the signals will be omitted frequently to simplify the notations.

For notational convenience, the shorthand notation

$$r := r_1 + Cr_2 \tag{3.6}$$

is introduced in order to rewrite (3.3) into a reduced form.

On the basis of the shorthand notation (3.6), the data coming from the plant G_0 operating under closed-loop conditions can be formulated as follows.

$$y = G_0 S_{in} r + S_{out} H_0 e \tag{3.7}$$

$$u = S_{in} r - C S_{out} H_0 e \tag{3.8}$$

where S_{in} and S_{out} are the input and output sensitivity function [61] defined with

$$S_{in} = (1 + CG_0)^{-1} \tag{3.9}$$

$$S_{out} = (1 + G_0 C)^{-1} \tag{3.10}$$

In the case that both unknown plant G_0 and controller C are single-input-single-output (SISO) transfer functions, the multiplication of C and G_0 is commutative and then $S_{in} = S_{out}$. In this dissertation, we only focus SISO problem, therefore, S_{in} and S_{out} are not discriminated.

For future use we introduce

$$\bar{G}_0 = G_0 S_{in}, \quad \bar{H} = S_{out} H_0 \tag{3.11}$$

so that we can rewrite (3.7) as

$$y = \bar{G}r + v_c, \quad v_c = \bar{H}e \tag{3.12}$$

3.2 Prediction error identification

In the prediction error identification, a following model structure $\mathcal{M}$ is considered.

$$y(t) = G(q,\theta)u(t) + H(q,\theta)\varepsilon(t,\theta) \tag{3.13}$$

where $G(q,\theta)$ is called plant model and $H(q,\theta)$ noise model. $\varepsilon(t,\theta)$ denotes the one step ahead prediction error. The parameter vector θ ranges over a set $\Theta_{\mathcal{M}}$ which is assumed to be compact and connect.

The one-step-ahead predictor of the open-loop system for the model structure is given by [59]

$$y(t|t-1,\theta) = H^{-1}(q,\theta)G(q,\theta)u(t) + (1 - H^{-1}(q,\theta))y(t). \tag{3.14}$$

Therefore, the prediction error can be determined

$$\varepsilon(t,\theta) = y(t) - y(t|t-1,\theta) = H^{-1}(q,\theta)\big[y(t) - G(q,\theta)u(t)\big] \tag{3.15}$$

For notational brevity $G_\theta = G(q,\theta)$ and $H_\theta = H(q,\theta)$ will be defined in the next. Rewrite (3.15) in terms of the input $u(t)$ and noise $e(t)$, we get

$$\varepsilon(t,\theta) = H_\theta^{-1}\left[(G_0 - G_\theta)u(t) + (H_0 - H_\theta)e(t)\right] + e(t) \tag{3.16}$$

Given the model (3.14) and measured data Z^N, the prediction error estimate [59] can be obtained by minimizing the filtered prediction error

$$\hat{\theta}_N = \arg\min_{\theta\in\Theta_{\mathcal{M}}} \frac{1}{N}\sum_{t=1}^{N} \varepsilon_F^2(t,\theta) \tag{3.17}$$

with $\varepsilon_F(t,\theta) = L(q)\varepsilon(t,\theta)$ and L(q) is a stable and monic filter that can be used to enhance wanted frequency regions. $L(q) = 1$ can be assumed in the remain text without loss of generality.

By Parseval's relation [59], the following frequency domain expression holds

$$\hat{\theta}_N = \arg \min_{\theta \in \Theta_{\mathcal{M}}} \frac{1}{2\pi} \int_{-\pi}^{\pi} \Phi_e(\omega, \theta)\, \mathrm{d}\omega \tag{3.18}$$

where $\Phi_e(\omega, \theta)$ denotes the (auto) spectrum of the prediction error $\varepsilon(t, \theta)$.

Under weak regularity condition this prediction error estimate is known to converge with probability 1 to θ^*.

$$\theta^* = \lim_{N \to \infty} \hat{\theta}_N = \arg \min_{\theta \in \Theta_{\mathcal{M}}} \frac{1}{2\pi} \int_{-\pi}^{\pi} \Phi_e(\omega, \theta)\, \mathrm{d}\omega \tag{3.19}$$

In the case of open loop identification, the input $u(t)$ and the noise $e(t)$ are uncorrelated. As a result the asymptotic expression of (3.19) for $N \to \infty$ can be represented by

$$\begin{aligned} \hat{\theta} = \arg \min_{\theta} \int_{-\pi}^{\pi} \left| H_\theta^{-1}(e^{j\omega}) \right|^2 \Big[\Big| G_0(e^{j\omega}) - G_\theta(e^{j\omega}) \Big|^2 \Phi_u(\omega) + \\ + \left| H_0(e^{j\omega}) - H_\theta(e^{j\omega}) \right|^2 \Phi_e(\omega) \Big]\, d\omega. \end{aligned} \tag{3.20}$$

and $\Phi_u(\omega)$ and $\Phi_e(\omega)$ are the spectral densities of input and noise, respectively.

From the above analysis, we know that the input $u(t)$ and output $y(t)$ signals of the plant G_0 are used directly to identify the plant model G_θ and disturbance model H_θ, and this is so-called direct identification method [59]. In this method the feedback is ignored and possible information with respect to the controller $C(q)$ or the reference signal $r(t)$ is not used.

For notational purposes, consider the definition of the model sets $\mathcal{G}$ and $\mathcal{H}$ with

$$\mathcal{G} := \{G_\theta \mid \theta \in \Theta_{\mathcal{M}}\} \tag{3.21}$$

$$\mathcal{H} := \{H_\theta \mid \theta \in \Theta_{\mathcal{M}}\} \tag{3.22}$$

where $\Theta_{\mathcal{M}}$ is the parameter space that guarantees stability of the prediction error (3.16). If the true system belongs to the model set, which is defined by $G_0 \in \mathcal{G}$ and $H_0 \in \mathcal{H}$, then a consistent identification of G_0 and H_0 is obtained [59]. In case $G_0 \notin \mathcal{G}$ and $H_0 \in \mathcal{H}$, an expression for the approximate identification of the models G_θ and H_θ can be obtained.

In the case that the signals u and y are obtained under feedback, substitution of (3.8) into (3.16) yields the prediction error

$$\varepsilon(t,\theta) = H_\theta^{-1}\left[(G_0 - G_\theta)\, S_{in} r(t) + \left((G_\theta - G_0)\, C S_{in} H_0 + (H_0 - H_\theta)\right) e(t)\right] + e(t) \tag{3.23}$$

The last term $e(t)$ can be ignored as it does not depend on θ and does not contribute to the minimization. Because $r(t)$ and $e(t)$ are uncorrelated, we can get a bias expression of $\hat{\theta}$ as

$$\begin{aligned}\hat{\theta} = \arg\min_\theta \int_{-\pi}^{\pi} \left|H_\theta^{-1}\right|^2 \Big[\left|G_0 - G_\theta\right|^2 \left|S_{in}\right|^2 \Phi_r + \\ + \left|(G_\theta - G_0)\, C S_{in} H_0 + (H_0 - H_\theta)\right|^2 \Phi_e\Big]\, d\omega\end{aligned} \tag{3.24}$$

and Φ_r is the spectral density of the reference signal r.

By comparing (3.24) and (3.20), it shows that in the closed-loop identification, the estimation of G_0 and H_0 will effect each other and no explicit tunable expression is obtained, even if the plant model G_θ and disturbance model H_θ are parametrized independently. However, a consistent identification of G_0 and H_0 is possible if the true system is in the model set. The bias of the plant model G_θ related to the bias of the noise model H_θ. If we have a good noise model and /or good signal to noise ratio Φ_r/Φ_e, then the bias of the estimation of plant model G_θ will be small [23].

The biased effect is more obvious when the disturbance model is parametrized independently and fixed to 1, as in an Output Error (OE) model structure. By using output error (OE) model structure, the parameter estimate can be characterized by

$$\hat{\theta} = \arg\min_\theta \int_{-\pi}^{\pi} \left[\left|G_0 - G_\theta\right|^2 \left|S_{in}\right|^2 \Phi_r + \left|(G_\theta C + 1) S_{in} H_0\right|^2 \Phi_e\right]\, d\omega. \tag{3.25}$$

When signal to noise ratio Φ_r/Φ_e is very small, it means that the spectrum of the noise dominates spectrum of the reference signal, and in the case of $-C^{-1} \in \mathcal{G}$, a biased estimation of G_θ is obtained with G_θ approaching to $-C^{-1}$, even if $G_0 \in \mathcal{G}$. As a result, the estimation of plant model G_θ will be biased, and it depends on the disturbance present on the closed-loop data.

In order to construct closed-loop approximate identification methods that have an explicit tunable bias expression we can consider indirect method [11]. This method is based on the idea of first estimating a closed-loop transfer function and then recalculating the model by using the knowledge of the controller C present in the estimated closed-loop transfer function. Even though it can provide an explicit tunable approximation expression, the McMillan degree of the model G_θ and H_θ founded by re-computation will be larger than the McMillan degree of the estimated closed-loop transfer function, and as a result, it is not attractive to us.

In the next sections, we will present some developments in the area of closed-loop approximate identification.

3.3 Two-stage identification

3.3.1 Method description

Two stage method can provide an explicitly tunable approximation criterion which is proposed in [81]. In the two-stage method, identification of the plant model and disturbance model in closed loop is performed in two separate steps. The two steps are used to eliminate the correlation between the input $u(t)$ and the noise $e(t)$ in case of closed-loop data. The two-stage method does not require the knowledge of the controller C. Only the knowledge of the reference signal $r(t)$ and the output signal $y(t)$ are needed and the method can be summarized as follows [81].

In the first step, a model S_β of the input sensitivity function S_{in} is estimated by considering the map from reference signal $r(t)$ to the plant input $u(t)$ in (3.8). Estimation is done by minimizing the prediction error

$$e_1(t, \beta) = u(t) - S_\beta(q)r(t)$$

using a high order model S_β for the sensitivity function. The model S_β is used only for filtering purposes in the second step of the method and no specific restrictions

on the order of S_β are imposed.

In the second step of the two-stage method, the estimate S_β is used to simulate a disturbance free input signal $u_r(t)$ via

$$u_r(t) = S_\beta(q)r(t).$$

that will be uncorrelated with noise $e(t)$ on the closed-loop data. In case a consistent estimate $S_\beta = S_{in}$ is obtained in the first step, (3.7) rewrites into

$$y(t) = G_0 u_r(t) + S_{in} H_0 e(t)$$

Subsequently, in the second step of this method a plant model G_θ (and possibly a disturbance model H_θ) can be estimated by minimizing the two-norm of the prediction error

$$\begin{aligned} \varepsilon_2(t,\theta) = H_\theta^{-1}[G_0 u(t) - G_\theta u_r(t) \\ +(H_0 - H_\theta)e(t)] + e(t) \end{aligned} \tag{3.26}$$

where G_θ and H_θ are again the desirable low order approximation of the plant G_0 and disturbance filter H_0.

In general, the two-stage method is used only to estimate (low order) models G_θ of G_0 in the second step and the estimation of disturbance filters is omitted. For comparison and analysis purposes, we also consider the estimation of disturbance models in the standard two-stage method. Rewriting (3.26) in terms of the reference signal yields

$$\begin{aligned} \varepsilon_2(t,\theta) = H_\theta^{-1}\left[(G_0 S_{in} - G_\theta S_\beta)\, r(t)\right. \\ \left. + (H_0 S_{in} - H_\theta)\, e(t)\right] + e(t) \end{aligned} \tag{3.27}$$

and we will compare the results of disturbance model estimation with the direct method and the extended two-stage method proposed in this dissertation.

3.3.2 Bias distribution for two-stage method

The minimization of the 2-norm of the prediction error in (3.27) during the second step of the two-stage method yields the asymptotic expression

$$\begin{aligned}\hat{\theta} = \arg\min_{\theta} \int_{-\pi}^{\pi} \left|H_{\theta}^{-1}\right|^2 [|\left(G_0 - G_{\theta}\right) S_{in} \\ +G_{\theta}\left(S_{in} - S_{\beta}\right)|^2 \Phi_r + \left|H_0 S_{in} - H_{\theta}\right|^2 \Phi_e] \, d\omega\end{aligned} \tag{3.28}$$

for $N \rightarrow \infty$ [81]. It can be observed that the estimation of the plant model G_{θ} depends on the estimate S_{β} of the input sensitivity function S_{in} in the first step. In case $S_{\beta} \neq S_{in}$ the term $G_{\theta}\left(S_{in} - S_{\beta}\right)$ influences the estimation of the model G_{θ}, but this term can be made small by estimating an accurate model S_{β} of the input sensitivity in the first step of the method [81].

An explicit tunable expression for the bias of the plant model can be obtained by using an independent parametrization of the plant model G_{ξ} and the disturbance model H_{η}. For example, for an OE-model with a fixed disturbance model $H_{\eta} = 1$, the asymptotic expression of (3.28) can be simplified to

$$\hat{\xi} = \arg\min_{\xi} \int_{-\pi}^{\pi} [|\left(G_0 - G_{\xi}\right)|^2 |S_{in}|^2 \Phi_r \, d\omega$$

in case $S_{\beta} = S_{in}$ and clearly indicates the tunable bias expression of the plant model estimate. Moreover, a consistent estimate of the plant dynamics G_0 can be obtained, even though H_{η} is fixed. Consistency of the plant model estimate for $H_{\eta} \neq H_0$ was not shared by the direct identification method.

Unfortunately, the favorable properties of consistency and tunable bias expression for the plant model do not carry over to the disturbance model estimate. It can be observed from (3.28) that the estimation of an independently parametrized disturbance model H_{η} will always be biased, as it aims at the approximation of the closed-loop disturbance model $H_0 S_{in}$. As a result, the estimation of the disturbance models in the two-stage identification method does not share the consistency and tunable bias expressions found for the plant model estimate.

3.4 Dual Youla method for closed loop identification

3.4.1 Coprime factorizations

The basic idea behind dual-Youla method is introduced by [30] in view of closed-loop experiment design. It was further elaborated and modified in [31]. It was applied for approximate identification in [29, 72, 73]. The main advantage of this method lies in the fact that the identified plant models are guaranteed to be stabilized by the present controller. In order to describe this method, following concepts will be needed.

Definition 3.4.1. *Let $N, D \in \mathcal{RH}_\infty$, then the pair (N, D) is called right coprime factorization (rcf) over $\mathcal{RH}_\infty$ if there exists $X, Y \in \mathcal{RH}_\infty$ such that*

$$XN + YD = I \tag{3.29}$$

Let $\tilde{N}, \tilde{D} \in \mathcal{RH}_\infty$, then the pair $(\tilde{D}, \tilde{N})$ is a left coprime factorization (lcf) if there exists $\tilde{X}, \tilde{Y} \in \mathcal{RH}_\infty$ such that

$$\tilde{N}\tilde{X} + \tilde{D}\tilde{Y} = I \tag{3.30}$$

Definition 3.4.2. *A rcf (N, D) is called a normalized right coprime factorization (nrcf) if it satisfies*

$$N^*N + D^*D = I \tag{3.31}$$

Similarly, a lcf $(\tilde{D}, \tilde{N})$ is called a normalized left coprime factorization (nlcf) if it satisfies

$$\tilde{N}\tilde{N}^* + \tilde{D}\tilde{D}^* = I \tag{3.32}$$

Definition 3.4.3. *Let (N, D) be a rcf and $(\tilde{D}, \tilde{N})$ be a lcf, then the pair (N, D) is a rcf of a system G if*

$$det\{D\} \neq 0, \quad G = ND^{-1}$$

Similarly, the pair $(\tilde{D}, \tilde{N})$ *is a lcf of a system* G *if*

$$det\{\tilde{D}\} \neq 0, \quad G = \tilde{D}^{-1}\tilde{N}$$

The requirement on the determinant of D and $\tilde{D}$ is needed to ensure that D^{-1} and $\tilde{D}^{-1}$ are well defined real rational transfer functions.

3.4.2 Method description

By using coprime factorization, a possibly unstable plant can be represented by a quotient of two stable transfer functions.

Lemma 3.1 ([15]). *Let* (N_c, D_c) *be a ref of a controller* C*, and let* (N_x, D_x) *be a rcf of any arbitrary system* G_x *that is stabilized by the controller* C*. Then, the plant* G_0 *with a rcf* (N_0, D_0) *is stabilized by the controller* C *if and only if there exists an* $R_0 \in \mathcal{RH}_\infty$ *such that*

$$\begin{aligned} N_0 &= N_x + D_c R_0 \\ D_0 &= D_x - N_c R_0 \end{aligned} \tag{3.33}$$

Proof: For a proof, one is refered to [93]. □

From Lemma 3.1 it shows that R_0 can vary over all possible transfer functions in $\mathcal{RH}_\infty$ such that $(D_x - N_c R_0)^{-1}$ is well defined, which characterizes a set of plant G_0 that are internally stabilized by the given controller C. R_0 in (3.33) is the only unknown stable transfer function, therefore, estimation of a model $\hat{R}$ of the stable transfer function R_0 would yield an estimate $(\hat{N}, \hat{D})$ of a rcf of the plant $\hat{G}$ described by

$$\begin{aligned} \hat{N} &= N_x + D_c \hat{R} \\ \hat{D} &= D_x - N_c \hat{R} \end{aligned} \tag{3.34}$$

If the estimate $\hat{R}$ is stable, then the model $\hat{G} = \hat{N}\hat{D}^{-1}$ estimated in (3.34) is guaranteed to be stabilized by the controller C.

Consider the feedback configuration presented in Fig. 3.1, the feedback connection $\mathcal{T}(G_0, C)$ can be replaced by a combination of a rcf (N_x, D_x) of any arbitrary plant G_x, a rcf (N_c, D_c) of the controller C and a stable transfer function R_0. The representation of $\mathcal{T}(G_0, C)$ in Fig. 3.1 can be found in Fig. 3.2

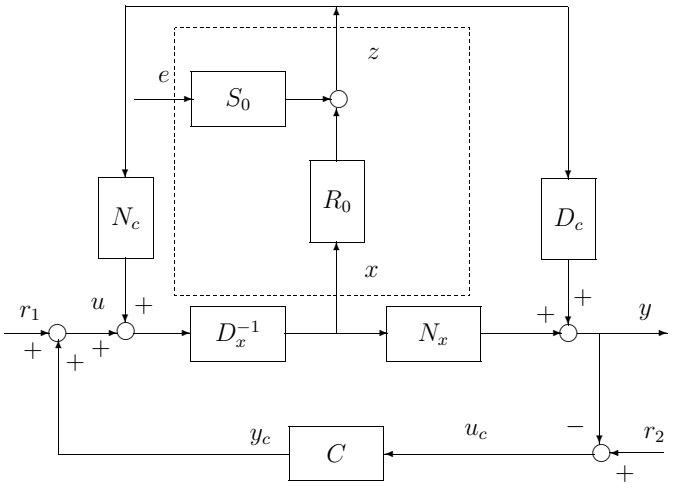

Figure 3.2. Block diagram of the dual Youla representation of the closed-loop data generating system

In order to estimate the dual-Youla parameter R_0 using the open loop identification algorithm, the following lemma is needed.

Lemma 3.2 ([11]). *Let (N_x, D_x) be a rcf of an auxiliary plant G_x over $\mathcal{RH}_\infty$, and (N_c, D_c) be a rcf of a given controller C such that $\mathcal{T}(G_x, C) \in \mathcal{RH}_\infty$, then the intermediate signals $x(t)$ and $z(t)$ can be considered as an input signal and an output signal*

$$z = R_0 x + S_0 e \tag{3.35}$$

The transfer functions R_0 and S_0 are given as

$$R_0 = D_c^{-1}(I + G_0 C)^{-1}(G_0 - G_x)D_x \tag{3.36}$$

$$S_0 = D_c^{-1}(I + G_0 C)^{-1} H_0 \tag{3.37}$$

Moreover, x is defined by the filter operation

$$x := (D_x + CN_x)^{-1} \begin{bmatrix} C & I \end{bmatrix} \begin{bmatrix} y \\ u \end{bmatrix} \tag{3.38}$$

The so-called dual-Youla signal z is defined by the filter operation

$$z := (D_c - G_x N_c)^{-1} \begin{bmatrix} I & -G_x \end{bmatrix} \begin{bmatrix} y \\ u \end{bmatrix} \tag{3.39}$$

where u can be obtained by $u = r - Cy$ and $r = r_1 - Cr_2$.

Proof: For a proof, one is referred to [11]. □

From Lemma 3.2, it can be observed that R_0 and S_0 are the only unknown transfer functions. If the intermediate signals x and z can be reconstructed from (3.38) and (3.39), respectively, in the case that the controller is known, then estimate of R_0 and S_0 is a standard open loop identification problem. When the models R_θ and S_θ are obtained, the model G_θ of the plant G_0 and the noise model H_θ of the noise filter H_0 can be obtained via

$$\begin{aligned} G_\theta &= (N_x + D_c R_{\theta)})(D_x - N_c R_\theta)^{-1} \\ H_\theta &= D_c(I + G_\theta C)S_\theta \end{aligned} \tag{3.40}$$

From (3.40) it can be observed that the McMillan degrees of G_θ and H_θ will be much higher because of the reparemetrization as presented in (3.40). This implies that in the identification discussed above, the McMillan degrees of the identified models G_θ and H_θ are not tunable. As a control point view, even though the identified models G_θ are guaranteed to be stabilized by the controller, it may not be a good choice to be used to design a low order controller because the complexity of identified model is a nontrivial problem to design a low order controller.

3.4.3 Bias distribution for dual-Youla parametrization

The asymptotic frequency domain expression of minimizing the 2-norm of the prediction error corresponding to (3.35) can be depicted as

$$\hat{\theta} = \arg\min_{\theta\in\Theta} \frac{1}{2\pi} \int_{-\pi}^{\pi} \left|S_\theta{}^{-1}\right|^2 \left[\left|R_0 - R_\theta\right|^2 \Phi_x + \left|S_0 - S_\theta\right|^2 \Phi_e\right] \, d\omega \tag{3.41}$$

(3.41) is almost the same as the open loop asymptotic frequency domain expression (3.20) in direct method. The only difference is that (3.41) is obtained under the closed loop experiment, but (3.20) in open loop experiment. As mentioned before, identification in closed loop experiments has more benefit than that in open loop experiments. The expression in (3.41) can be made an explicit and tunable expression if an independent parametrization is used. Specifically, if we use an output error structure to estimate R_θ and fix S_θ to 1, the asymptotic estimate

$$\hat{\theta} = \arg\min_{\theta\in\Theta} \frac{1}{2\pi} \int_{-\pi}^{\pi} \left[\left|R_0 - R_\theta\right|^2 \Phi_x\right] \, d\omega \tag{3.42}$$

is a simple explicit tunable expression for R_θ. The resulting plant model G_θ can be calculated according to

$$G_\theta = \left[N_x + D_c R_\theta\right] \left[D_x - N_c R_\theta\right]^{-1}$$

3.5 Coprime factor identification

3.5.1 Method description

An alternative to the dual-Youla parametrization described in the previous section is coprime factor identification [72, 73]. Unlike the dual-Youla parametrization in which the complexity of the model G_θ is highly dependent on the controller, the auxiliary model G_x and the model R_θ, this method is directed towards estimate of the coprime factors of a plant G_0. Therefore, the order of the resulting model can be controlled more efficiently.

Rewrite the closed loop data generating system in (3.7) and (3.8) into a compact form

$$\begin{bmatrix} y \\ u \end{bmatrix} = \begin{bmatrix} G_0 S_{in} \\ S_{in} \end{bmatrix} r + \begin{bmatrix} S_{out} H_0 \\ -C S_{out} H_0 \end{bmatrix} e \tag{3.43}$$

Now, consider a stable filter F that create an intermediate signal x according to $x = Fr$ which is shown in Fig. 3.3. Then (3.43) can be rewritten as

$$\begin{aligned} \begin{bmatrix} y \\ u \end{bmatrix} &= \begin{bmatrix} G_0 S_{in} F^{-1} \\ S_{in} F^{-1} \end{bmatrix} x + \begin{bmatrix} S_{out} H_0 \\ -C S_{out} H_0 \end{bmatrix} e \\ &= \begin{bmatrix} G_0 S_{in} F^{-1} \\ S_{in} F^{-1} \end{bmatrix} x + \begin{bmatrix} D_c \\ -N_c \end{bmatrix} S_0 e \end{aligned} \tag{3.44}$$

where S_0 is defined as

$$S_0 = D_c^{-1}(I + G_0)^{-1} H_0$$

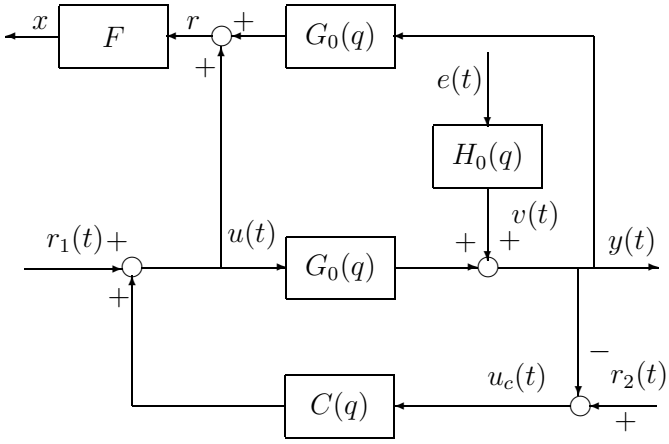

Figure 3.3. Construction of intermediate signal x

Define

$$\begin{aligned} N_0 &= G_0 S_{in} F^{-1} \\ D_0 &= S_{in} F^{-1} \end{aligned} \tag{3.45}$$

Then according to the scheme shown in Fig. 3.4, the identification of N_0 and D_0 can be done with a standard open loop identification because the intermediate signal x and the noise e are uncorrelated. The plant model G_θ is then constructed from $G_\theta = N_\theta D_\theta^{-1}$.

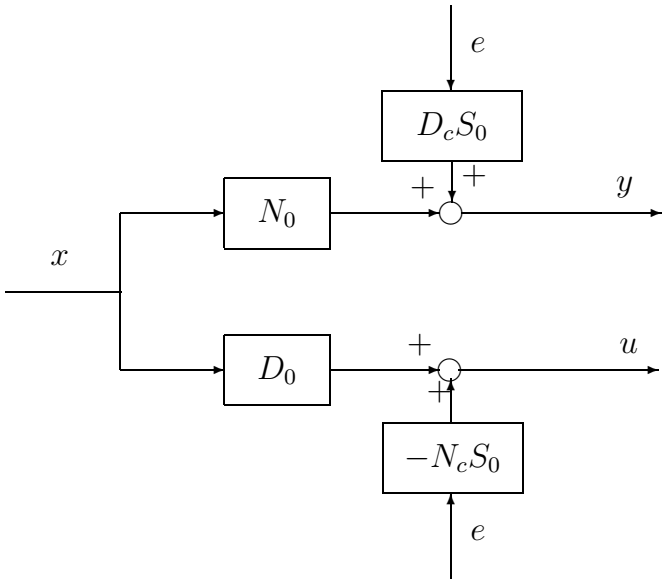

Figure 3.4. Open loop identification of coprime factors

In order to keep N_0 and D_0 to be stable and the intermediate signal x to be bounded, then how to choose the filter F is crucial and the result is given in [82].

Corollary 3.5.1. *A filter F yields stable mappings $(y,u) \to x$ and $x \to (y,u)$ if and only if there exists an auxiliary system G_x with a rcf (N_x, D_x), stabilized by the controller C, such that*

$$F = (D_x + CN_x)^{-1}$$

Furthermore, for all such F, N_0 and D_0 are a pair rcf of system G_0 with $G_0 = N_0 D_0^{-1}$

Proof: For a proof, one is referred to [11] □

After F has been chosen from the above corollary, coprime factors N_θ, D_θ and the noise filter S_θ can be estimated by minimizing the 2-norm of the prediction error described as

$$\varepsilon(t,\theta) = \begin{bmatrix} \frac{1}{D_cS_\theta} & 0 \\ 0 & -\frac{1}{N_cS_\theta} \end{bmatrix} \begin{bmatrix} y - N_\theta x \\ u - D_\theta x \end{bmatrix} \tag{3.46}$$

in terms of the intermediate signal x and noise e.

The plant model G_θ and noise model H_θ can be obtained with a re-computation.

$$\begin{aligned} G_\theta &= N_\theta D_\theta^{-1} \\ H_\theta &= D_c(I + G_\theta C)S_\theta \end{aligned} \tag{3.47}$$

From (3.47) it can be observed that the estimate of G_θ only depends on the estimate of N_θ and D_θ. Therefore, the complexity of the plant model G_θ can be largely simplified. The noise filter model H_θ also depends on the order of D_c, G_θ and S_θ which is the same formula as used in the dual-Youla parametrization.

3.5.2 Bias distribution for coprime factor identification

The asymptotic frequency domain expression for the minimization of the 2-norm of the prediction error in (3.46) is given as follows.

$$\begin{aligned} \hat{\theta} \;=\; \arg\min_{\theta\in\Theta} \int_{-\pi}^{\pi} \begin{bmatrix} \left|\frac{1}{D_c S_\theta}\right|^2 & \left|\frac{1}{N_c S_\theta}\right|^2 \end{bmatrix} \left\{ \begin{bmatrix} |N_0 - N_\theta|^2 \\ |D_0 - D_\theta|^2 \end{bmatrix} \Phi_x + \right. \\ \left. + \begin{bmatrix} |D_c|^2 \\ |N_c|^2 \end{bmatrix} |S_0 - S_\theta|^2 \Phi_e \right\} d\omega \end{aligned} \tag{3.48}$$

Although (3.48) yields an expression for the resulting estimate obtained by approximate identification, it is not an explicit expression for the misfit among N_0, D_0 and S_0 being estimated. This is due to the fact that the estimated S_θ will influence the approximate estimate N_θ, D_θ. The mutual influence of the estimation of S_0 and N_0, D_0 can be decoupled by applying an independently parametrized model structure such as BJ-model structure. Therefore an explicit and tunable expression for the bias or misfit between N_0, D_0 and N_θ, D_θ can be obtained. If we only want to estimate the plant model G_θ, then a OE-model structure can be chosen by setting the filter $S_\theta = 1$. Then (3.48) becomes

$$\hat{\theta} \;=\; \arg\min_{\theta\in\Theta} \int_{-\pi}^{\pi} \left[\left|\frac{1}{D_c}\right|^2 \quad \left|\frac{1}{N_c}\right|^2 \right] \left\{ \begin{bmatrix} |N_0 - N_\theta|^2 \\ |D_0 - D_\theta|^2 \end{bmatrix} \Phi_x \right\} d\omega \qquad (3.49)$$

(3.49) is also an explicit and tunable expression for the bias between N_0, D_0 and N_θ, D_θ. It can be observed that (3.49) is zero when $D_\theta = D_0$ and $N_\theta = N_0$ in case $G_0 \in \mathcal{G}$.

Chapter 4

Extended Two-Stage Method

4.1 Extended two-stage method

4.1.1 Method description

The extended two-stage method is similar to the previously mentioned two-stage method. But the main difference lies in the use of a disturbance model estimate in the two subsequent steps of this method. The estimate of the disturbance filter in the first step of the method is being used to create filtered signals for the low order model approximation of both plant and disturbance dynamics in the second step of the method.

To explain the extended two-stage method in more details, the closed loop data generating system shown in Fig. 4.1 is considered. $\bar{G} = G_0 S_{in}$ and $\bar{H} = H_0 S_{in}$ are defined for notational convenience. The notations $\bar{G}$ and $\bar{H}$ are used to respectively indicate the closed-loop reference signal filter and the closed-loop disturbance filter. With this definition, (3.7) can be rewritten into

$$y(t) = \bar{G}r(t) + \bar{H}e(t) \tag{4.1}$$

$$y(t) = G_0(1 - C\bar{G})r(t) + H_0(1 - C\bar{G})e(t) \tag{4.2}$$

where the knowledge of the controller C is exploited. From (4.2) it can be observed

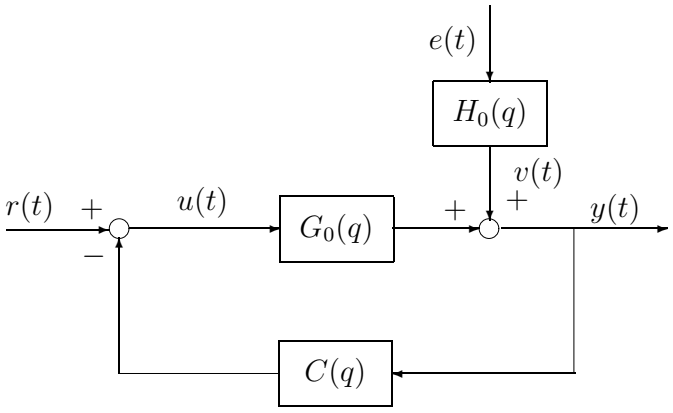

Figure 4.1. Closed-loop data generating system

that with knowledge of $\bar{G}$, the controller C and a time realization of $e(t)$, the estimation of G_0 and H_0 on the basis of closed-loop data becomes a standard open-loop identification problem. A time realization of $e(t)$ can be obtained via an accurate estimation of $\bar{G}$, $\bar{H}$ on the basis of the closed-loop data in (4.1).

Consistent estimation of the closed-loop disturbance filter $\bar{H}$ is possible in the prediction error framework if $\bar{H}$ is a stable and stably invertible filter. If the controller C internally stabilizes the plant G_0, and the open-loop disturbance filter H_0 is stable and stably invertible, then it is straightforward to see that $\bar{H}$ is stable and stably invertible provided both C and G_0 are stable. Under these conditions, the consistent estimation of $\bar{G}$, $\bar{H}$ on the basis of the closed-loop data in (4.1) also becomes a standard open-loop identification problem. From these observations, the extended two-stage method can be summarized by the following two steps:

1. In the first step, a standard open-loop identification of $\bar{G}$ and $\bar{H}$ is performed on the basis of the closed-loop reference $r(t)$ and output $y(t)$ signal in (4.1). Using the estimated models $\bar{G}_*$ and $\bar{H}_*$, the closed-loop prediction error

$$\varepsilon_{cl}(t) = \bar{H}_*^{-1}\left(y(t) - \bar{G}_* r(t)\right). \tag{4.3}$$

   is computed to obtain a realization of the (unfiltered white) noise present on

the closed-loop data.

2. In the second step of the method, the estimated models $\bar{G}_*$ and $\bar{H}_*$ are used to create a filtered input $u_f(t)$ and a filtered prediction error $\varepsilon_f(t)$:

$$u_f(t) := (1 - C\bar{G}_*)r(t) \tag{4.4}$$

$$\varepsilon_f(t) := (1 - C\bar{G}_*)\varepsilon_{cl}(t) \tag{4.5}$$

using the knowledge of the feedback controller C. Subsequently, the signals $u_f(t)$ and $\varepsilon_f(t)$ according to (4.2) are used to estimate low order models G_θ and H_θ by minimizing the two-norm of the output error

$$\varepsilon(t,\theta) = y(t) - [G_\theta(q)\ H_\theta(q)] \begin{bmatrix} u_f(t) \\ \varepsilon_f(t) \end{bmatrix} \tag{4.6}$$

that allows for a low order approximation of the open-loop plant G_0 and disturbance filter H_0.

During the open-loop identification of $\bar{G}$ and $\bar{H}$ in the first step of this method, a stable plant model $\bar{G}$ and a stable and stably-invertible disturbance model $\bar{H}$ are estimated. The reason for the construction of the closed loop residuals in (4.3) in the first step of the method is to allow control over the order of the estimated disturbance model in the second step. An alternative would be to compute a disturbance model H_θ from the estimate $\bar{H}_*$ using knowledge of C and a model G_θ, but this would lead to a higher order estimate of the disturbance model H_θ. Furthermore, it can be noted that only the signals $r(t)$ and $y(t)$ are used in this method, but the knowledge of the controller C can be replaced by an additional measurement of $u(t)$.

Similar to the standard two-stage method [81], the models in the first step are only used for filtering purposes and no restriction on the order of these models is required. A similar idea was also exploited in [44] to obtain consistent estimates of plant and disturbance models, but the results in this dissertation also include the

approximation of plant and disturbance dynamics. Moreover, the computation of the prediction error $\varepsilon_{cl}(t)$ can be used for model validation purposes [59] to address the accuracy of the models $\bar{G}_*$ and $\bar{H}_*$ being estimated in the first step.

4.1.2 Bias distribution for the extended two-stage method

The asymptotic frequency domain expression for the minimization of the 2-norm of the prediction error in (4.6) depends on the estimation results of $\bar{G}_*$ and $\bar{H}_*$ in the first step of the method. In case modeling errors are made in the first step, i.e. $\bar{G}_* \neq G_0 S_{in},\ \bar{H}_* \neq H_0 S_{in}$, then the following asymptotic bias expression is obtained.

Theorem 4.1. *Consider the first step in the extended two-stage method where estimates $\bar{G}_*$ and $\bar{H}_*$ satisfy*

$$\bar{G}_* \neq\ \bar{G} = G_0 S_{in}, \quad \bar{H}_* \neq \bar{H} = H_0 S_{in} \tag{4.7}$$

then for $N \to \infty$ the two-norm minimization of the output error in (4.6) is equivalent to

$$\begin{aligned} \min_{\theta} \int_{-\pi}^{\pi} \Big[\left| (G_0 - G_\theta) S_{in} + (\bar{G}_* - \bar{G})(G_\theta C + H_\theta (1 - C\bar{G}_*)\bar{H}_*^{-1}) \right|^2 \Phi_r(\omega) + \\ + \left| (H_0 - H_\theta) S_{in} + H_\theta (S_{in} - (1 - C\bar{G}_*)\bar{H}\bar{H}_*^{-1}) \right|^2 \Phi_e(\omega) \Big]\ d\omega \end{aligned} \tag{4.8}$$

where G_θ and H_θ denote the models estimated in the second step of the extended two-stage method.

Proof: With the biased estimates of (4.7), the closed-loop prediction error in (4.3) can be rewritten into

$$\varepsilon_{cl}(t) = \bar{H}_*^{-1}(\bar{G} - \bar{G}_*) r(t) + \bar{H}_*^{-1} \bar{H} e(t) \tag{4.9}$$

The output error in (4.6) satisfies

$$\begin{aligned} \varepsilon(t,\theta) &= y(t) - G_\theta u_f - H_\theta \varepsilon_f \\ &= G_0 S_{in} r(t) + H_0 S_{in} e(t) - G_\theta u_f - H_\theta \varepsilon_f \end{aligned} \tag{4.10}$$

Using (4.4), (4.5) and (4.9), the output error in (4.10) can be written as

$$\begin{aligned}\varepsilon(t,\theta) = &\left[(G_0 - G_\theta)S_{in} + (\bar{G}_* - \bar{G})(G_\theta C + H_\theta(1 - C\bar{G}_*)\bar{H}_*^{-1})\right] r(t) + \\ &+ \left[(H_0 - H_\theta)S_{in} + H_\theta(S_{in} - (1 - C\bar{G}_*)\bar{H}\bar{H}_*^{-1})\right] e(t)\end{aligned} \tag{4.11}$$

Using the fact that the closed-loop (unfiltered white) noise $e(t)$ is uncorrelated with the reference signal $r(t)$, autocorrelation of $\varepsilon(t,\theta)$ and application of Parseval's theorem leads to the bias distribution given in (4.8).

Although the result in (4.8) is fairly general, it provides little insight in the bias distribution of plant model estimate G_θ and disturbance model estimate H_θ. It can be seen that in the general situation of $\bar{G}_* \neq G_0 S_{in}$, $\bar{H}_* \neq H_0 S_{in}$, the plant model estimate G_θ will be influenced by the second term $(\bar{G}_* - \bar{G})(G_\theta C + H_\theta(1 - C\bar{G}_*)\bar{H}_*^{-1})$ which again depends on the disturbance model H_θ. However, this second term can be made small in case a consistent estimate $\bar{G}_*$ is obtained of the closed-loop transfer function $G_0 S_{in}$. This effect was also observed in the standard two-stage method. However the bias expression is slightly more complicated due to estimation of the disturbance model H_θ which is now also based on a filtered prediction error $\varepsilon(t)$.

More simplified expressions of the bias distribution can be obtained by assuming that consistent estimate of the closed-loop transfer functions $G_0 S_{in}$ and/or $H_0 S_{in}$ are obtained in the first step of the method. A bias distribution similar to the standard two-stage method is obtained by assuming the consistent estimation $\bar{G}_* = G_0 S_{in}$ and the result is summarized in the following.

Corollary 4.1.1. *Let $\bar{G}_* = \bar{G}$, $\bar{H}_* \neq \bar{H}$ in the first step in the extended two-stage method, then for $N \to \infty$ the two-norm minimization of the output error in (4.6) is equivalent to*

$$\begin{aligned}\min_\theta \int_{-\pi}^{\pi} &\left[\left|(G_0 - G_\theta)\right|^2 \left|S_{in}\right|^2 \Phi_r(\omega) + \right. \\ &\left. + \left|(H_0 - H_\theta)S_{in} + H_\theta(1 - \bar{H}\bar{H}_*^{-1})S_{in}\right|^2 \Phi_e(\omega)\right] d\omega\end{aligned} \tag{4.12}$$

Proof: Substitution of $\bar{G}_* = G_0 S_{in}$, $\bar{H}_* \neq \bar{H}$ into (4.8) yields the result of (4.12).

In the case $\bar{G}_* = G_0 S_{in}$, $\bar{H}_* \neq \bar{H}$, a tunable bias expression for the model estimate G_θ is obtained that is weighted by the sensitivity function and the spectrum of the reference signal. In case of an independent parametrization of plant model G_θ and disturbance H_θ, the bias distribution of the model in the minimization of (4.12) can be decoupled from the disturbance model estimation. However the disturbance model estimate H_θ will still be biased due to the influence of the term $H_\theta(1 - \bar{H}\bar{H}_*^{-1})S_{in}$, which is an effect that can be eliminated only if $\bar{H}_* = H_0 S_{in}$.

It should be noted that exchanging the consistency conditions $\bar{G}_* \neq G_0 S_{in}$ and $\bar{H}_* = H_0 S_{in}$ does not provide the converse of the result mentioned in (4.12). The result is summarized in the following corollary.

Corollary 4.1.2. *Let $\bar{G}_* \neq G_0 S_{in}$, $\bar{H}_* = \bar{H}$ in the first step in the extended two-stage method, then for $N \to \infty$ the two-norm minimization of the output error in (4.6) is equivalent to*

$$\min_\theta \int_{-\pi}^{\pi} \Big[\left| (G_0 - G_\theta) S_{in} + (\bar{G}_* - \bar{G})(G_\theta C + H_\theta (1 - C\bar{G}_*)\bar{H}_*^{-1}) \right|^2 \Phi_r(\omega) + \\ + \left| (H_0 - H_\theta) S_{in} + (\bar{G}_* - \bar{G}) C H_\theta \right|^2 \Phi_e(\omega) \Big] \, d\omega \tag{4.13}$$

Proof: Substitute $\bar{G}_* \neq G_0 S_{in}$, $\bar{H}_* = \bar{H}$ into (4.8) and the result in (4.13) is obtained.

In case $\bar{G}_* \neq G_0 S_{in}$, $\bar{H}_* = \bar{H}$, two terms including $(\bar{G}_* - \bar{G})$ remain and will effect the bias distribution of G_θ and H_θ. The biased estimation of $\bar{G}$ will effect both the estimation of the plant model and the disturbance model. As a result, no explicit tunable expressions of the misfit between G_0 and G_θ, and between H_0 and H_θ are obtained.

The most simplified results is obtained when consistent estimates of both the closed-loop transfer function $G_0 S_{in}$ and $H_0 S_{in}$ are obtained in the first step of the

method. In that case explicit tunable expressions for both the plant model P_θ and the disturbance model H_θ can be derived.

Corollary 4.1.3. *Let $\bar{G}_* = \bar{G}$, $\bar{H}_* = \bar{H}$ in the first step in the extended two-stage method, then for $N \to \infty$ the two-norm minimization of the output error in (4.6) is equivalent to*

$$\begin{aligned} \min_{\theta} \int_{-\pi}^{\pi} \big[|\ G_0 - G_\theta|^2 \, |S_{in}|^2 \, \Phi_r(\omega) + \\ + |H_0 - H_\theta(|^2 \, |S_{in}|^2 \, \Phi_e(\omega) \big] \ d\omega \end{aligned} \tag{4.14}$$

Proof: Substitute $\bar{G}_* = G_0 S_{in}$, $\bar{H}_* = \bar{H}$ into (4.8), then (4.14) is obtained.

It is easily observed that in the case $\bar{G}_* = G_0 S_{in}$ and $\bar{H}_* = H_0 S_{in}$, the difference $|G_0 - G_\theta|^2$ is weighted by the reference spectrum Φ_r and the difference $|H_0 - H_\theta|^2$ is weighted by noise spectrum Φ_e, while both are weighted by the input sensitivity function S_{in}. As a result, explicit tunable bias expressions are obtained for both plant and noise model dynamics. Moreover, consistent models for plant or disturbance dynamics can be obtained if either $G_0 \in \mathcal{G}$ or $H_0 \in \mathcal{H}$.

4.2 Case study

Several parameter identification methods that address the posed identification problem have been proposed in this dissertation. In most of the existing methods, the emphasis is placed on the control-relevant approximation of the system dynamics only and ignore the approximate modeling of the disturbance that is relevant in disturbance control. The new methodology extended two stage method we proposed allows the estimation of low order control relevant plant and disturbance models based on the time series $r(t)$ and $y(t)$, and allows for a control-relevant estimation of low order models of both system and disturbance dynamics. With this method, a tunable bias distribution of the plant model and disturbance model is obtained.

A case study will be given in this section and be used to illustrate the identification concepts proposed and analyzed in this dissertation. The case study consists of a discrete-time sixth order plant $G_0(q)$ and monic stable and stably invertible disturbance filter $H_0(q)$. The dynamics of the plant and disturbance filter are given by

$$G_0(q) = \frac{1}{100} \cdot \frac{-7.737q^5 + 1.113q^4 - 4.014q^3 + 1.377q^2 - 6.016q - 2.493}{q^6 - 1.441q^5 + 2.296q^4 - 1.791q^3 + 2.181q^2 - 1.317q + 0.9206}$$
$$H_0(q) = \frac{q^6 - 0.5574q^5 + 1.293q^4 - 0.7303q^3 + 1.269q^2 - 0.2837q + 0.4032}{q^6 - 1.441q^5 + 2.296q^4 - 1.791q^3 + 2.181q^2 - 1.317q + 0.9206}$$

and follow an [6,6,6,1]-ARMAX structure [59] with a common denominator. An amplitude Bode plot of the sixth order plant G_0 and disturbance H_0 is given in Fig. 4.2, where it can be observed that the plant G_0 exhibits a large resonance frequency at approximately 1 rad/s and small resonance modes on either side. Due to the common dynamics in G_0 and H_0, the disturbance filter exhibits a similar dynamic behavior, but has different zero locations. The dynamics of G_0 and H_0 is characteristic for a mechanical system subjected to external disturbances that excite the same resonance modes.

As G_0 and H_0 are known in this case study, the knowledge of the plant G_0 and disturbance dynamics H_0 is used to design a simple 2nd order discrete time lead/lag feedback controller

$$C(q) = \frac{0.9455q + 0.9347}{q^2 - 0.1315q + 0.3956}$$

that is used for the reduction of the main resonance mode at approximately 1 rad/s. The feedback controller $C(s)$ is tuned in such a way that the main resonance mode in the open-loop disturbance dynamics $H_0(q)$ in (3.4) has been eliminated in the closed-loop disturbance filter $S_{in}(q)H_0(q)$ of (3.7). For identification purposes, the closed-loop input $u(t)$ and output $y(t)$ signals in (3.8) and (3.7) are generated of $N = 4096$ points, where the $r(t)$ and $e(t)$ are chosen as independent Gaussian

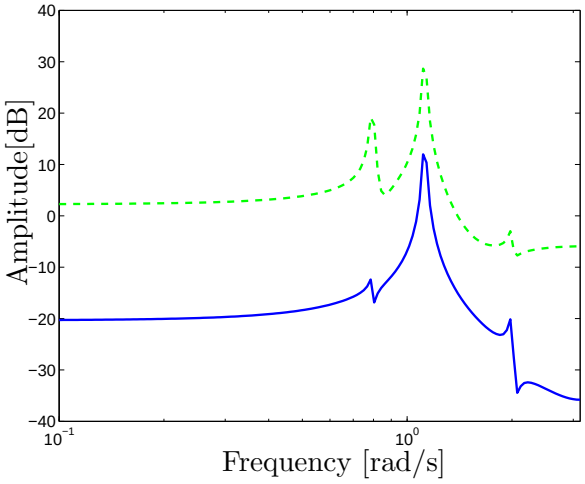

Figure 4.2. Amplitude Bode plot of system dynamics G_0 (solid) and disturbance dynamics H_0 (dashed).

distributed white noise signals. The reference signal $r(t)$ has a unit variance, whereas the noise $e(t)$ has a variance $\lambda = 0.04$.

The objective of the case study is fairly straightforward: find low (2nd order) models G_θ and H_θ that capture the main resonance mode in G_0 and H_0 on the basis of closed-loop data. Since the mutual influence of the estimation between the input-output model and the noise model can be decoupled by employing an independent parametrization, the low order models are parametrized using a BJ structure:

$$\begin{aligned} G(q,\theta) &= \frac{b_2 q^{-2} + b_1 q^{-1} + b_0}{q^{-2} + a_1 q^{-1} + a_0} \\ H(q,\theta) &= \frac{q^{-2} + c_1 q^{-1} + c_0}{q^{-2} + d_1 q^{-1} + d_0} \end{aligned} \tag{4.15}$$

$$\theta = [\ a_1 \quad a_0 \quad b_2 \quad b_1 \quad b_0 \quad c_1 \quad c_0 \quad d_1 \quad d_0\ ] \in \mathbb{R}^{1\times 9}$$

The estimated low order models G_θ and H_θ can then be used to design an optimal low order controller for disturbance suppression of the main resonance mode. The case study is illustrative for the methodologies discussed in this dissertation, as it requires the estimation of low order models that describe the system dynam-

ics and the disturbance dynamics to design a low order controller for disturbance reduction. Three different methods are compared: direct identification, two-stage method and the proposed extended two-stage method. To distinguish between the bias and variance effects of the different closed-loop identification methods, several low order models will be estimated using Monte-Carlo simulations on the basis of different stochastic realizations of the closed-loop data. The identification results are shown in Fig. 4.3, Fig. 4.4 and Fig. 4.5, respectively.

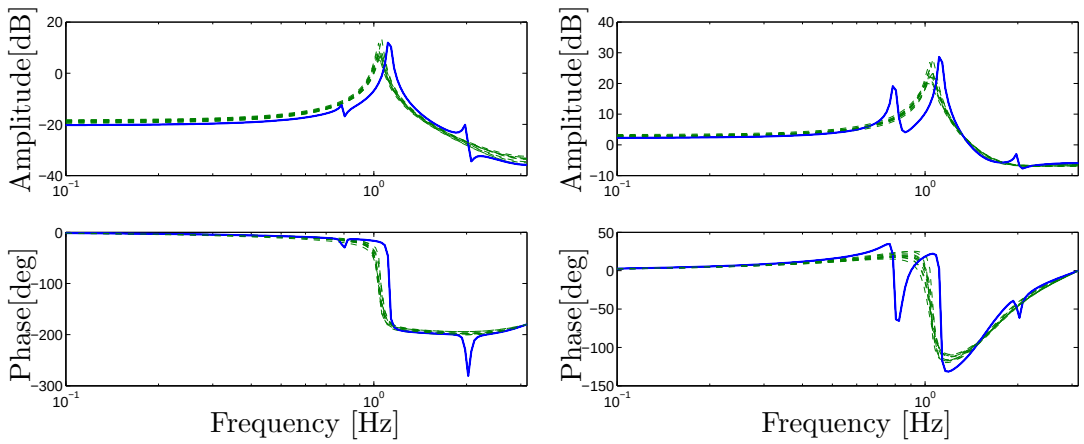

Figure 4.3. Identification results of direct identification. Left: Bode plot of plant G_0 (solid) and the 2nd order model G_θ (dashed). Right: Bode plot of H_0 (solid) and the 2nd order noise model H_θ (dashed).

From Fig. 4.3, it can be observed that the estimate of both plant model G_θ and H_θ can not fit the real system very well even though they are estimated separately. The possible reason for the bias of both plant model G_θ and H_θ lies in the fact that the signal to noise ratio used in this case study is 11, and it may be too small for direct method to get a good identification results.

From Fig. 4.4 it can obtained that the estimate of the plant model G_θ can get a consistent identification, but the estimate of the noise model H_θ can not fit the real noise filter very well. From the description of the two stage method, we know that the estimate of the noise model are always bias and it will tend to the closed

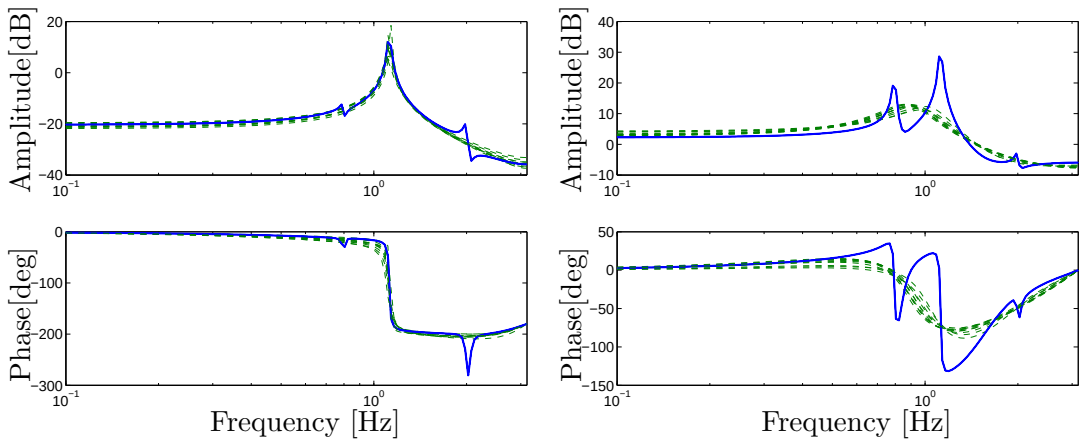

Figure 4.4. Identification results of two-stage method. Left: Bode plot of plant G_0 (solid) and the 2nd order model G_θ (dashed). Right: Bode plot of H_0 (solid) and the 2nd order noise model H_θ (dashed).

loop noise filter $H_0 S_{in}$.

From Fig. 4.5, it is obvious to see that the estimate of both plant model G_θ and noise model H_θ can get a consistent fit of the real system. By comparing the identification results of these three method, we can conclude that the extended two stage method gives a much better approximation of the plant model and noise model than direct method and two stage method.

4.3 Application to Hard Disk Drive

4.3.1 Experimental setting

Due to the extreme miniaturization of the components, and the importance of the hard disk's role in the PC, the entire hard disk is manufactured to a high degree of precision. The main part of the disk is isolated from outside air to ensure that no contaminants get onto the platters, which could cause damage to the read/write heads. In order to obtain reliable and realistic experimental data to measure

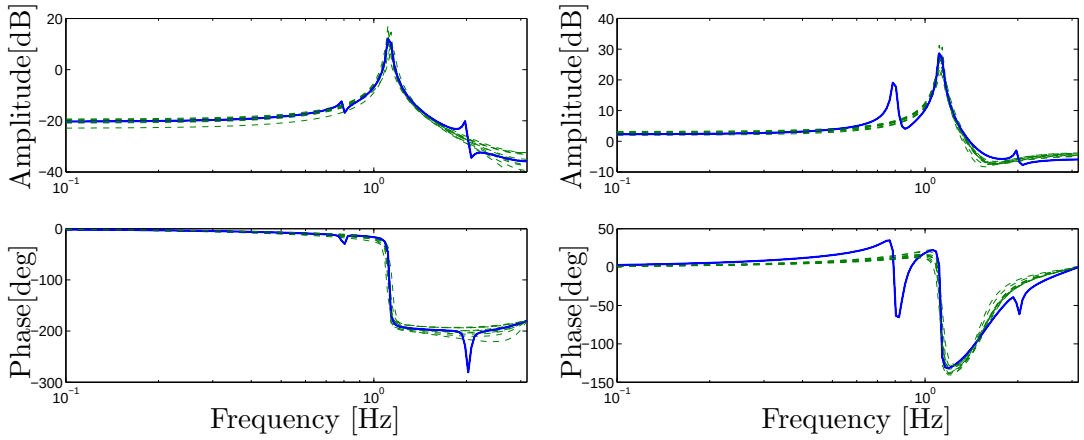

Figure 4.5. Identification results of extended two-stage method. Left: Bode plot of plant G_0 (solid) and the 2nd order model G_θ (dashed). Right: Bode plot of H_0 (solid) and the 2nd order noise model H_θ (dashed).

windage disturbance, the cover of the hard disk drive should keep untouched. So, the same closure with an aperture covered by a transparent material for LDV on hard disk is needed which is illustrated in left part of Fig. 4.6. It can be seen that the cover has been left intact while a small plastic transparent apperture is used to measure the read/write head position with a LDV. The schematic representation of the experiment setup is also depicted in the right part of Fig. 4.6, where it can be seen that the LDV measurement is fed back through an external controller. An additive reference signal $r(t)$ is applied for excitation and identification purposes.

In Fig. 4.7, a block diagram of experiment configuration of hard disk drive is shown. Here $G_0(q)$ indicates the dynamics of voice-coil motor (VCM), E-block and suspension, and $H_0(q)$ denotes the external windage disturbance. For experimentation purposes the external controller $C(q)$ is a discrete time PD controller given by

$$C(q) = \frac{4.219e005q - 4.097e005}{q - 0.1879} \tag{4.16}$$

where $C(q)$ is used only to stabilize the VCM during the experiments. Without such a controller, the open loop marginally unstable VCM drifts and LDV mea-

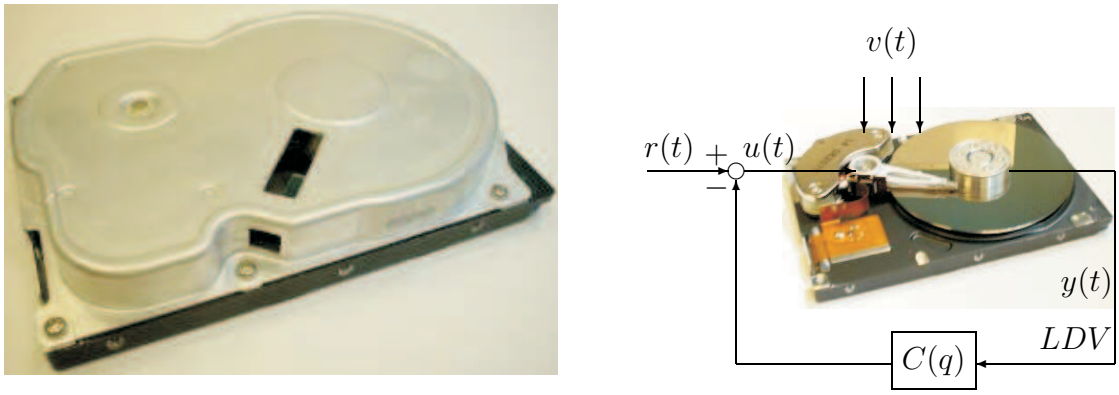

Figure 4.6. Hard disk drive with a slot for LDV measurement (left); Experiment configuration of HDD and servo controller C for track following (right)

surements are compromised.

4.3.2 Experiments and spectral analysis

The experiment setup indicated in Fig. 4.6 is used to gather time sequences of external reference signal $r(t)$, input signal $u(t)$ and output position error signal $y(t)$. To analyze the effect of windage disturbance dynamics in the hard disk drive, experiments were conducted with the read/write head located at 3 different positions on the disk. The VCM was positioned via a feedback controller at the OD (outer diameter), the MD (middle diameter) and ID (inner diameter) of the platter.

For validating the parametric estimation results of actuator dynamics $G_0(q)$ and windage disturbance dynamics $H_0(q)$ with extended two-stage identification method, non-parametric estimates of $G_0(q)$ and $H_0(q)$ are needed, which can be

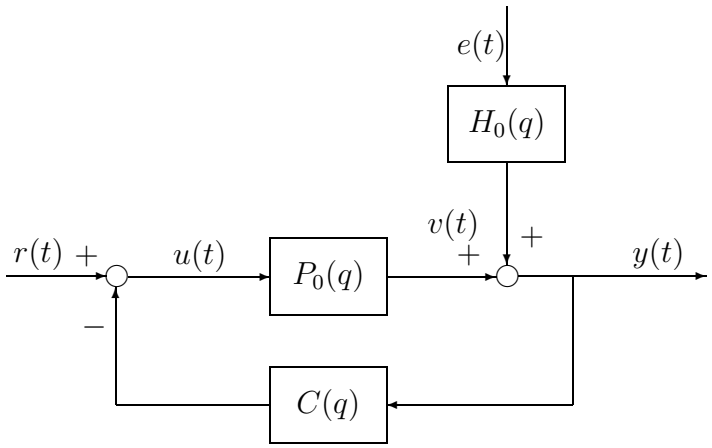

Figure 4.7. Closed-loop data generating system

obtained by a spectral analysis [59], and given by

$$\hat{P}(\omega) := \hat{\Phi}_{ru}^{-1}(\omega)\hat{\Phi}_{ry}(\omega) \tag{4.17}$$

$$\hat{H}(\omega) := \sqrt{(\hat{\Phi}_{yy}(\omega) - \hat{\Phi}_{ry}^{2}(\omega)\hat{\Phi}_{rr}(\omega))\hat{\Phi}_{ru}^{-1}(\omega)\lambda^{-1}} \tag{4.18}$$

where $\hat{\Phi}_{ru}(\omega)$ denotes an approximation of the transfer function from reference signal $r(t)$ to input signal $u(t)$, $\hat{\Phi}_{ry}(\omega)$ denotes an approximation of the transfer function from reference signal $r(t)$ to output position error signal $y(t)$, $\hat{\Phi}_{yy}(\omega)$ and $\hat{\Phi}_{rr}(\omega)$ are approximations of the (auto) spectra of output position error signal $y(t)$ and reference signal $r(t)$, respectively. λ is the variance of the external disturbance.

It should be noted that $\hat{G}(\omega)$ and $\hat{H}(\omega)$ will only be used as a validation tool for the parametric models G_θ and H_θ being estimated with extended two-stage method.

4.3.3 Application of extended two-stage method

In this section, the extended two-stage method discussed in Section 4.1 is applied to data measured using closed loop experiments.

In the case when the VCM located at the OD (outer diameter) of the platter, reference signals $r(t)$, input signal $u(t)$ and output position error signal $y(t)$

measured in closed-loop experiment setting (Fig. 4.7) are plotted in Fig. 4.8. In the first step of the method, a 17th order ARMAX model structure is selected to estimate the closed-loop actuator dynamics $\bar{G}$ and closed-loop windage disturbance dynamics $\bar{H}$ which are used for later filtering purposes. The minimization of the prediction error (4.3) leads to 12th order model estimates of the open-loop actuator dynamics G_0 and windage disturbance dynamics H_0 which are depicted in Fig. 4.9 and Fig. 4.10, respectively.

Fig. 4.9 presents the amplitude plots of the non-parametric estimate of actuator dynamics G_0 and the 12th order parametric model G_θ. Fig. 4.10 shows the amplitude plot of non-parametric estimate of windage disturbance dynamics H_0 and 12th order parametric model H_θ. It can be observed that a good estimation of E-block resonance mode, torsion mode and sway mode is obtained in G_θ and H_θ that are parametrized to share the same resonance modes.

To analyze the effect of windage disturbance dynamics in the hard disk drive, other two experiments also were conducted when VCM was positioned at the MD (middle diameter) and ID (inner diameter) of the platter, respectively. Similar to the process of analyzing the data measured in the case when the VCM located at the OD (outer diameter) of the platter, the estimate models G_θ and H_θ are obtained and compared for illustration in Fig. 4.11 and Fig. 4.12.

Fig. 4.11 and Fig. 4.12 present the amplitude plot of 12th order parametric model G_θ and H_θ when VCM was located at 3 different positions of the platter, respectively. From Fig. 4.11, we can observe that the positions of resonant modes of system dynamics keep the same even though data was measured at different positions. From Fig. 4.12, it can be seen that the position of VCM will affect the magnitude of the windage disturbance dynamics.

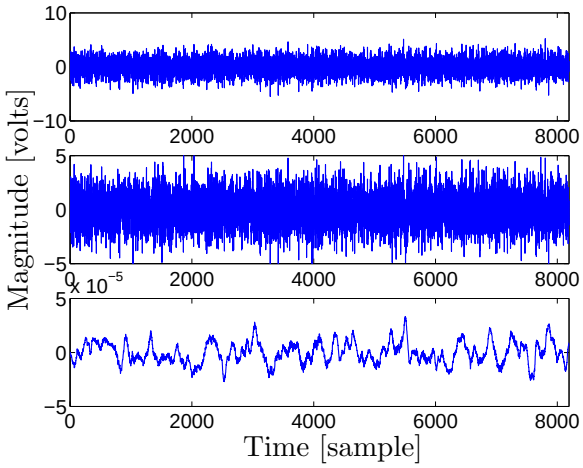

Figure 4.8. Time plots of measured data: $r(t)$ (top); $u(t)$ (middle); $y(t)$ (bottom)

4.4 Conclusions

In this chapter, a new control relevant parametric identification scheme is introduced and analyzed and is so called extended two-stage identification algorithm. In this method, high order models are estimated in the first step for filtering purposes. In the second step, filtered signals are used to provide means for low order model approximation of both actuator and disturbance dynamics which can be used to design a low order control for disturbance rejection. Comparing with other identification methods such as two stage method and direct methods, the extended two stage methods can be not only used to estimate a low order plant model, but also a low order disturbance model which can be used to design a low order control design for disturbance rejection.

Acknowledgements

The text of Chapter 4, in part, is a reprint of the material as it appears in 13th IFAC Symposium on System Identification and in Proc. IEEE International Conference on Mechatronics, and in part, has been submitted for publication in Automatica. The dissertation author was the primary researcher and author in these works

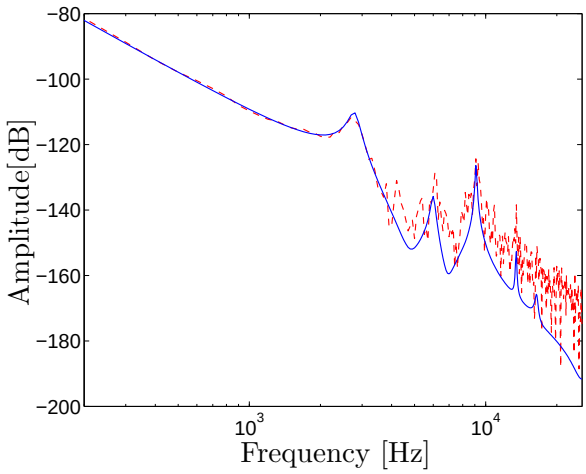

Figure 4.9. Amplitude plot of spectral estimate of system plant (dashed) and 12th order parametric model $G_\theta(q)$ (solid)

and the co-author listed in these publications directed and supervised the research which forms the basis for this chapter.

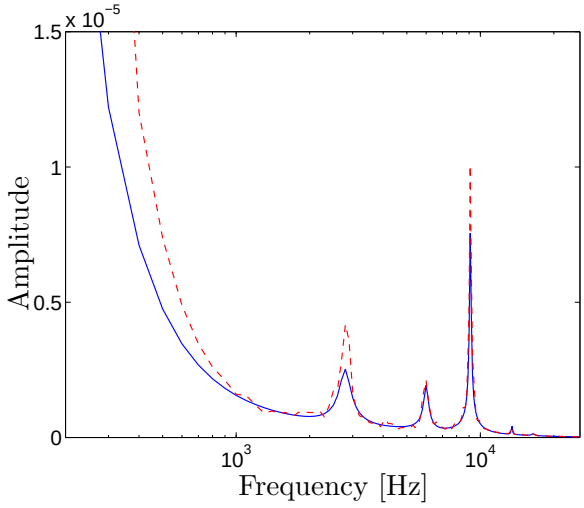

Figure 4.10. Amplitude plot of spectral estimate of disturbance filter (dashed) and 12th order parametric model $H_\theta(q)$ (solid)

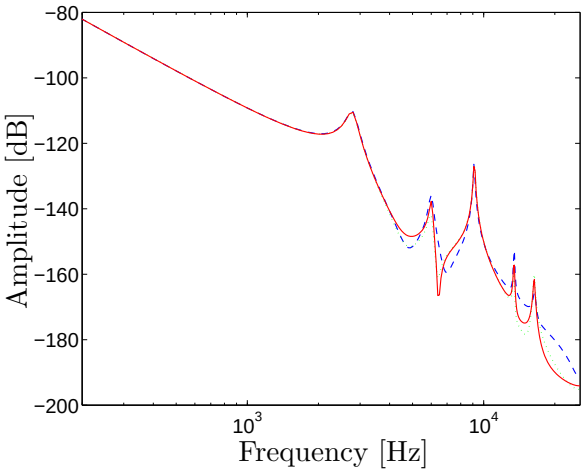

Figure 4.11. Amplitude plot of 12th order parametric estimate model $G_\theta(q)$ when data is measured at different positions: outer diameter (dashed); middle diameter (dotted); inner diameter (solid)

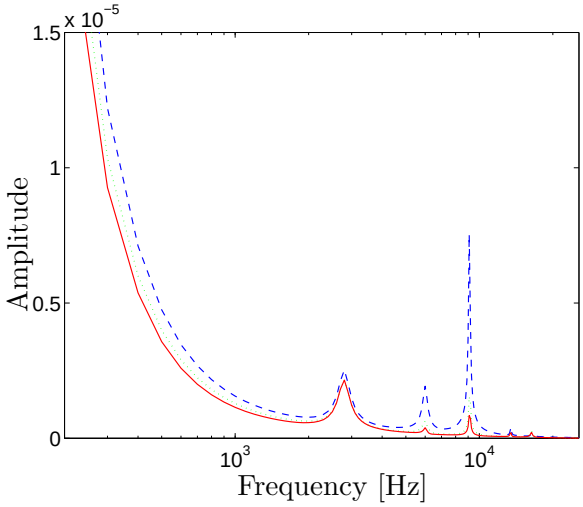

Figure 4.12. Amplitude plot of 12th order parametric estimate model $H_\theta(q)$ when data is measured at different positions: outer diameter (dashed); middle diameter (dotted); inner diameter (solid)

Chapter 5

Modele matching using orthonormal basis functions

5.1 Introduction

Affine model parametrizations using orthonormal basis functions have been widely used in system identification and adaptive signal processing [36, 65, 14, 64, 80, 13, 35, 37]. The main advantage of using orthonormal basis functions in a (generalized) orthonormal Finite Impulse Response (FIR) filter lies in the possibility of incorporating prior knowledge of the system dynamics into the identification and approximation process. As a result, more accurate and simplified models can be obtained with a limited number of parameters in the offline model representation. In this chapter the linear parameter structure of a generalized FIR filter is used to formulate analytic solutions for model matching problems.

In the constructions of the orthonormal basis functions, Laguerre and Kautz basis have been used successfully in system identification and signal processing [85, 86]. A unifying construction [65] generalized both the Laguerre and Kautz basis in the context of system identification. Laguerre basis can be used for the identification of well-damped dynamical systems with one dominant first-order

[85], whereas Kautz basis is suitable for the identification of dynamical systems with second order resonant modes [86]. A further generalization of these results for arbitrary dynamical systems was reported in [36] and is called generalized (orthonormal) basis functions. The generalized orthonormal basis and unifying construction can be used for systems with wide range of dominant modes, i.e, both high frequency and low frequency behavior.

It has been shown in [36] that if the dynamics of the orthonormal basis functions approaches the dynamics of the system to be approximated, the convergence rate of the affine series expansion will increase and as a result the number of the parameters to be determined to accurately approximate the system will be much smaller. Therefore, the choice of the orthonormal basis becomes an important issue in order to obtain accurate models.

In this chapter, the use of a generalized FIR filter $F(q,\theta)$ is considered to solve a model matching problem of the form

$$\min_{\theta} \|H(q) - F(q,\theta)G(q)\|_2 \tag{5.1}$$

where $H(q)$ and $G(q)$ are models that are stable but not necessarily have a stable inverse. The model matching in (5.1) occurs in many applications that require the computation of a stable filter to approximate an unstable system. The problem (5.1) arises for example in Active Noise Control (ANC), there $H(q)$ is primary noise path, $G(q)$ is second noise path, and $F(q,\theta)$ is a feedforward controller to be designed [92]. This chapter provides analytic solutions to the optimization of (5.1) in case $F(q,\theta)$ is a generalized FIR filter, parameterized using an orthonormal basis function. Furthermore, a comparison is made between the approximation results for different orthonormal basis functions that use the same prior knowledge on the system dynamics of $H(q)$ and $G(q)$ both of which can be estimated from closed loop identification method depicted in Chapter 4.

5.2 Structure of orthonormal basis functions

Consider a linear time invariant stable discrete time system $F(q)$ written as

$$F(q) = \sum_{k=0}^{\infty} F_k q^{-k} \tag{5.2}$$

where $\{F_k\}_{k=0,1,2\cdots}$ are the sequence of Markov parameters. In general, the system $F(q)$ can be approximated by $\hat{F}(q)$ using a finite number of expansion coefficients $\theta = \{F_k\}_{k=0,1,\cdots,N-1}$ through

$$\hat{F}(q,\theta) = \sum_{k=0}^{N-1} F_k q^{-k} \tag{5.3}$$

The model $\hat{F}(q)$ represented via (5.3) is a Finite Impulse Response (FIR) model and has some favorable properties. First, it is linearly parameterized. Secondly, least square estimation of the parameters θ on the basis of input/output measurements of $F(q)$ is robust against colored noise on the output measurements, which is one of the main features exploited in model identification.

However, it is known that for a dynamical system including both high and low frequency dynamics, a large number of coefficients N are required in order to capture the most important dynamics of the system $F(q)$ into the model $\hat{F}(q)$. Therefore, the FIR model structure in general is too simple to capture a system with a broad-band dynamics.

Suppose $\{V_k(q)\}_{k=0,1,2,\cdots}$ is an orthonormal basis sequence for the set of systems in $\mathcal{H}_2$. Then there exists a unique expansion

$$F(q) = \sum_{k=0}^{\infty} L_k V_k(q) \tag{5.4}$$

where $\{L_k\}_{k=0,1,2,\cdots}$ are the generalized orthonormal expansion coefficients for the basis $\{V_k(q)\}$. Based on this rationale, a model of the dynamical system $F(q)$ can be represented by an finite length N series expansion

$$\hat{F}(q,\theta) = \sum_{k=0}^{N-1} L_k V_k(q),\ \theta = [L_0^T, \cdots, L_{N-1}^T]. \tag{5.5}$$

When $V_k(q)$ are chosen as $V_k(q) = q^{-k}$, then (5.5) simplifies to (5.3). Therefore, (5.5) will be called a generalized FIR filter in the remainder of the chapter. The orthornomal basis sequence $\{V_k(q)\}_{k=0,1,2,\cdots}$ can incorporate the possible prior knowledge of the system to be approximated, and the model $\hat{F}(q)$ can be more accurate for a finite number of coefficients N compared to a standard FIR model structure. It is obvious that the accuracy of the model $\hat{F}(q)$ depends on the choice of the basis function $V_k(q)$.

A well-known orthonormal basis function expansion is based on the Laguerre functions [85] and described by

$$V_k(q) = \sqrt{1-a^2}q\frac{(1-aq)^k}{(q-a)^{k+1}}, \qquad |a| < 1 \tag{5.6}$$

where the variable a should be chosen in a range that matches the dominating dynamics of the system to be approximated. Although useful, the Laguerre functions $V_k(q)$ can only include knowledge of a single pole. For moderately damped systems, Kautz functions [86] have been employed and they are given as

$$V_k(q) = \begin{cases} \dfrac{\sqrt{(1-b^2)(1-c^2)}}{q^2-b(c+1)q+c}\left(\dfrac{cq^2-b(c+1)q+1}{q^2-b(c+1)q+c}\right)^k \\ \dfrac{(q-b)\sqrt{(1-c^2)}}{q^2-b(c+1)q+c}\left(\dfrac{cq^2-b(c+1)q+1}{q^2-b(c+1)q+c}\right)^k \end{cases} \tag{5.7}$$

where $|b| < 1$ and $|c| < 1$.

A unifying construction of the orthonormal basis function was presented in [65] and given by

$$V_k(q) = \left(\frac{\sqrt{1-|\xi_k|^2}}{q-\xi_k}\right)\prod_{i=0}^{k-1}\left(\frac{1-\bar{\xi}_i q}{q-\xi_i}\right) \tag{5.8}$$

where $\{\xi_i\}_{i=0,1,2,\cdots,N-1}$ is the variety of the poles. A model structure using unifying construction is illustrated in Fig. 5.1. The advantage of using the unifying construction (5.8) lies in the possibility to include knowledge of multiple possible pole locations in the generalized FIR filter, while the orthonormality of basis $V_k(q)$ is still preserved. This property may lead to a more accurate model $\hat{F}(q,\theta)$ of the system $F(q)$ to be approximated.

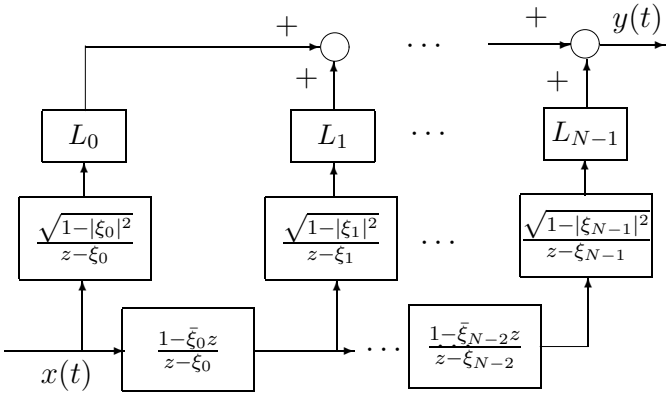

Figure 5.1. Illustration of model structure using unifying construction of the basis functions.

The set of (generalized) orthonormal basis functions presented in [36] provides an alternative way to construct an orthonormal basis with all-pass functions. For details on the construction of the generalized basis functions $V_k(q)$ one is referred to [36]. The following result shows the existence and construction of the inner function which is crucial to create the orthonormal basis functions.

Proposition 5.2.1. *Let (A, B) be the state matrix and input matrix of an input balanced realization of a discrete time transfer function $H \in \mathcal{RH}_2^{p\times m}$ ($\mathcal{RH}_2^{p\times m}$ indicates the set of real rational $p \times m$ matrix functions) with a McMillan degree $n > 0$, and with $rank(B) = m$. Then*

(a) *There exist matrices C, D such that (A, B, C, D) is a minimal balanced realization of a square inner function P.*

(b) *A realization (A, B, C, D) has the property mentioned in (a) if and only if*

$$\begin{aligned} C &= UB^T(I_n + A^T)^{-1}(I_n + A) \\ D &= U[B^T(I_n + A^T)^{-1}B - I_m] \end{aligned} \tag{5.9}$$

where I_n is $n\times n$ identity matrix, I_m is $m\times m$ identity matrix, and $U \in R^{m\times m}$ is any unitary matrix.

Proof: This proposition is original described in [36]. For the proof, one is referred to [36].

Proposition 5.2.1 yields a square $m \times m$ inner transfer function $P(q) = D + C(qI - A)^{-1}B$, where (A, B, C, D) is a minimal balanced realization. With the information obtained in Proposition 5.2.1, the orthonormal basis functions can be created with following proposition.

Proposition 5.2.2. *Let $P(q)$ is a square inner function with McMillan degree $n > 0$ and (A, B, C, D) is a minimal balanced realization of $P(q)$. Define the input to state transfer function $V_0(q) := (qI - A)^{-1}B$ and*

$$\begin{aligned} V_k(q) &= (qI - A)^{-1}BP^k(q) \\ &= V_0(q)P^k(q) \end{aligned} \tag{5.10}$$

then the set of functions $\{V_k(q)\}_{k=0,1,2,\cdots}$ are orthonormal basis functions which have the following property

$$\frac{1}{2\pi j}\oint V_i(q)V_j^T(1/q)\frac{dq}{q} = \begin{cases} I & i = j \\ 0 & i \neq j \end{cases} \tag{5.11}$$

Proof: For the proof, one is referred to [37].

Proposition 5.2.1 and Proposition 5.2.2 show how to use an inner function to construct the orthonormal basis function $V_k(q)$. In summary, if an orthonormal basis with poles at $\{\xi_i\}_{i=0,1,2,\cdots,N-1}$ is desired, then from Proposition 5.2.1 an inner function $P(q)$ with these poles can be created. As a result, a balanced realization (A, B, C, D) of inner function $P(q)$ can be found to form the orthonormal basis function $V_k(q)$ as in (5.10). The construction of a generalized FIR filter on the basis of the (generalized) orthonormal basis function is shown in Fig. 5.2.

The difference between the generalized basis functions in (5.10) and the unifying construction (5.8) is that using (5.10) the poles of $\hat{F}(q)$ are restricted to a

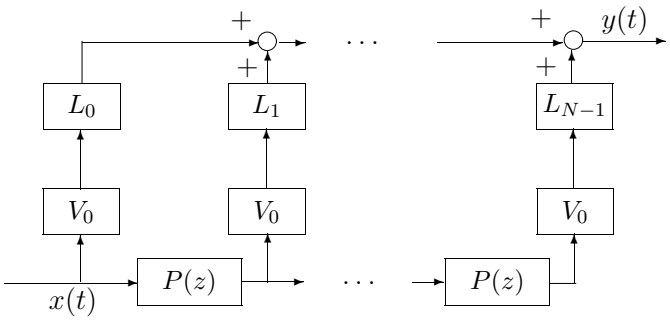

Figure 5.2. Illustration of model structure based on (generalized) orthonormal basis functions.

finite set $\{\xi_0, \cdots, \xi_{n-1}\}$. Using unifying construction (5.8), the poles of $\hat{F}(q)$ can be extended to infinite. The reason the generalized basis functions can only incorporate finite modes is that the order of the inner function $P(q)$ in the orthonormal basis functions is finite. A more general orthonormal basis functions which can incorporate an infinite number of poles is summarized in the following proposition.

Proposition 5.2.3. *Consider a sequence of inner function $P_i(q),\ i = 0, 1, 2, \cdots$, each $P_i(q)$ having a corresponding balanced realization (A_i, B_i, C_i, D_i) and defining $\Phi_i(q) = (qI - A_i)^{-1}B_i$. Then the set of functions $\{V_i(q)\}_{i=0,1,2,\cdots}$ with*

$$\begin{aligned} V_0(q) &= \Phi_0(q) \\ V_i(q) &= \Phi_i(q)P_0(q)P_1(q)\cdots P_{i-1}(q) \end{aligned} \tag{5.12}$$

is mutually orthonormal.

Proof: The proof is similar to the proof for Proposition 5.2.2, and is omitted for sake of brevity.

Because the set of functions $\{V_i(q)\}_{i=0,1,2,\cdots}$ are mutually orthonormal, then $V_i(q)$ can constitute a set of orthonormal basis functions. The construction of

orthonormal basis function described in Proposition 5.2.3 is named (generalized) mutual orthonormal basis functions. With $V_i(q)$ in place, the model $\hat{F}(q)$ of a dynamical system $F(q)$ can be represented as

$$\begin{aligned} \hat{F}(q) &= \sum_{k=0}^{N-1} L_k \Phi_k(q) P_0(q) P_1(q) \cdots P_{k-1}(q) \\ &= \sum_{k=0}^{N-1} L_k V_k(q). \end{aligned} \tag{5.13}$$

If $P(q) = P_0(q) = P_1(q) = \cdots = P_{N-2}(q)$, then (5.12) can be simplified to (5.10) and therefore the construction of the basis functions in (5.12) is the generalization of the construction of basis functions in (5.10).

A model structure using (generalized) mutual orthonormal basis functions is illustrated in Fig. 5.3.

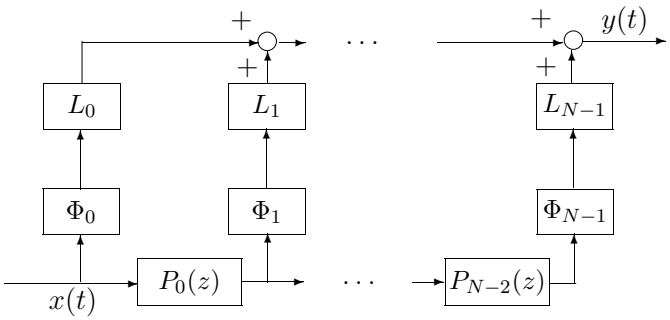

Figure 5.3. Illustration of model structure using (generalized) mutual orthonormal basis functions

Compared with Fig. 5.3 and Fig. 5.1, it is easy to observe that when each $P_i(q)$ in Fig. 5.3 only include one pole ξ_i, then the construction of generalized mutual orthonormal basis functions (5.12) is equal to unifying construction (5.8). Therefore, the unifying construction described in (5.8) is again a special case of the generalized mutual basis functions given in (5.12).

5.3 Model matching with generalized FIR filters

Given the parametrization results for a filter $F(q,\theta)$ using generalized mutual orthonormal basis function, the model matching problem defined earlier in (5.1) will be solved. The model matching in (5.1) occurs in many applications that require the computation of a stable filter to approximate an unstable system and arises for example in feedforward control design algorithms for active noise control.

For the model matching problem (5.1), let the dynamical systems $H(q)$ and $G(q)$ be given by the state space realizations (A_h, B_h, C_h, D_h) and (A_g, B_g, C_g, D_g), where $H(q)$ is stable and stable invertible, and $G(q)$ is stable but not stable invertible. As a result, the filter $F(q,\theta)$ can not be directly obtained by using $H(q)/G(q)$. Furthermore, the objective is to find a filter $F(q,\theta)$ such that

$$\|H(q) - F(q,\theta)G(q)\|_2 \tag{5.14}$$

is minimized, where $F(q,\theta)$ is parametrized affinely using an orthonormal FIR expansion. It is straightforward to show that the minimization of (5.14) is equivalent to minimizing

$$\|\bar{H}(q,\theta)\|_2,\ \bar{H}(q,\theta) := H(q) - F(q,\theta)G(q)$$

where $\bar{H}(q,\theta)$ is parametrized by a state-space representation $(A, B, C(\theta), D(\theta))$ in which the output matrix $C(\theta)$ and the feedthrough matrix $D(\theta)$ depend affinely on the parameter θ. To formulate an analytic solution to (5.1), first an expression for the state space realization $(A, B, C(\theta), D(\theta))$ is derived in case $F(q,\theta)$ is parametrized using an orthonormal FIR expansion. The state space realization of the orthonormal FIR expansion $F(q,\theta)$ is given by the following two propositions.

Proposition 5.3.1. *Suppose a square inner transfer function $P(q)$ has a minimal balanced realization (A_b, B_b, C_b, D_b) with the state dimension $n_b > 0$, then for any $k > 1$ the realization (A_k, B_k, C_k, D_k) of $P(q)^k$ can be computed with the recursive*

forms

$$\begin{aligned} A_k &= \begin{bmatrix} A_{k-1} & 0 \\ B_b C_{k-1} & A_b \end{bmatrix} \\ B_k &= \begin{bmatrix} B_{k-1} \\ B_b D_{k-1} \end{bmatrix} \\ C_k &= \begin{bmatrix} D_{k-1} C_b & C_{k-1} \end{bmatrix} \\ D_k &= D_b D_{k-1} \end{aligned} \tag{5.15}$$

and is a minimal balanced realization of $P(q)^k$ *with state dimension* $n \cdot k$.

Proof: For the proof, one is referred to [36].

Proposition 5.3.2. *Given an orthonormal FIR expansion* $F(q,\theta)$ *in the form of*

$$F(q,\theta) = D_f + \sum_{k=1}^{n} L_{k-1} V_{k-1}(q), \ \theta = [D_f, L_0^T, \cdots, L_{n-1}^T]$$

where $V_{k-1}(q)$ *are obtained from (5.10). Let the inner function* $P(q)^{n-1}$ *has a minimal balanced realization* $(A_{n-1}, B_{n-1}, C_{n-1}, D_{n-1})$*, then* $(A_{n-1}, B_{n-1}, C_f, D_f)$ *is a realization of* $F(q,\theta)$*, where* $C_f = [L_0^T, L_1^T, \cdots, L_{n-1}^T]$.

Proof: The proof of this proposition follows by inspection.

If (5.12) is chosen to create the orthonormal basis function $V_k(q)$, i.e, many different all-pass functions $P_i(q)$ are selected to create the orthonormal basis function $V_k(q)$, then the state space realization of orthonormal FIR can still be easily obtained following the similar procedures described in Proposition 5.3.1 and Proposition 5.3.2.

With the state space realization of $H(q)$, $G(q)$ and $F(q,\theta)$, the state space realization $(A, B, C(\theta), D(\theta))$ of $H(q) - F(q,\theta)G(q)$ is given by

$$\begin{aligned} A &= \begin{bmatrix} A_h & 0 & 0 \\ 0 & A_g & 0 \\ 0 & B_{n-1} C_g & A_{n-1} \end{bmatrix}, B = \begin{bmatrix} B_h \\ B_g \\ B_{n-1} D_g \end{bmatrix} \\ C(\theta) &= \begin{bmatrix} C_h & -D_f C_g & -C_f \end{bmatrix}, D(\theta) = [D_f D_g] \\ \theta &= [D_f, L_0^T, \cdots, L_{n-1}^T] \end{aligned} \tag{5.16}$$

With these results, the minimization of $\|\bar{H}(q,\theta)\|_2$ can be computed as a function of θ and the result is summarized in the following theorem.

Theorem 5.1. *Consider the discrete-time system $\bar{H}(q,\theta)$, Minimization of $\|\bar{H}(q,\theta)\|_2^2$ is equivalent to*

$$\min_{\theta}\{tr\left[D(\theta)D(\theta)^T + C(\theta)QC(\theta)^T\right]\} \tag{5.17}$$

where Q is the solution to the Lyapunov (Stein) equation

$$AQA^T - Q + BB^T = 0$$

The optimization in (5.17) can be solved via a SemiDefinite Programming (SDP) problem

$$\begin{gathered}\min_{\gamma,X_1,X_2,\theta}\gamma \text{ such that} \\ \gamma - tr\{X_1\} - tr\{X_2\} > 0,\ \begin{bmatrix} X_1 & C(\theta) \\ C(\theta)^T & Q^{-1} \end{bmatrix} > 0, \\ \begin{bmatrix} X_2 & D(\theta) \\ D(\theta)^T & I \end{bmatrix} > 0\end{gathered} \tag{5.18}$$

where γ is a positive real number.

Proof: Since $C(\theta)$ and $D(\theta)$ depend affinely on the parameter θ, the condition

$$\mathrm{tr}\{D(\theta)D(\theta)^T\} + \mathrm{tr}\{C(\theta)QC(\theta)^T\} \leq \gamma$$

can be recasted as a Linear Matrix Inequality (LMI). The LMI will be of the form

$$\begin{gathered}\mathrm{tr}\{X_1\} + \mathrm{tr}\{X_2\} < \gamma,\ \begin{bmatrix} X_1 & C(\theta) \\ C(\theta)^T & Q^{-1} \end{bmatrix} > 0, \\ \begin{bmatrix} X_2 & D(\theta) \\ D(\theta)^T & I \end{bmatrix} > 0\end{gathered}$$

where $X_1 = X_1^T$ and $X_2 = X_2^T$ are two new (slack) variables of appropriate dimension needed to formulate the convex constraints. As a result, the SDP problem

$$\min_{\gamma, X_1, X_2, \theta} \gamma \text{ such that}$$
$$\gamma - \text{tr}\{X_1\} - \text{tr}\{X_2\} > 0, \begin{bmatrix} X_1 & C(\theta) \\ C(\theta)^T & Q^{-1} \end{bmatrix} > 0,$$
$$\begin{bmatrix} X_2 & D(\theta) \\ D(\theta)^T & I \end{bmatrix} > 0$$

can be used to find the value of the parameter θ that minimizes $\|\bar{H}(q,\theta)\|_2 = \sqrt{\gamma}$.

A more efficient algorithm to compute θ is by exploiting the structure of $C(\theta)$ and $D(\theta)$. Since $\bar{H}(q,\theta)$ is defined as $H(q) - F(q,\theta)G(q)$, it follows that $C(\theta) = [C_h \ -D_f C_g \ -C_f]$ and $D(\theta) = D_h - D_f D_g$ where the pairs (C_h, D_h), (C_g, D_g) and (C_f, D_f) are the output matrices of $H(q)$, $G(q)$ and $F(q,\theta)$ respectively. Defining the parameter θ as

$$\theta = \begin{bmatrix} D_f & C_f \end{bmatrix}$$

the minimization of $\|\bar{H}(q,\theta)\|_2$ can also be written as a weighted least squares problem. The result is summarized in the following corollary.

Corollary 5.3.1. *The analytic solution for the minimization*

$$\min_{\theta} \{ tr \left[D(\theta) D(\theta)^T + C(\theta) Q C(\theta)^T \right] \} \tag{5.19}$$

is given by

$$\theta = [Y X^T][X X^T]^{-1} \tag{5.20}$$

where

$$Y = \begin{bmatrix} D_h & C_h & 0 & 0 \end{bmatrix} H, \ X = \begin{bmatrix} D & C \end{bmatrix} H$$

$$C = \begin{bmatrix} 0 & C_g & 0 \\ 0 & 0 & I \end{bmatrix}, \ D = \begin{bmatrix} D_g \\ 0 \end{bmatrix}$$

and H is found by a Cholesky factorization of the positive definite matrix $\bar{Q} = \begin{bmatrix} I & 0 \\ 0 & Q \end{bmatrix}$.

Proof: Matrices $C(\theta)$ and $D(\theta)$ in (5.16) can be rewritten as

$$C(\theta) = \begin{bmatrix} C_h & 0 & 0 \end{bmatrix} - \theta C,\ D(\theta) = D_h - \theta D,$$
$$C := \begin{bmatrix} 0 & C_g & 0 \\ 0 & 0 & I \end{bmatrix},\ D := \begin{bmatrix} D_g \\ 0 \end{bmatrix}$$

Define

$$E = \begin{bmatrix} D_h & C_h & 0 & 0 \end{bmatrix} - \theta \begin{bmatrix} D & C \end{bmatrix},\ \bar{Q} = \begin{bmatrix} I & 0 \\ 0 & Q \end{bmatrix}$$

then (5.19) can be rewritten as

$$\|\bar{H}(q,\theta)\|_2^2 = \mathrm{tr}\{E\bar{Q}E\}$$

where H is found by a Cholesky factorization $\bar{Q} = HH^T$ of the positive definite matrix $\bar{Q}$. With the definition of

$$Y = \begin{bmatrix} D_h & C_h & 0 & 0 \end{bmatrix} H,\ X = \begin{bmatrix} D & C \end{bmatrix} H$$

E is defined as $E = Y - \theta X$ and the minimization of $\mathrm{tr}\{E\bar{Q}E\}$ for $\bar{Q} > 0$ is a standard weighted least squares optimization problem for which the analytic solution can be computed via (5.20).

5.4 Model error bounds

With full knowledge of the dynamics of $H(q)$ and $G(q)$, the modeling matching problem in (5.1) can be seen as an H_2-optimal control or filtering problem. In case no restrictions on the parametrization of $F(q,\theta)$ are imposed, the minimization $\|H(q) - F(q,\theta)G(q)\|_2$ can be solved with standard H_2 optimal control solutions [93]. Including a requirement on the parametrization of $F(q,\theta)$ in the form of an

affine orthonormal FIR model structure, only allows the model $F(q,\theta)$ to approach the optimal solution $F_{opt}(q)$.

To formulate error bounds for the model error between $F(q,\theta)$ and $F_{opt}(q)$, the model error is quantified by the 2-norm

$$\|H(q) - F(q,\theta)G(q)\|_2 \tag{5.21}$$

and the optimal solution $F_{opt}(q)$ gives a lower bound $\|H(q) - F_{opt}(q)G(q)\|_2$ for the model error in (5.21). An upper bound for (5.21) can be formulated by considering the poles ξ_i of the basis functions, when $F(q,\theta)$ is parametrized using an affine orthonormal FIR model structure. The result is summarized in the following proposition.

Proposition 5.4.1. *Let $\{\kappa_i\}$ be the set of stable poles of $H(q)$ and stable zeros of $G(q)$, let $\{\sigma_i\}$ be the set of unstable zeros of $G(q)$ and let the all-pass transfer function $P(q)$ used for the construction of the orthonormal basis functions have poles ρ_j, $j = 1, \cdots, n_p$. Define*

$$\lambda := \max_i \prod_{j=1}^{n_p} \left| \frac{\nu_i - \rho_j}{1 - \nu_i \rho_j} \right|, \ \nu_i = \kappa_i \cup \sigma_i^{-1}$$

and denote

$$F(q,\theta) = D_f + \sum_{k=1}^{n} L_{k-1} V_{k-1}(q), \ \theta = [D_f, L_0^T, \cdots, L_{n-1}^T].$$

Then there exists a finite constant $c \in \mathbf{R}$ and any $\eta \in \mathbf{R}$, $\lambda < \eta < 1$ such that

$$\|H(q) - F(q,\theta)G(q)\|_2 \leq c \frac{\eta^{n+1}}{\sqrt{1-\eta^2}}$$

Proof: Let $F_{opt}(q)$ be the solution to (5.21), where $F_{opt}(q)$ is freely parametrized, e.g. F_{opt} is not restricted to be an affine orthonormal FIR. Then it is straightforward to show that (5.21) is an *LQG* control problem that minimizes

$$\sum_{t=1}^{\infty} z^T(t) z(t), z(t) = H(q)d(t) + u(t),$$
$$u(t) = F_{opt}(q)G(q)d(t)$$

in which only the variance of the control signal $u(t)$ is being penalized. For such a minimum variance controller it was shown in [4] the zeros of $G(q)$ should be mapped into the unit circle in order to obtain a stable minimum variance controller. As a result, the poles of $F_{opt}(q)$ will include all stable poles of $H(q)$, all stable zeros of $G(q)$, and all unstable zeros of $G(q)$ which are mapped into the unit circle, e.g. $\nu_i = \kappa_i \cup \sigma_i^{-1}$. Therefore, $\min_\theta \|H(q) - F(q,\theta)G(q)\|_2$ is equivalent to $\min_\theta \|F_{opt}(q) - F(q,\theta)\|_2$. For computation of the upper bound of model error $\|F_{opt} - F(q,\theta)\|_2$, one is referred to the work of [34].

The above proposition shows that if the poles $\{\rho_j\}$ of $P(q)$ approach the poles $\{\nu_i\}$, then $\lambda = 0$ and the upper bound of model error $\|H(q) - F(q,\theta)G(q)\|_2$ will decrease drastically. Therefore, from Proposition 5.4.1 it can be observed that an appropriate selection of the poles of the all-pass function will have an important contribution to the reduction of the model error $\|H(q) - F(q,\theta)G(q)\|_2$. This is due to the improvement in the convergence rate of the coefficient $\{L_{k-1}\}_{k=1,\ldots,n}$ in the generalized FIR filter expansion.

5.5 Case study

For the case study, consider a 4th order system $H(q)$ and a 2nd order system $G(q)$

$$\begin{gathered} H(q) = \frac{q^2 - 1.2q + 0.4}{q^2 - 1.8q + 0.8} \cdot \frac{q^2 - q + 0.5}{q^2 - q + 0.89}, \\ \text{with poles at } 0.9 \pm 0.3i,\ 0.5 \pm 0.8i \\ G(q) = \frac{q^2 - 1q + 1.94}{q^2 - q + 0.74}, \\ \text{with poles at } 0.5 \pm 0.7i, \text{zeros at } 0.5 \pm 1.3i \\ \text{sampling time } \Delta T = 1 \end{gathered} \tag{5.22}$$

The objective is to find optimal ORTFIR models

$$\begin{gathered} F(q,\theta) = D_f + \textstyle\sum_{k=1}^{n} L_{k-1} V_{k-1}(q), \\ \theta = [D_f, L_0^T, \cdots, L_{n-1}^T] \end{gathered} \tag{5.23}$$

with a limited number of parameters, such that

$$\|H(q) - F(q,\theta)G(q)\|_2 \tag{5.24}$$

is being minimized. Using H_2 optimal control design technique, an optimal $F_{opt}(q)$ can be obtained as

$$F_{opt}(q) = \frac{b_5q^5 + b_4q^4 + b_3q^3 + b_2q^2 + b_1q + b_0}{q^6 + a_5q^5 + a_4q^4 + a_3q^3 + a_2q^2 + a_1q + a_0}$$

where $b_0 = -0.08646$, $b_1 = 0.2046$, $b_2 = -0.2522$, $b_3 = 0.1443$, $b_4 = -0.0267$, $b_5 = 0.004005$. $a_0 = 0.4129$, $a_1 = -1.7032$, $a_2 = 3.941$, $a_3 = -5.796$, $a_4 = 5.549$, $a_5 = -3.315$. The poles of $F_{opt}(q)$ are $q_1, \bar{q}_1 = 0.9 \pm 0.3i$, $q_2, \bar{q}_2 = 0.5 \pm 0.8i$ and $q_3, \bar{q}_3 = 0.2577 \pm 0.6701i$. With $F_{opt}(q)$ in place, the lower bound of model error can be computed as $\|H(q) - F_{opt}(q)G(q)\|_2 = 1.2243$. Since $F_{opt}(q)$ is computed with a feed-through matrix $D_f = 0$, the feed-through term D_f in (5.23) also be set to 0 for comparison purposes.

For the sake of illustration in this case study, it is assumed only the first two (conjugate) poles $\{q_1, \bar{q}_1, q_2, \bar{q}_2\}$ of the model $F_{opt}(q)$ are known for the construction of basis functions $V_k(q)$. Actually, these poles are also the poles of $H(q)$. Obviously, if all pole locations of $F_{opt}(q)$ were known beforehand, n can be set to $n = 1$ as only one unique coefficient L_0 will be able to represent $F_{opt}(q)$. However, in this case incomplete knowledge of the pole locations of $F_{opt}(q)$ is assumed, requiring theoretically an infinite number of parameters for an accurate representation of $F_{opt}(q)$, increasing the McMillan degree of $F(q)$. To make a fair comparison between the usage of different basis functions, n is limited such that $F_{opt}(q)$ will have a McMillan degree that is less than or equal to 20.

The quality of the approximation measured by (5.24) is compared for different sets of basis functions. The first set of basis function consists of the standard orthonormal FIR expansion as presented in Section 5.2 and based on the all-pass function $P(q)$ that uses the knowledge of the two (conjugate) poles $q_1, \bar{q}_1$ and $q_2, \bar{q}_2$ of $F_{opt}(q)$. Since $P(q)$ is a fourth order all-pass function, the parametrization of

the first orthonormal FIR expansion $F_1(q)$ is given by

$$F_1(q) = \sum_{k=1}^{5} L_{k-1} V_{k-1}(q),\ V_{k-1}(q) = \Phi_0(q) P(q)^{k-1} \tag{5.25}$$

where $\Phi_0(q) = (qI - A)^{-1}B$ in which (A, B) are computed from an input balanced state-space realization of $P(q)$. With the fourth order all-pass function $P(q)$, it can be seen from (5.25) that n has been limited to $n = 5$ to ensure that $F(q)$ has a McMillan degree that is less than or equal to 20.

Instead of a single basis function $V_k(q)$, an alternative approach would be to create mutually orthonormal basis functions on the basis of the two all-pass functions $P_1(q)$ and $P_2(q)$ that separate the knowledge of the (conjugate) poles location at $q_1, \bar{q}_1$ and $q_2, \bar{q}_2$. On the basis of the two all-pass functions $P_1(q)$ and $P_2(q)$, following the parametrization given in Proposition 5.2.3, the following orthonormal FIR $F_m(q)$ is considered:

$$\begin{aligned} F_m(q) &= \sum_{k=1}^{10} L_{k-1} V_{k-1}(q) \text{ where} \\ V_{k-1}(q) &= \begin{cases} \Phi_1(q) P_1(q)^{k-1},\ k = 1, \ldots, m \\ \\ \Phi_2(q) P_1(q)^m P_2(q)^{k-m-1},\ k = 1+m, \ldots, 10 \end{cases} \end{aligned} \tag{5.26}$$

where $\Phi_1(q) = (qI - A_1)^{-1}B_1$ in which (A_1, B_1) are computed from an input balanced state-space realization of $P_1(q)$ and $\Phi_2(q) = (qI - A_2)^{-1}B_2$ in which (A_2, B_2) are computed from an input balanced state-space realization of $P_2(q)$.

In case the orthonomal basis functions are simply set to $V_k(q) = q^{-k}$ to obtain a 20th order FIR model $F_{fir}(q, \theta)$, then the model error becomes $\|H(q) - F_{fir}G(q)\|_2 = 1.2586$. With the 4th order all-pass function $P(q)$ and the construction of the orthonormal basis functions in (5.25), the computations of 5 coefficients L_i for a 20th ORTFIR model $F_1(q)$ reduces the model error to $\|H(q) - F_1(q)G(q)\|_2 = 1.2257$. This illustrates that a generalized FIR filter can provide much better approximation results than a conventional FIR filter.

Different combinations m of basis functions in the mutual orthonormal basis functions in (5.26) to construct $F_m(q, \theta)$ will give different model error results. As

a final comparison for this case study, the modeling error of $\|H(q)-F_m(q,\theta)G(q)\|_2$ is calculated and shown in Fig. 5.4

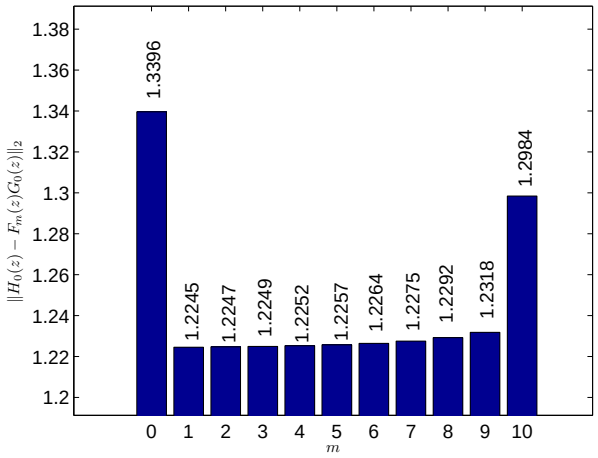

Figure 5.4. Comparison of model error using 20th order ORTFIR filter $F_m(q,\theta)$ with different combinations m of mutual orthonormal basis functions

From Fig. 5.4, the following observations can be made. Firstly, if only the 2nd order $P_1(q)$, $m = 10$ or $P_2(q)$, $m = 0$ all-pass function is used to create orthonormal basis functions, the approximation result is worse than choosing 4th order basis function $P(q)$ or any linear combination of $P_1(q)$ and $P_2(q)$ as all-pass functions. Hence. higher order orthonormal basis functions which include more poles of the dynamic system to be approximated is preferable to reach an improvement in model approximation.

Secondly, the smallest model error is obtained when $m = 1$. This implies that the quality of the approximation is not only related to the location of the poles of the basis function, but is also determined by the number of coefficients used for building the series expansion on the basis of a specific basis function. In this case study, only two poles of F_{opt} are used to create an orthonormal basis. A possible explanation for the approximation results lies in the location of the poles, as indicated by Proposition 5.4.1. Since the poles $q_3, \bar{q}_3$ are closer to $q_2, \bar{q}_2$ than to

$q_1, \bar{q}_1$ less coefficients ($m = 1$) are needed to obtain a better approximation.

5.6 H_∞ norm model matching problem

Let $H(q)$ and $G(q)$ are stable proper transfer functions, the H_∞ norm model matching problem is to find a stable transfer function $F(q)$ to minimize the H_∞ norm of $H(q) - F(q)G(q)$. The H_∞ norm model matching problem can be interpreted as this: $H(q)$ is a model, $G(q)$ is a plant, and $F(q)$ is a controller to be designed so that $F(q)G(q)$ can approximate $H(q)$. The contoller $F(q)$ can be designed with the use of generalized FIR filter

$$\begin{aligned} F(q,\theta) &= D_f + \textstyle\sum_{k=1}^{n} L_{k-1} V_{k-1}(q), \\ \theta &= [D_f, L_0^T, \cdots, L_{n-1}^T] \end{aligned} \tag{5.27}$$

to solve a model matching problem with the form of H_∞ norm

$$\min_{\theta} \|H(q) - F(q,\theta)G(q)\|_\infty \tag{5.28}$$

Given the state space realization $(A, B, C(\theta), D(\theta))$ of $H(q) - F(q,\theta)G(q)$ in (5.16), the minimization of $\|H(q) - F(q,\theta)G(q)\|_\infty$ can be computed by using Linear Matrix Inequalities (LMIs), which is given in the following proposition.

Proposition 5.6.1. *Given the system matrix* $\begin{bmatrix} A & B \\ C(\theta) & D(\theta) \end{bmatrix}$ *of a discrete time system* $\bar{H}(q,\theta) := H(q) - F(q,\theta)G(q)$, $\|\bar{H}(q,\theta)\|_\infty < \gamma$ *is equivalent to there exists a positive definite symmetric matrix* $P > 0$, *such that*

$$\begin{bmatrix} A^T P A - P & A^T P B & C(\theta)^T \\ B^T P A & B^T P B - \gamma^2 I & D(\theta)^T \\ C(\theta) & D(\theta) & I \end{bmatrix} < 0 \tag{5.29}$$

where $C(\theta)$ *and* $D(\theta)$ *can be written as*

$$C(\theta) = \begin{bmatrix} C_h & 0 & 0 \end{bmatrix} - \theta C, \; D(\theta) = D_h - \theta D,$$
$$C := \begin{bmatrix} 0 & C_g & 0 \\ 0 & 0 & I \end{bmatrix}, \; D := \begin{bmatrix} D_g \\ 0 \end{bmatrix}$$

and

$$\theta = \begin{bmatrix} D_f & C_f \end{bmatrix}$$

Proof: It is well known that $\|\bar{H}(q,\theta)\|_\infty < \gamma$ is equivalent to there exists a positive definite matrix P such that

$$A^TPA - P + C^TC - (A^TPB + C^TD)(B^TPB + D^TD - \gamma^2 I)^{-1}(B^TPA + D^TC) < 0 \tag{5.30}$$

Perform schur complement for (5.30), then we can obtain (5.29).

From Proposition 5.6, it is easy to know that H_∞ norm model matching using the orthonormal basis function can be transferred to a standard LMI problem which is easy to be solved.

5.7 Conclusions

In this chapter an analytic solution for a H_2-norm based model matching problem, typically found in problems associated to feedforward active noise control design, is formulated on the basis of an affine model structure parametrized by generalized orthonormal basis functions. The analytic solution is formulated in terms of Semidefinite Programming problem to a quadratic optimization problem that can also be generalized to H_∞-norm specifications. Exploiting the structure of the quadratic optimization problem, an analytic solution is presented on the basis of a weighted least-squares optimization that can be solved reliably even for a relatively large model approximation order.

A model error bound for the model approximation is formulated and using the analytic solution, different orthonormal basis functions for the construction of generalized FIR filter are compared in a case study. The results show that during the construction of the orthonormal basis functions, a high order orthonormal basis function with a small number of coefficients is preferred over a low order orthonormal basis functions with a larger number of parameters.

Chapter 6

Feedforward Active Noise Control

6.1 Basic principles of feedforward active noise control

Active noise control is based on either feedforward control or feedback control. Feedforward control can be classified into broad-band feedforward control system and narrow-band feedforward control system. In this chapter, only a broad-band feedforward active noise control system will be introduced. Usually in a feedforward control system, a reference sensor, a secondary source, a control actuator and an error sensor will be essential to obtain a good active noise control performance. This standard feedforward ANC system can be exemplified by a single channel airduct ANC shown in Fig. 6.1

In Fig. 6.1, the reference signal is picked by the reference microphone and is processed by a ANC system to generate a control signal to drive the control loudspeaker to create an anti-phase signal to cancel the primary noise. The error microphone is used to monitor the performance of the ANC system. The objective of the feedforward controller is to minimize the measured acoustic noise by creating a secondary path noise to cancel the primary noise.

Fig. 6.2 shows the block diagram of the single channel feedforward ANC system

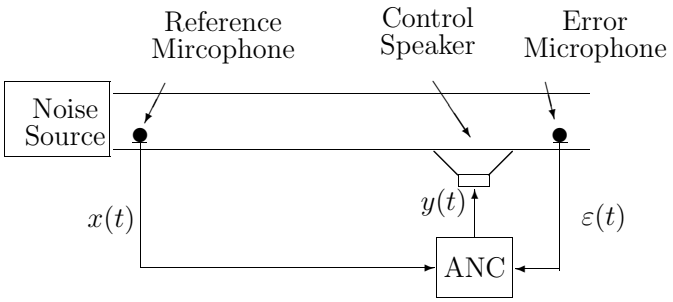

Figure 6.1. Active noise control system in an airduct

setup in Fig. 6.1. Following this block diagram, dynamic relationship between signals in the ANC system are characterized by discrete time transfer functions, with $qx(t) = x(t+1)$ indicates a unit step delay. The primary path $H_0(q)$ models the propagation path between the reference microphone and error microphone, and $G_0(q)$ is the secondary path between the control speaker and the error microphone.

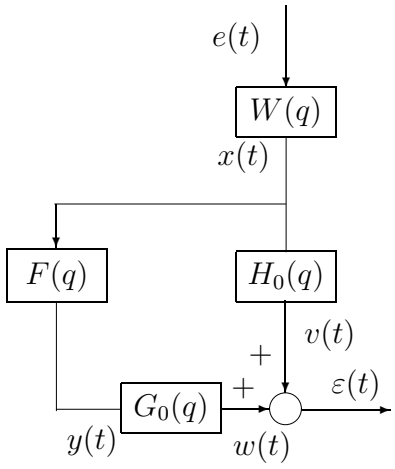

Figure 6.2. Block diagram of ANC system with feedforward

For the analysis we assume in this section that all transfer functions in Fig. 6.2

are stable and known. The error microphone signal $e(t)$ can be described by

$$\varepsilon(t) = [H_0(q) + G_0(q)F(q)]\, x(t), \quad x(t) = W(q)e(t) \tag{6.1}$$

In case the transfer functions in Fig. 6.2 are known, perfect feedforward noise cancellation can be obtained in case

$$F(q) = -\frac{H_0(q)}{G_0(q)} \tag{6.2}$$

and can be implemented as a feedforward compensator in case $F(q)$ is a stable and causal transfer function.

In general, the filter $F(q)$ in (6.2) is not a causal or stable filter due to the dynamics of $G_0(q)$ and $H_0(q)$ that dictate the solution of the feedforward compensator. Therefore, an optimal approximation has to be made to find the best causal and stable feedforward compensator. With (6.1) the variance of the discrete time error signal $e(t)$ is given by

$$\frac{\lambda}{2\pi}\int_{-\pi}^{\pi} \left|H_0(\mathrm{e}^{j\omega}) + G_0(\mathrm{e}^{j\omega})F(\mathrm{e}^{j\omega})\right|^2 \left|W(\mathrm{e}^{j\omega})\right|^2 \mathrm{d}\omega$$

where λ denotes the variance of $e(t)$. In case variance minimization of the error microphone signal $\varepsilon(t)$ is required for ANC, the optimal feedforward controller is found by the minimization

$$\begin{gathered} \min_\theta \textstyle\int_{\omega=-\pi}^{\omega=\pi} |L(\mathrm{e}^{j\omega},\theta)|^2 \mathrm{d}\omega := \min_\theta \|L(q,\theta)\|_2, \\ L(q,\theta) = [H_0(q) + G_0(q)F(q,\theta)]\, W(q) \end{gathered} \tag{6.3}$$

where the parametrized filter $F(q,\theta)$ is required to be a causal and stable filter. The minimization in (6.3) is standard 2-norm based feedback control and model matching problems [5, 40] that can be solved in case the dynamics of $W(q)$, $G_0(q)$ and $H_0(q)$ are known. Actually, the dynamics of $W(q)$ can be obtained automatically via spectrum analysis of $x(t)$, and the dynamics of $G_0(q)$ and $H_0(q)$ can be estimated with the use of closed loop identification techniques. Instead of separately estimating the unknown transfer functions and computing the feedforward controller via an adaptive optimization from (6.3), a direct estimation of the feedforward controller can also be performed.

Defining the signals

$$y(t) := H_0(q)x(t),\ x_f(t) := -G_0(q)x(t) \tag{6.4}$$

(6.1) can be rewritten as

$$\varepsilon(t,\theta) = y(t) - F(q,\theta)x_f(t)$$

for which the minimization

$$\min_{\theta} \frac{1}{N}\sum_{t=1}^{N} \varepsilon(t,\theta) \tag{6.5}$$

to compute the optimal feedforward filter $F(q,\theta)$ is a standard output error (OE) minimization problem in a prediction error framework [59]. Using the fact that the input signal $x(t)$ satisfies $\|x\|_2 = |W(q)|^2\lambda$, the minimization of (6.5) for $\lim_{N\to\infty}$ can be rewritten into the frequency domain expression

$$\min_{\theta} \int_{\pi}^{-\pi} |H_0(\mathrm{e}^{j\omega}) + G_0(\mathrm{e}^{j\omega})F(\mathrm{e}^{j\omega},\theta)|^2 |W(\mathrm{e}^{j\omega})|^2 d\omega \tag{6.6}$$

using Parceval's theorem [59]. Due to the equivalency of (6.6) and (6.3), the same 2-norm objectives for the computation of the optimal feedforward compensator are used.

From above analysis, we know that the design of a feedforward controller $F(q,\theta)$ can be seen as a system identification problem and can be solved with standard open loop identification technique. However, as mentioned before, because the characteristics of the acoustic noise and the environment may be time varying, the frequency content, amplitude, phase, and sound velocity of the undesired noise are possible nonstationary, an ANC system with adaptive filter would be required to accommodate with these possible variations. The adaptive filter for ANC application is presented in Fig. 6.3.

From Fig. 6.3, it can be observed that the coherence between the error microphone signal $\varepsilon(t)$ and the reference microphone signal $x(t)$ determines the performance of the adaptive feedforward ANC.

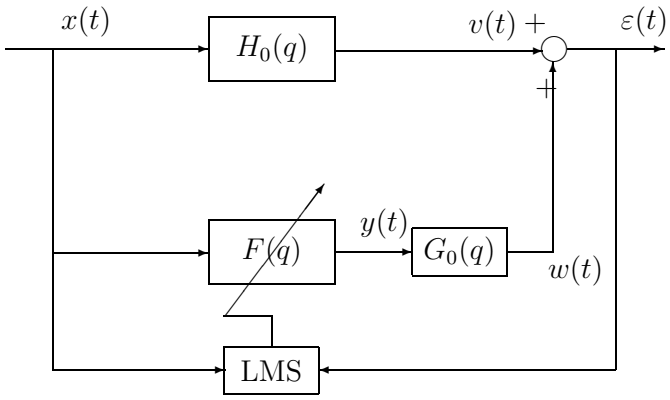

Figure 6.3. Block diagram of adaptive feedforward ANC system

The coherence function in the frequency domain between two stationary random processes $v(t)$ and $x(t)$ is defined as

$$\gamma_{vx}(\omega) = \frac{S_{vx}(\omega)}{\sqrt{S_{vv}(\omega)S_{xx}(\omega)}} \tag{6.7}$$

where $S_{vx}(\omega)$ is the cross spectrum between $v(t)$ and $x(t)$, $S_{vv}(\omega)$ and $S_{xx}(\omega)$ are the auto spectrum of $v(t)$ and $x(t)$, respectively.

The coherence function $\gamma_{vx}(\omega)$ is a dimensionless function of frequency having only the real part and values in the range 0 to 1.

The spectrum of error microphone signal $\varepsilon(t)$ is given by

$$\begin{aligned} S_{\varepsilon\varepsilon}(\omega) &= E\left|V(\omega) + G_0(\omega)F(\omega)X(\omega)\right|^2 \\ &= S_{vv}(\omega) + F^*(\omega)G_0^*(\omega)S_{vx}(\omega) + G_0(\omega)F(\omega)S_{vx}^*(\omega) + \\ &\quad + \left|G_0(\omega)F(\omega)\right|^2 S_{xx}(\omega) \\ &= \left[1 - \frac{|S_{vx}(\omega)|^2}{S_{vv}(\omega)S_{xx}(\omega)}\right] S_{vv}(\omega) + \left|G_0(\omega)F(\omega) + \frac{S_{vx}(\omega)}{S_{xx}(\omega)}\right|^2 S_{xx}(\omega) \end{aligned} \tag{6.8}$$

Define

$$|\gamma_{vx}(\omega)|^2 = \frac{|S_{vx}(\omega)|^2}{S_{vv}(\omega)S_{xx}(\omega)} \tag{6.9}$$

and with the optimal filter $F_o(\omega)$ that minimizes (6.8) given by

$$F_o(\omega) = -G_0^{-1}(\omega)\frac{S_{vx}(\omega)}{S_{xx}(\omega)} = -G_0^{-1}(\omega)H_0(\omega)$$

which is the same as (6.2).

Then (6.8) becomes

$$S_{\varepsilon\varepsilon}(\omega) = [1 - |\gamma_{vx}(\omega)|^2]S_{vv}(\omega) \tag{6.10}$$

(6.10) shows that the performance of the adaptive feedforward ANC system is dependent on the coherence between $v(t)$ and $x(t)$. In order to obtain a good feedforward ANC performance, it is necessary to have a very high coherence at frequencies for which there is significant disturbance energy, so $v(t)$ and $x(t)$ should have a very good correlation, i.e $\gamma_{vx}(\omega) \approx 1$.

In general, the adaptive filter $F(q)$ in Fig. 6.3 can be realized with finite impulse response (FIR) structure and infinite impulse response (IIR) structure. Because the FIR filter incorporates only zeros, always stable and provides a linear phase response, it is a more popular adaptive filter widely used in the adaptive control. The structure of FIR filter is depicted in Fig. 6.4.

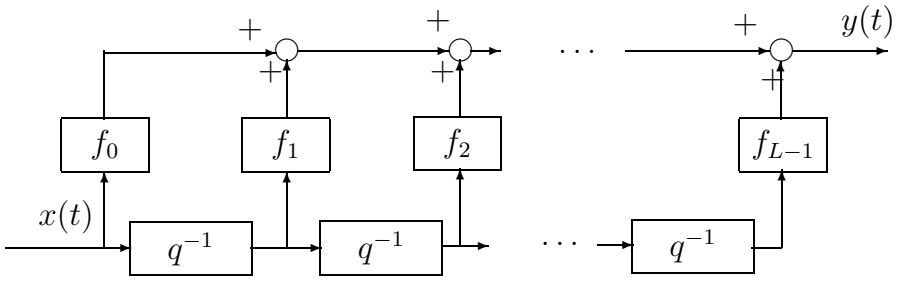

Figure 6.4. Block diagram of digital FIR filter

From Fig. 6.4, It can be obtained that by using FIR filter $F(q)$ can be presented as

$$F(q) = \sum_{k=0}^{L-1} f_k q^{-k} \tag{6.11}$$

Given a set of L filter coefficients $f_l(t)$, $l = 0, 1, \ldots, L-1$, and a data sequences $x(t), x(t-1), \ldots, x(t-L+1)$, the output signal $y(t)$ constructed by a

FIR structure can be computed as

$$y(t) = \sum_{l=0}^{L-1} f_l(t)x(t-l) \tag{6.12}$$

where the filter coefficients f_l are time-varying and updated by the adaptive algorithms.

Define the reference vector at time t as

$$\mathbf{x}(t) = [x(t) \quad x(t-1) \quad \dots \quad x(t-L+1)]^T$$

and the weight vector at time t as

$$\mathbf{f}(t) = [f_0(t) \quad f_1(t) \quad \dots \quad f_{L-1}(t)]^T$$

Then the output signal $y(t)$ in (6.12) can be expressed by

$$y(t) = \mathbf{f}^T(t)\mathbf{x}(t) \tag{6.13}$$

$$= \mathbf{x}^T(t)\mathbf{f}(t) \tag{6.14}$$

The error signal $e(t)$ then can be computed as

$$\varepsilon(t) = v(t) + g_0(t) * y(t) = v(t) + g_0(t) * [\mathbf{f}^T(t)\mathbf{x}(t)] \tag{6.15}$$

where $g_0(t)$ is the impulse response of secondary path $G_0(q)$ at time t, $*$ is linear convolution.

The objective is to determine the weight vector so that the mean square value of the error signal is minimized by using adaptive algorithms.

6.2 Filtered-X LMS algorithm

Using the standard LMS algorithm when the secondary path transfer function following the controller will cause instability [18], this is because the error signal is not correctly "aligned" in time with the reference signal due to the presence of

$G_0(q)$ [47]. Filter-X LMS algorithm which is first derived by [89] is an alternative form of the standard LMS algorithm for ANC application to ensure the convergence when there has a transfer function in the second path following the adaptive filter.

Generally, in order to minimize the instantaneous squared error value of the error signal, $\hat{\xi}(t) = \varepsilon^2(t)$, a most widely used method to achieve this is the stochastic gradient, or LMS algorithm. By using this method, the coefficient vector is updated in the negative gradient direction with step size μ which is given by

$$\mathbf{f}(t+1) = \mathbf{f}(t) - \frac{\mu}{2}\nabla\hat{\xi}(t) \tag{6.16}$$

where $\nabla\hat{\xi}(t)$ is an instantaneous estimate of the mean square error (MSE) gradient at time t, and can be depicted as

$$\nabla\hat{\xi}(t) = \nabla\varepsilon^2(t) = 2\nabla\varepsilon(t)\varepsilon(t) \tag{6.17}$$

From (6.15) we get

$$\nabla\varepsilon(t) = g(t) * \mathbf{x}(t) \tag{6.18}$$

Define

$$\mathbf{x}_f(t) = g(t) * \mathbf{x}(t) \tag{6.19}$$

Then (6.17) can be rewritten as

$$\nabla\hat{\xi}(t) = 2\mathbf{x}_f(t)\varepsilon(t) \tag{6.20}$$

where $\mathbf{x}_f(t) = [x_f(t) \quad x_f(t-1) \quad \dots \quad x_f(t-L+1)]^T$ and $x_f(t) = g(t) * x(t)$

Substitute (6.20) into (6.16), then the FXLMS algorithm can be obtained

$$\mathbf{f}(t+1) = \mathbf{f}(t) - \mu\mathbf{x}_f(t)\varepsilon(t) \tag{6.21}$$

In practical ANC applications, the secondary path $G_0(q)$ is unknown and it must be replaced by a model $G(q)$ in order to utilize the FXLMS algorithm. Fortunately, the model $G(q)$ can be easily estimated with system identification technique. Therefore, the filtered reference signal is generated by passing the reference

signal through the estimated model $G(q)$ of the second path $G_0(q)$.

$$\mathbf{x}_f(t) = g(t) * \mathbf{x}(t) \tag{6.22}$$

where $g(t)$ is the estimated impulse response of the secondary path model $G(q)$.

The block diagram of feedforward ANC system using the FXLMS algorithm is depicted in Fig. 6.5

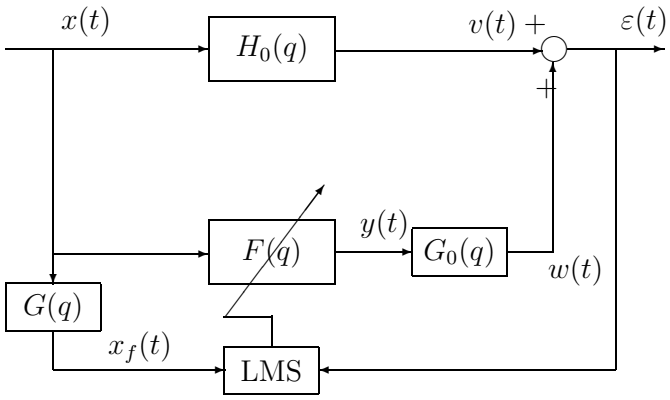

Figure 6.5. Block diagram of feedforward ANC system using FXLMS algorithm

The FXLMS algorithm is not sensitive to the model errors in the estimate of $G_0(q)$ by $G(q)$. In [63], the analysis shows that within the limit of slow adaptation, the algorithm will converge with nearly 90° of phase error between $G_0(q)$ and $G(q)$. Therefore, an offline modeling $G(q)$ can be used to instead $G_0(q)$ for most ANC applications.

The step size μ in (6.16) and (6.21) is difficult to determine in real applications. Improper selection of μ might make the convergence speed unnecessarily slow or introduce large excess mean square error. If the signal is non-stationary and real time tracking capability is crucial for a given application, then a large μ should be selected. If the signal is stationary and convergence rate is not important, a small μ should be chosen to achieve a better performance in steady state. In some

applications, usually a larger μ is used at the beginning of the operation for a faster initial convergence, then a smaller μ is used to achieve a better steady-state performance.

The maximum step size that can be used in the FXLMS algorithm is approximated in [19] as

$$\mu_{max} = \frac{1}{P_{x_f}(L+\Delta)} \tag{6.23}$$

where $P_{x_f} = E[x_f^2(t)]$ is the power of the filtered reference signal $x_f(t)$, and Δ is the number of samples corresponding to the overall delay in the second path transfer function $G_0(q)$. From (6.23), it can be observed that the delay in the secondary path influences the dynamic response of the ANC system by reducing the maximum step size of the FXLMS algorithm.

6.3 Recursive least square algorithm for ANC

6.3.1 Recursive least square algorithm

The recursive least square (RLS) algorithm can be used with an adaptive FIR filter to provide faster convergence and smaller steady-state error than the FXLMS algorithm. In this section, the detail of RLS algorithm will be discussed.

To derive the RLS algorithm, we assume that the weight vector $\mathbf{f}(t)$ is constant during the time interval $(1, t)$. The error signal at time i can be described as

$$\varepsilon(i) = v(i) - \mathbf{f}^T(t)\mathbf{x}(i), \quad 1 \leqslant i \leqslant t \tag{6.24}$$

where

$$\mathbf{f}(t) = [f_0(t) \quad f_1(t) \ldots \quad f_{L-1}(t)]^T$$

is the current weight vector of the Lth-order adaptive filter and

$$\mathbf{x}(i) = [x(i) \quad x(i-1) \quad \ldots \quad x(i-L+1)]^T$$

is the $L \times 1$ reference signal vector at time i.

The cost function at time t is expressed by

$$\mathrm{J}(t) = \sum_{i=1}^{t} \lambda^{t-i} e^2(i) \tag{6.25}$$

where $0 \leqslant \lambda \leqslant 1$ is a forgetting factor, which is used to weight recent data more heavily in order to accommodate nonstationary signals.

Substituting (6.24) into (6.25), we can get

$$\mathrm{J}(t) = \sum_{i=1}^{t} \lambda^{t-i} v^2(i) - 2\mathbf{f}^T(t) \left[\sum_{i=1}^{t} \lambda^{t-i} v(i)\mathbf{x}(i) \right] + \mathbf{f}^T(t) \left[\sum_{i=1}^{t} \lambda^{t-i} \mathbf{x}(i)\mathbf{x}^T(i) \right] \mathbf{f}(t) \tag{6.26}$$

Define the autocorrelation matrix as

$$\mathbf{R}(t) = \sum_{i=1}^{t} \lambda^{t-i} \mathbf{x}(i)\mathbf{x}^T(i) \tag{6.27}$$

and define the cross correlation vector as

$$\mathbf{p}(t) = \sum_{i=1}^{t} \lambda^{t-i} v(i)\mathbf{x}(i) \tag{6.28}$$

Then (6.26) can be written as

$$\mathrm{J}(t) = \sum_{i=1}^{t} \lambda^{t-i} v^2(i) - 2\mathbf{p}^T(t)\mathbf{f}(t) + \mathbf{f}^T(t)\mathbf{R}(t)\mathbf{f}(t) \tag{6.29}$$

$\mathrm{J}(t)$ can be minimized with respect to $\mathbf{f}(t)$ at time t by setting the gradient of $\mathrm{J}(t)$ respect to $\mathbf{f}(t)$ to zero, this will yield

$$\mathbf{R}(t)\mathbf{f}^o(t) = \mathbf{p}(t) \tag{6.30}$$

where $\mathbf{f}^o(t)$ is the optimum weight vector at time t that minimizes the weighted sum of squared errors $\xi(t)$. If the inverse matrix $\mathbf{R}^{-1}(t)$ exists, then a unique solution for $\mathbf{f}^o(t)$ can be obtained by solving equation (6.30).

Because the time index t could increase to a very large value in real-time processing, computation of $\mathbf{R}(t)$ and $\mathbf{p}(t)$ will become very difficult. This problem

can be solved by using a recursive algorithm, which computes $\mathbf{R}(t)$ and $\mathbf{p}(t)$ from previous $\mathbf{R}(t-1)$ and $\mathbf{p}(t-1)$.

Isolating the term corresponding to $i = t$ from the rest of the summation on the right hand of (6.27), it yields

$$\begin{aligned}\mathbf{R}(t) &= \sum_{i=1}^{t-1} \lambda^{t-i}\mathbf{x}(i)\mathbf{x}^T(i) + \lambda^0\mathbf{x}(t)\mathbf{x}^T(t) \\ &= \lambda \sum_{i=1}^{t-1} \lambda^{(t-1)-i}\mathbf{x}(i)\mathbf{x}^T(i) + \mathbf{x}(t)\mathbf{x}^T(t) \\ &= \lambda\mathbf{R}(t-1) + \mathbf{x}(t)\mathbf{x}^T(t) \end{aligned} \tag{6.31}$$

(6.31) shows that the current correlation matrix $\mathbf{R}(t)$ can be obtained recursively from the previous correlation matrix $\mathbf{R}(t-1)$ and the matrix product $\mathbf{x}(t)\mathbf{x}^T(t)$.

Similarly, the recursive update of the cross-correlation vector $\mathbf{p}(t)$ can also be obtained from (6.28), and expressed as

$$\mathbf{p}(t) = \lambda\mathbf{p}(t-1) + v(t)\mathbf{x}(t) \tag{6.32}$$

To compute the least-square estimate $\mathbf{f}^o(t)$ according to (6.30), the inverse of the correlation matrix $\mathbf{R}(t)$ have to be computed. However, the computation of $\mathbf{R}^{-1}(t)$ can be quite time consuming, particularly when the number of coefficients, L is large. Therefore, in practice, we try to avoid computing $\mathbf{R}^{-1}(t)$ directly, instead we apply the matrix inversion lemma to compute the inverse of $\mathbf{R}(t)$ to reduce the computation requirement.

The matrix inversion lemma is given [33] by

$$(\mathbf{A} + \mathbf{BCD})^{-1} = \mathbf{A}^{-1} - \mathbf{A}^{-1}\mathbf{B}(\mathbf{DA}^{-1}\mathbf{B} + \mathbf{C}^{-1})^{-1}\mathbf{DA}^{-1} \tag{6.33}$$

where $\mathbf{A}$, $\mathbf{B}$, $\mathbf{C}$, $\mathbf{D}$ are any dimensionally compatible matrices.

Now, define

$$\mathbf{A} = \lambda \mathbf{R}(t-1) \tag{6.34}$$

$$\mathbf{B} = \mathbf{x}(t) \tag{6.35}$$

$$\mathbf{C} = 1 \tag{6.36}$$

$$\mathbf{D} = \mathbf{x}^T(t) \tag{6.37}$$

$$\tag{6.38}$$

Then (6.31) can be expressed as

$$\begin{aligned} \mathbf{R}(t) &= \lambda \mathbf{R}(t-1) + \mathbf{x}(t)\mathbf{x}^T(t) \\ &= \mathbf{A} + \mathbf{BCD} \end{aligned} \tag{6.39}$$

Therefore, $\mathbf{R}^{-1}(t)$ can be described as

$$\begin{aligned} \mathbf{R}^{-1}(t) &= (\mathbf{A} + \mathbf{BCD})^{-\mathbf{1}} \\ &= \lambda^{-1}\mathbf{R}^{-1}(t-1) - \frac{\lambda^{-2}\mathbf{R}^{-1}(t-1)\mathbf{x}(t)\mathbf{x}^T(t)\mathbf{R}^{-1}(t-1)}{1 + \lambda^{-1}\mathbf{x}^T(t)\mathbf{R}^{-1}(t-1)\mathbf{x}(t)} \end{aligned} \tag{6.40}$$

For notational and computational convenience, define

$$\mathbf{Q}(t) = \mathbf{R}^{-1}(t) \tag{6.41}$$

and

$$\mathbf{k}(t) = \frac{\lambda^{-1}\mathbf{Q}(t-1)\mathbf{x}(t)}{1 + \lambda^{-1}\mathbf{x}^T(t)\mathbf{Q}(t-1)\mathbf{x}(t)} \tag{6.42}$$

(6.40) can be rewritten as

$$\mathbf{Q}(t) = \lambda^{-1}\mathbf{Q}(t-1) - \lambda^{-1}\mathbf{k}(t)\mathbf{x}^T(t)\mathbf{Q}(t-1) \tag{6.43}$$

(6.43) shows that matrix $\mathbf{Q}(t)$ can be computed in a recursive fashion, this will save much computation time.

Rearranging (6.42), we can obtain

$$\begin{aligned} \mathbf{k}(t) &= \lambda^{-1}\mathbf{Q}(t-1)\mathbf{x}(t) - \lambda^{-1}\mathbf{k}(t)\mathbf{x}^T(t)\mathbf{Q}(t-1)\mathbf{x}(t) \\ &= \left[\lambda^{-1}\mathbf{Q}(t-1) - \lambda^{-1}\mathbf{k}(t)\mathbf{x}^T(t)\mathbf{Q}(t-1)\right]\mathbf{x}(t) \\ &= \mathbf{Q}(t)\mathbf{x}(t) \end{aligned} \tag{6.44}$$

Combine (6.30), (6.32) and (6.41), the recursive equation for updating the weight vector is given by

$$\begin{aligned}\mathbf{f}^o(t) &= \mathbf{R}^{-1}(t)\mathbf{p}(t) \\ &= \mathbf{Q}(t)\mathbf{p}(t) \\ &= \mathbf{Q}(t)\left[\lambda\mathbf{p}(t-1) + v(t)\mathbf{x}(t)\right] \\ &= \lambda\mathbf{Q}(t)\mathbf{p}(t-1) + v(t)\mathbf{Q}(t)\mathbf{x}(t) \qquad (6.45)\end{aligned}$$

Substituting (6.43) for $\mathbf{Q}(t)$ in the first term only on the right hand side of (6.45), we can get

$$\begin{aligned}\mathbf{f}^o(t) &= \mathbf{Q}(t-1)\mathbf{p}(t-1) - \mathbf{k}(t)\mathbf{x}^T(t)\mathbf{Q}(t-1)\mathbf{p}(t-1) + v(t)\mathbf{Q}(t)\mathbf{x}(t) \qquad (6.46)\\ &= \mathbf{f}^o(t-1) - \mathbf{k}(t)\mathbf{x}^T(t)\mathbf{f}^o(t-1) + v(n)\mathbf{k}(t) \qquad (6.47)\\ &= \mathbf{f}^o(t-1) + \mathbf{k}(t)\left[v(t) - \mathbf{f}^{oT}(t-1)\mathbf{x}(t)\right] \qquad (6.48)\\ &= \mathbf{f}^o(t-1) + \mathbf{k}(t)\xi(t) \qquad (6.49)\end{aligned}$$

Here,

$$\xi(t) = v(t) - \mathbf{f}^{oT}(t-1)\mathbf{x}(t)$$

is the a priori estimation error. The inner product of $\mathbf{f}^{oT}(t-1)\mathbf{x}(t)$ represents an estimate of the desired response $v(t)$, based on the previous weight vector that was made at time $t-1$.

Therefore, the RLS algorithm is thus derived and summarized as follows.

First, initialize the algorithm by setting

$$\begin{aligned}\mathbf{f}^o(0) &= \mathbf{0} \\ \mathbf{Q}(0) &= \delta^{-1}\mathbf{I}\end{aligned}$$

where

$$\delta = \begin{cases} small\, positive\, constant\, for\, high\, signal\, noise\, ratio\, (SNR) \\ large\, positive\, constant\, for\, low\, SNR \end{cases} \qquad (6.50)$$

Then, compute the gain vector $\mathbf{k}(t)$ and the weighting vector $\mathbf{f}^o(t)$

$$\pi(t) = \mathbf{Q}(t-1)\mathbf{x}(t) \tag{6.51}$$

$$\mathbf{k}(t) = \frac{\pi(t)}{\lambda + \mathbf{x}^T(t)\pi(t)} \tag{6.52}$$

$$\xi(t) = v(t) - \mathbf{f}^{oT}(t-1)\mathbf{x}(t) \tag{6.53}$$

$$\mathbf{f}^o(t) = \mathbf{f}^o(t-1) + \mathbf{k}(t)\xi(t) \tag{6.54}$$

Finally, update the inverse correlation matrix $\mathbf{Q}(t)$.

$$\mathbf{Q}(t) = \lambda^{-1}\mathbf{Q}(t-1) - \lambda^{-1}\mathbf{k}(t)\mathbf{x}^T(t)\mathbf{Q}(t-1) \tag{6.55}$$

It is well known that RLS algorithm at steady-state operation exhibits a windup problem if the forgetting factor λ remains constant, which will deteriorate the estimation results. As a results, a variable forgetting factor RLS algorithm [50, 94, 76] can be employed to prevent this problem from occurring.

In (6.44), if we assume that $\mathbf{Q}(t) = \mu\mathbf{I}$, then $\mathbf{k}(t) = \mu\mathbf{x}(t)$, and (6.16) becomes

$$\mathbf{f}^o(t) = \mathbf{f}^o(t-1) + \mu\mathbf{x}(t)\xi(t) \tag{6.56}$$

(6.56) is actually the LMS algorithm we described before. Instead of compute $\mathbf{Q}(t)$, the LMS algorithm simply assume that $\mathbf{Q}(t) = \mu\mathbf{I}$, and this assumption greatly simplifies the algorithm. However, the cost is the lose of the performance advantage in convergence rate and steady-state error. The computation of $\mathbf{Q}(t)$ in RLS algorithm results in faster convergence rate and lower residual error than with the LMS algotirhm.

6.3.2 Feedforward ANC using RLS algorithm

Same as the modification of LMS algorithm because of the secondary path $G(q)$ following the feedforward filter $F(q)$ in Section 6.2, the RLS algorithm described

in Section 6.3.1 needs to be modified to ensure the convergence. Therefore, (6.24) is modified as

$$\varepsilon(i) = v(i) - g(t) * [\mathbf{f}^T(t)\mathbf{x}(i)] \tag{6.57}$$

$$= v(i) - \mathbf{f}^T(t)\mathbf{x}_f(i) \tag{6.58}$$

where $g(t)$ is the impulse response of the model $G(q)$ of the secondary path $G_0(q)$, and $\mathbf{x}_f(i) = g(t) * \mathbf{x}(i)$ is the reference signal $\mathbf{x}(t)$ filtered through the secondary path transfer function $G(q)$. The modified RLS algorithm for feedforward ANC can be derived the same procedure as before, the results can be summarized as follows.

$$\mathbf{x}_f(t) = g(t) * \mathbf{x}(t) \tag{6.59}$$

$$\pi(t) = \mathbf{Q}(t-1)\mathbf{x}_f(t) \tag{6.60}$$

$$\mathbf{k}(t) = \frac{\pi(t)}{\lambda + \mathbf{x}_f^T(t)\pi(t)} \tag{6.61}$$

$$\xi(t) = v(t) - \mathbf{f}^{oT}(t-1)\mathbf{x}_f(t) \tag{6.62}$$

$$\mathbf{f}^o(t) = \mathbf{f}^o(t-1) + \mathbf{k}(t)\xi(t) \tag{6.63}$$

$$\mathbf{Q}(t) = \lambda^{-1}\mathbf{Q}(t-1) - \lambda^{-1}\mathbf{k}(t)\mathbf{x}_f^T(t)\mathbf{Q}(t-1) \tag{6.64}$$

6.4 Acoustic coupling effects in ANC

Generally, in an acoustic ANC system illustrated in Fig. 6.1, a reference microphone is used to pick up the reference noise in order to process this noise through an adaptive filter to generate an anti-phase sound to cancel the primary noise. However, the anti-phase sound coming from the control speaker will not only be used to cancel the primary noise, but also radiate upstream to the reference microphone to interfere the reference signal. The coupling of the acoustic wave from the control speaker to the reference microphone is called acoustic coupling or acoustic feedback. A block diagram of a feedforward ANC system that includes the acoustic coupling is shown in Fig. 6.6.

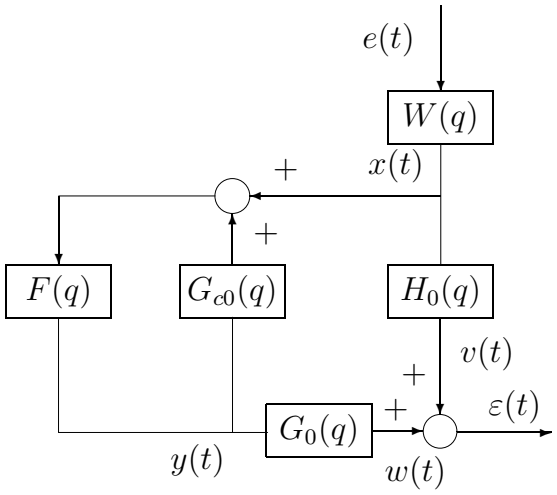

Figure 6.6. Block diagram of feedforward ANC system with acoustic coupling

In Fig. 6.6, $G_{c0}(q)$ is used to indicate the acoustic coupling from control speaker to the reference microphone that creates a positive feedback loop with the feedforward controller $F(q)$. For the analysis we assume in this section that all transfer functions in Fig. 6.2 are stable and known. The error microphone signal $\varepsilon(t)$ can be described by

$$\varepsilon(t) = \left[H_0(q) + \frac{G_0(q)F(q)}{1 - G_{c0}(q)F(q)} \right] x(t), \quad x(t) = W(q)e(t) \tag{6.65}$$

In case the transfer functions in Fig. 6.6 are known, perfect feedforward noise cancellation can be obtained in case

$$F(q) = -\frac{H_0(q)}{G_0(q) - H_0(q)G_{c0}(q)} \tag{6.66}$$

and can be implemented as a feedforward compensator in case $F(q)$ is a stable and causal transfer function.

It should be noted that the optimal feedforward controller derived in (6.66) assumed that there is not measurement noise in the reference input. However, in practice, (6.66) should be modified to include the effects of the measurement noise

[71] as

$$F(q) = -\frac{\alpha H_0(q)}{G_0(q) - \alpha H_0(q) G_{c0}(q)} \tag{6.67}$$

where α is given as

$$\alpha = \frac{SNR}{1 + SNR} \tag{6.68}$$

and SNR is the signal to noise ration at the reference microphone. In this dissertation, we assume that $\alpha = 1$ for analysis convenience.

Refer to Fig. 6.6, a closed loop transfer function $L(q)$ between $x(t)$ and $y(t)$ can be given as

$$L(q) = \frac{F(q)}{1 - G_{c0}(q) F(q)} \tag{6.69}$$

The closed loop transfer function $L(q)$ is unstable if we did not consider the effect of $G_{c0}(q)$ in the design process of the feedforward controller. In order to avoid the negative effects of the acoustic coupling $G_{c0}(q)$, one way is to constrain the effect of acoustic coupling $G_{c0}(q)$ to the feedforward controller such as directional microphones and loudspeakers, feedback neutralization and dual-microphone reference sensing. The other way is to consider the effect of the acoustic coupling $G_{c0}(q)$ during the design process of the feedforward controller $F(q)$ such as using IIR filter and H_2/H_∞ control design algorithm. Some popular methods to be used to design the feedforward control in the case that acoustic coupling is present in the ANC system will be discussed in the next.

6.4.1 Feedback neutralization

In this method, a model $G_c(q)$ of acoustic coupling $G_{c0}(q)$ is used to cancel or neutralize the feedback effect of acoustic coupling within the positive feedback loop. The model $G_c(q)$ can be estimated offline with standard open loop identification technique [59]. This method is exactly the same technique as that in acoustic echo cancellation [77]. A feedforward ANC system with feedback neutralization is illustrate in Fig. 6.7.

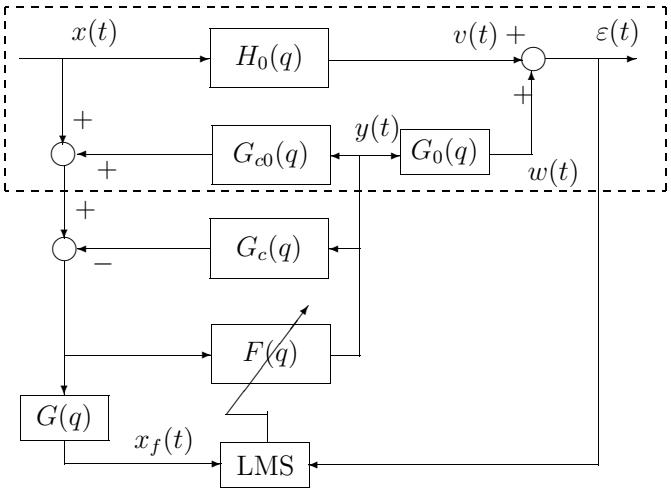

Figure 6.7. Block diagram of a feedforward ANC system with acoustic feedback neutralization

From Fig. 6.7, feedback neutralization filter $G_c(q)$ takes the output $y(t)$ of the $F(q)$ as its input, and the reference signal $x(t)$ is produced to design feedforward controller $F(q)$ by the output of $G_c(q)$ subtracted by the signal measured by the reference microphone.

Refer to Fig. 6.7, the error signal $e(t)$ is given as

$$\begin{aligned}\varepsilon(t) &= H_0(q)x(t) + G_0(q)y(t) \\ &= H_0(q)x(t) + G_0(q)F(q)\left[x(t) + (G_{c0}(q) - G_c(q))y(t)\right] \end{aligned} \tag{6.70}$$

From (6.70) It can be observed that in the case that a perfect model of acoustic coupling can be obtained, that is, $G_c(q) = G_{c0}(q)$, the resulting transfer function from the controller speaker to the reference microphone is zero, which means that the ANC system appears to be no acoustic coupling existing. At this case, the error signal $\varepsilon(t)$ is reduced to

$$\varepsilon(t) = \left[H_0(q) + G_0(q)F(q)\right]x(t) \tag{6.71}$$

which is the same as the standard feedforward ANC system we have discussed in Section 6.1.

Let us discuss the case that $G_c(q) \neq G_{c0}(q)$. Assuming modeling error $G_c(q) - G_{c0}(q) = \Delta$ is bounded by $\|\Delta\|_\infty \leqslant 1/\gamma$ with $\gamma > 0$. Based on the small gain theory [93], robust stability is guaranteed for all $\Delta(q) \in \mathcal{RH}_\infty$ if and only if $\|\Delta(q)F(q)\|_\infty < 1$. That means that if the error Δ is small, the feedforward controller $F(q)$ can be large to obtain a good ANC performance, and even if the modeling error Δ is large, we also can make $F(q)$ small to guarantee the internally stability of the closed loop system. Of course, this will cause the performance of feedforward ANC system getting deteriorated.

6.4.2 IIR filter to compensate the acoustic coupling

FIR filter has been widely used in the adaptive filter algorithm because of the property of linear parameters and linear phase. However, In order to model a very complicated dynamical system such as airduct, FIR filter will need a very high order to incorporate the frequency modes of the airduct, but a small step size μ has to be used for stationary purposes. This results in slow convergence and computational complexity, which is undesirable for some ANC applications. When computation burden becomes a big issue, an IIR filter is a good substitute because the poles of the IIR filter make it possible to obtain the same performance as the FIR filter with a relative much lower order comparing to FIR filter. Another important property of IIR filter is that it could consistent match both poles and zeros of a dynamical system, whereas FIR filter only can give an approximation to the poles because FIR filter only has zeros. Therefore, IIR filter can further minimize the mean square error of the adaptive filter, and this is very important in ANC applications. Except that IIR filter can replace the FIR filter in some feedforward ANC applications, IIR fitler can also used to solve the acoustic coupling problem. In Section 6.4.1, it shows one way to solve the effect of acoustic coupling by use an additional filter to neutralize the negative effect of acoustic coupling. Therefore, the performance of ANC application is largely dependent on the accuracy of this additional filter. In order to overcome this drawback, IIR filter is an alternative

method because it can automatically incorporate the acoustic coupling as a part of the overall plant model [20]. In this method, acoustic coupling was considered as a part of the system and the adaptive IIR filter deal with it directly as part of the problem. A block diagram of an adaptive IIR ANC system is shown in Fig. 6.8.

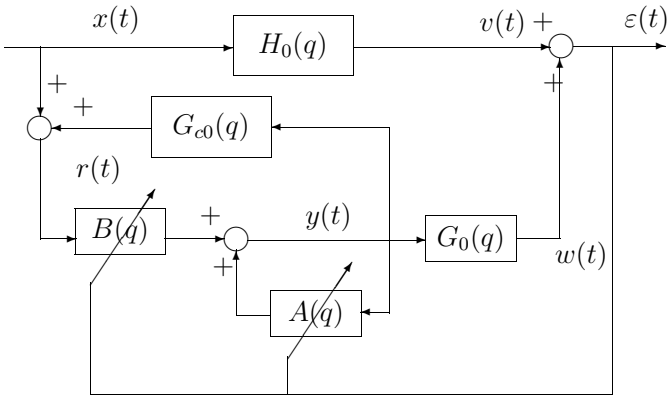

Figure 6.8. Block diagram of a feedforward ANC system with IIR adaptive filter

In Fig. 6.8, the error microphone signal $\varepsilon(t)$ is given as

$$\varepsilon(t) = v(t) + g_0(t) * y(t) \tag{6.72}$$

and the output signal $y(t)$ is

$$y(t) = \mathbf{b}^T(t)\mathbf{r}(t) + \mathbf{a}^T(t)\mathbf{y}^T(t-1) \tag{6.73}$$

where $\mathbf{a}(t)$ is the coefficient vector of $A(q)$ and given as

$$\mathbf{a}(t) = [a_1(t) \quad a_1(t) \quad \dots \quad a_N(t)]^T \tag{6.74}$$

The coefficient vector $\mathbf{b}(t)$ is

$$\mathbf{b}(t) = [b_0(t) \quad b_1(t) \quad \dots \quad a_M(t)]^T \tag{6.75}$$

and $\mathbf{y}(t-1)$ is the output vector delayed by one sample defined as

$$\mathbf{y}(t-1) = [y(t-1) \quad y(t-2) \quad \dots \quad y(t-N)]^T \tag{6.76}$$

Define

$$\mathbf{f}(t) = \begin{bmatrix} \mathbf{b}(t) \\ \mathbf{a}(t) \end{bmatrix} \tag{6.77}$$

and define

$$\mathbf{u}(t) = \begin{bmatrix} \mathbf{r}(t) \\ \mathbf{y}(t-1) \end{bmatrix} \tag{6.78}$$

Then (6.73) can be simplified as

$$y(t) = \mathbf{f}^T(t)\mathbf{u}(t) \tag{6.79}$$

which is a linear regression. (6.72) can be rewritten as

$$\varepsilon(t) = v(t) + g_0(t) * \mathbf{f}^T(t)\mathbf{u}(t) \tag{6.80}$$

The error gradient can be calculated as

$$\begin{aligned} \nabla\varepsilon(t) &= \left[\frac{\partial\varepsilon(t)}{\partial b_0(t)} \quad \dots \quad \frac{\partial\varepsilon(t)}{\partial b_{M-1}(t)} \quad \frac{\partial\varepsilon(t)}{\partial a_0(t)} \quad \dots \quad \frac{\partial\varepsilon(t)}{\partial a_N(t)}\right] \\ &= g_0(t) * \left[\frac{\partial y(t)}{\partial b_0(t)} \quad \dots \quad \frac{\partial y(t)}{\partial b_{M-1}(t)} \quad \frac{\partial y(t)}{\partial a_0(t)} \quad \dots \quad \frac{\partial y(t)}{\partial a_N(t)}\right] \end{aligned} \tag{6.81}$$

where

$$\frac{\partial y(t)}{\partial b_p(t)} = r(t-p) + \sum_{j=1}^{M} a_j(t)\frac{\partial y(t-j)}{\partial b_p(t)}, \quad p = 0, 1, \dots, M-1 \tag{6.82}$$

and

$$\frac{\partial y(t)}{\partial a_q(t)} = y(t-q) + \sum_{i=1}^{M} a_i(t)\frac{\partial y(t-j)}{\partial a_q(t)}, \quad q = 1, \dots, N \tag{6.83}$$

Assuming that the step size μ is small, then we can get

$$\frac{\partial y(t-j)}{\partial a_q(t)} \approx \frac{\partial y(t-j)}{\partial a_q(t-j)} \tag{6.84}$$

$$\frac{\partial y(t-j)}{\partial b_p(t)} \approx \frac{\partial y(t-j)}{\partial b_p(t-j)} \tag{6.85}$$

and assuming that the recursion based on the old output gradients is negligible [22], we have

$$\frac{\partial y(t-j)}{\partial a_q(t-j)} = \frac{\partial y(t-j)}{\partial b_p(t-j)} = 0 \tag{6.86}$$

Therefore, the error gradient $\nabla\varepsilon(t)$ can be rewritten as

$$\begin{aligned}\nabla\varepsilon(t) &= g_0(t) * [r(t) \quad r(t-1) \quad \dots \quad r(t-M-1) \quad y(t-1) \quad \dots \quad y(t-N)]^T \\ &= g_0(t) * \mathbf{u}(t)\end{aligned} \tag{6.87}$$

The mean square error gradient estimate in (6.17) can expressed as

$$\begin{aligned}\nabla\hat{\xi}(t) &= \nabla\varepsilon^2(t) = 2\nabla\varepsilon(t)\varepsilon(t) \\ &= 2g_0(t) * \mathbf{u}(t)\varepsilon(t)\end{aligned} \tag{6.88}$$

Substitute (6.88) into (6.16), we can get the filtered-U recursive LMS algorithm for IIR filter

$$\begin{aligned}\mathbf{f}(t+1) &= \mathbf{f}(t) - \frac{\mu}{2}\nabla\hat{\xi}(t) \\ &= \mathbf{f}(t) - \mu[g_0(t) * \mathbf{u}(t)]\varepsilon(t) \\ &= \mathbf{f}(t) - \mu\mathbf{u}_f(t)\varepsilon(t)\end{aligned} \tag{6.89}$$

where

$$\mathbf{u}_f(t) = g_0(t) * \mathbf{u}(t) \tag{6.90}$$

In practice, $g_0(t)$ is replace by $g(t)$ which is the impulse response of the estimated model $G(q)$ of the secondary path transfer function $G_0(q)$.

(6.89) can separated into two vector equations for adaptive filter $A(q)$ and $B(q)$ as follows.

$$\mathbf{b}(t+1) = \mathbf{b}(t) - \mu\mathbf{r}_f(t)e(t) \tag{6.91}$$

and

$$\mathbf{a}(t+1) = \mathbf{a}(t) - \mu\mathbf{y}_f(t-1)e(t) \tag{6.92}$$

where $\mathbf{r}_f(t) = g(t) * \mathbf{r}(t)$ and $\mathbf{y}_f(t-1) = g(t) * \mathbf{y}(t-1)$

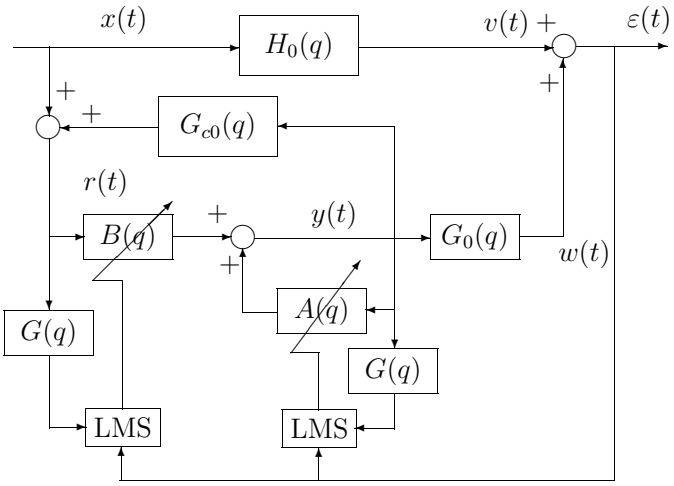

Figure 6.9. Block diagram of a feedforward ANC system using the filtered-U recursive LMS algorithm

The filtered-U recursive LMS algorithm applied an ANC system is illustrated in Fig. 6.9.

The filtered-U recursive LMS algorithm uses the same error microphone error $\varepsilon(t)$ in the adaptation process for both filters $A(q)$ and $B(q)$. Therefore, Both filters $A(q)$ and $B(q)$ will stop adapting when $\varepsilon(t)$ reaches its minimum. Actually, filter $A(q)$ models $-H_0(q)/G_0(q)$, and filter $B(q)$ models $H_0(q)G_{c0}(q)/G_0(q)$. However, global convergence and stability of the filter-U recursive LMS algorithm have never been proved formally. A filtered-U recursive LMS algorithm with a posteriori estimates has been proposed [70] and shows that the reference signal contamination from $G_{c0}(q)$ does not require any algorithmic modification.

An important property of adaptive IIR filter is to generate poles corresponding to the ideal response. However, the trajectory of the filter poles during the convergence is unpredictable, one or several poles may move outside of the unite circle and lead to instability. The problem with unstable filter poles can be solved by use of the leaky LMS algorithm [55]. A modified leaky version of the simplified hyperstable adaptive recursive filter algorithm [54] has also developed for ANC

applications to improve the stability of IIR filter. In that algorithm, a low pass filter is used to smooth the error signal for the filtered-U recursive LMS algorithm.

Chapter 7

Generalized FIR Filter for Feedforward ANC Applications

7.1 Generalized FIR filter

Filter estimation using FIR models converge to optimal and unbiased feedforward compensators irrespective of the coloring of the noise as indicated in (6.3). However, a FIR filter is usually too simple to model the dynamics of a complex sound control system with many resonance modes. As a result, many tapped delay coefficients of the FIR filter are required to approximate the optimal feedforward compensator.

To improve the approximation properties of the feedforward compensator in ANC, the linear combination of tapped delay functions q^{-1} in the FIR filter in (6.11) are generalized to

$$F(q) = f_0 + \sum_{k=1}^{L-1} f_k V_k(q)$$

where $V_k(q)$ are generalized (orthonormal) basis functions [36] that may contain knowledge on system dynamics.

For details on the construction of the functions $V_k(q)$ one is referred to Chapter 5 and [36].

Given an inner transfer function $P(q) = D + C(qI - A)^{-1}B$, where (A, B, C, D) is a minimal balanced realization, define $V_0(q) := (qI - A)^{-1}B$ and

$$V_k(q) = (qI - A)^{-1}BP^k(q) = V_0(q)P^k(q) \tag{7.1}$$

then a generalized FIR filter can be constructed that consists of a linear combination of the basis functions $f_0 + \sum_{k=0}^{L-1} f_k V_k$. This yields a generalized FIR filter

$$F(q) = \left[f_0 + \sum_{k=0}^{L-1} f_k V_0(q) P^k(q) \right] \tag{7.2}$$

A block diagram of the generalized FIR filter $F(q)$ in (7.2) is depicted in Fig. 7.1 and it can be seen that it exhibits the same tapped delay line structure found in a conventional FIR filter, with the difference of more general basis functions $V_k(q)$.

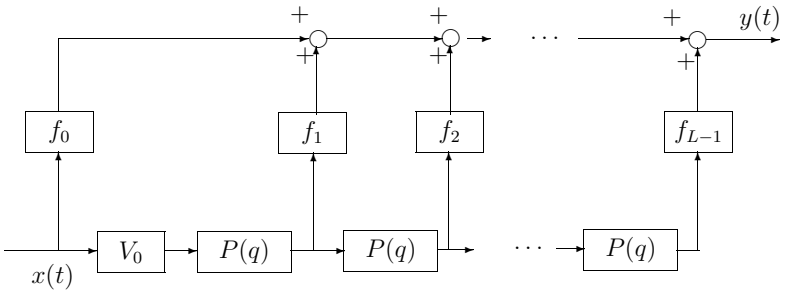

Figure 7.1. Block diagram of generalized FIR filter

An important property and advantage of the generalized FIR filter is that knowledge of the (desired) dynamical behavior can be incorporated in the basis function $V_k(q)$. Without any knowledge of desired dynamic behavior, the trivial choice of $V_k(q) = q^{-k}$ reduces the generalized FIR filter to the conventional FIR filter. If a more elaborate choice for the basis function $V_k(q)$ is incorporated, then (7.2) can exhibit better approximation properties for a much smaller number of parameters L than used in a conventional FIR filter. Consequently, the accuracy of the optimal feedforward controller will substantially increase. In the next section

we will elaborate on the choice of the basis function $V_k(q)$ and the use of the generalized FIR filter in the role of ANC based on feedforward compensation.

7.2 Estimation of Generalized FIR filter

7.2.1 Construction of basis functions

To facilitate the use of the generalized FIR filter, the basis function $V_k(q)$ in (7.1) have to be selected. A low order model for the basis functions will suffice, as the generalized FIR model will be expanded on the basis of $V_k(q)$ to improve the accuracy of the feedforward compensator. In order to more easily analyze the estimation of generalized FIR filter, let us recall the block dialog of of a feedforward ANC system Fig. 6.2 again for illustration purpose.

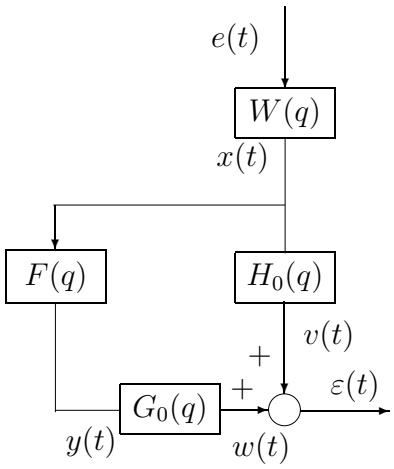

Figure 7.2. Block diagram of ANC system with feedforward

With no feedforward compensator in place, the signal $y(t)$ is readily available via

$$y(t) := v(t) = H_0(q)x(t) \tag{7.3}$$

and an initial low order IIR model $\hat{F}(q)$ of the feedforward filter $F(q)$ can be

estimated using the OE-minimization

$$\hat{F}(q) = F(q, \hat{\theta}),\ \hat{\theta} = \min_{\theta} \frac{1}{N} \sum_{t=0}^{N} \varepsilon^2(t, \theta) \tag{7.4}$$

of the prediction error

$$\varepsilon(t, \theta) = y(t) - F(q, \theta) x_f(t)$$

where $x_f(t)$ is given as

$$x_f(t) = g(t) * x(t) \tag{7.5}$$

and θ is defined as $\theta = [f_0 \quad f_1 \quad f_2 \quad \dots \quad f_{L-1}]$

The initial low order IIR model $\hat{F}(q)$ can be used to generate the basis functions $V_k(q)$ of the generalized FIR filer of the feedforward compensator $F(q)$. An input balanced state space realization of the low order model $\hat{F}(q)$ is used to construct the basis function $V_k(q)$ in (7.1).

With a known (initial) feedforward $F(q, \hat{\theta})$ in place, the signal $y(t)$ can be generated via

$$y(t) := H_0(q)x(t) = \varepsilon(t) + F(q, \hat{\theta}) x_f(t) \tag{7.6}$$

and requires measurement of the error microphone signal $\varepsilon(t)$, and the filtered input signal $x_f(t) = G(q)x(t)$. Since the feedforward filter is based on the generalized FIR model, the input $x_f(t)$ is also filtered by the tapped delay line of basis functions. A new filtered input signal $\bar{x}_k(t)$ can be defined as

$$\bar{x}_k(t) = V_k(q)G(q)x(t) \tag{7.7}$$

With the signal $y(t)$ in (7.6), $x_f(t)$ in (7.5), $\bar{x}_k(t)$ in (7.7) and the basis function $V_k(q)$ in (7.1) from the initial low order model in (7.4), the system dynamics can be rewritten as a linear regression form

$$y(t) = \phi^T(t)\theta, \quad \theta = [f_0, f_1, ..., f_{L-1}]^T \tag{7.8}$$

where $\phi^T(t) = [\bar{x}_1^T(t), ..., \bar{x}_{L-1}^T(t)]$ is the available input data vector and θ is the parameter vector to be estimated of the generalized FIR feedforward compensator.

7.2.2 Recursive estimation

The objective is to identify (estimate) the values of the parameters θ in (7.8) such that the feedforward controller minimizes the error signal $\varepsilon(t)$. The parameters θ can be identified with the available input-output data up to time t by a standard recursive least square (RLS) algorithm [33]. It is known that RLS algorithm at steady-state operation exhibits a windup problem if the forgetting factor remains constant, which will deteriorate the estimation results. As a result, a variable forgetting factor [50] be employed to prevent this problem from occurring. The parameters ϑ can be estimated by RLS algorithm with variable forgetting factor through two steps in each sample time:

1. Compute the gain vector $k(t)$ and the parameters $\hat{\theta}(t)$ at the current sample time

$$k(t) = \frac{P(t-1)\phi(t)}{\lambda_1(t) + \phi^T(t)P(t-1)\phi(t)} \tag{7.9}$$

$$\xi(t) = y(t) - \hat{\theta}^T(t-1)\phi(t) \tag{7.10}$$

$$\hat{\theta}(t) = \hat{\theta}(t-1) + k(t)\xi^*(t) \tag{7.11}$$

2. Update the inverse correlation matrix $P(t)$ and the forgetting factor $\lambda_1(t)$

$$\begin{aligned} P(t) = \lambda_1(t)^{-1}P(t-1) - \\ \lambda_1(t)^{-1}k(t)\phi^T(t)P(t-1) \end{aligned} \tag{7.12}$$

$$\lambda_1(t) = \lambda_0\lambda_1(t-1) + 1 - \lambda_0; 0 < \lambda_0 < 1 \tag{7.13}$$

where the typical values can be: $\lambda_1(0) = 0.95 \sim 0.99$; $\lambda_0 = 0.95 \sim 0.99$.

Relationship (7.13) leads to a forgetting factor that asymptotically tends towards 1. The recursive least square minimization will be

$$J(t) = \sum_{i=1}^{t} \lambda_1(i)^{t-i}[y(i) - \hat{\theta}(t)^T\phi(i)]^2 \tag{7.14}$$

The algorithm is initialized by setting

$$\hat{\theta}(0) = 0, \quad P(0) = \delta^{-1} I$$

a typical value for δ choose in this paper is $\delta = 0.001$.

From (7.9), we can see that even though the input data vector $\phi(t)$ is zero at some time t, the gain vector $k(t)$ does not increase because $\lambda_1 \neq 0$. A zero or small input data vector $\phi(t)$ can occur when the sound disturbance $x(t)$, measured by the reference microphone, is small. In that event, the recursive estimation routine will be robust in the presence of lack of excitation from the sound disturbance. As a result, $\hat{\theta}(t) = \hat{\theta}(t-1)$, and the parameters $\theta(t)$ of the generalized FIR filter at the current sample time t remain constant when only a small or no inlet disturbance signal $x(t)$ is being measured. An additional advantage of the usage of a variable forgetting factor $\lambda_1(t)$ computed by (7.13) is a rapid decrease of the inverse correlation matrix. In general this results in an accelerating convergence by maintaining a high adaptation at the beginning of the estimation when the parameters θ are still far from the optimal value.

7.3 Low order modeling of secondary path G_0

From (7.7), it is obtained that the modeling of secondary path $G_0(q)$ is needed for filtering purpose. Therefore a high order of model $G(q)$ of secondary path $G_0(q)$ may be estimated for filtering purpose by the standard open loop/closed loop identification technique. Even though a high order model $G(q)$ is desired in the filtering process in order to obtain a accurate filtered signal, a low order model $G(q)$ may be acceptable if it can maintain a good performance of feedforward compensation. In this section a low order model estimation of secondary path $G_0(q)$ is discussed and analyzed.

Suppose the performance of a feedforward controller applied to a system which is shown in Fig. 7.2 can be described by $\|(H_0(q) - F(q)G_0(q))W(q)\|$. Then

$\|(H_0(q) - F(q)G_0(q))W(q)\|$ can be bounded by

$$\|(H_0 - FG_0)W\| \leq \|(H_0 - FG)W\| + \|(FG_0 - FG)W\| \tag{7.15}$$

where G is the model of secondary path G_0, F is the feedforward controller, and W is a tunable weighting function.

As indicated in (7.15), a model G can be used to formulate an upper bound for $\|(H_0 - FG_0)W\|$, and a tight upper bound can be obtained by minimizing $\|(FG_0 - FG)W\|$. For a given feedforward controller F, the minimization of $\|(FG_0 - FG)W\|$ is so called control relevant identification problem [83].

Given the optimal (ideal) control F with $F = \frac{H_0}{G_0}$, $\|(FG_0 - FG)W\|$ can be rewritten as

$$\|(FG_0 - FG)W\| = \|(G_0 - G)FW\| = \|G_0 - G\|\|\frac{H_0}{G_0}\|\|W\|$$

Defining $\Phi_u = \|\frac{H_0}{G_0}\|\|W\|$, we can get

$$\|(FG_0 - FG)W\| = \|G_0 - G\|\Phi_u$$

Then the estimation of a model G of the secondary path G_0 is a standard open loop prediction error framework identification problem, and a low order model G may be obtained with the guarantee of the performance of active noise cancellation.

7.4 Applications to feedforward ANC

7.4.1 Modeling of the system dynamics

For the experimental verification of the proposed feedforward noise cancellation, the ACTA silencer depicted in Fig. 7.3 was used. The system is an open-ended airduct located at the System Identification and Control Laboratory at UCSD that will be used as a case study for the ANC algorithm presented in this chapter. Experimental data and real time digital control is implemented at a sampling

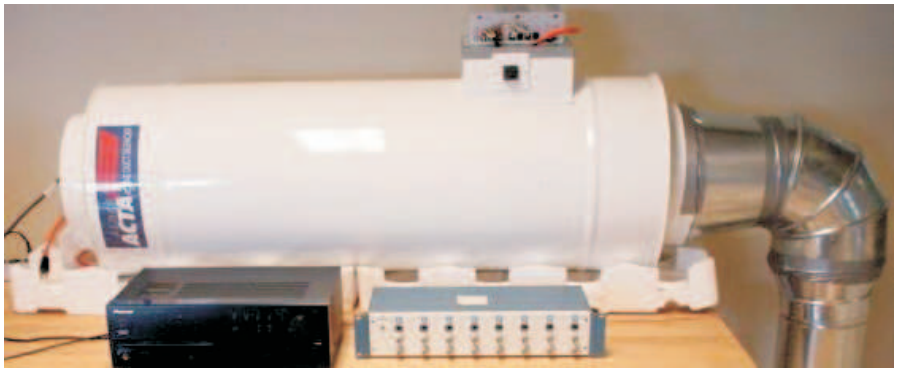

Figure 7.3. ACTA airduct silencer located in the System Identification and Control Laboratory at UCSD

frequency of 2.56kHz and experimental data of the error and input microphone were gathered for the initialization of the feedforward controller.

In order to create the filtered input digital $x_f(t)$ in (7.5) and $\bar{x}_k(t)$ in (7.7), a 21th order ARX model $G(q)$ which can pick most main resonance modes of $G_0(q)$ was estimated for filtering purposes.

The identification results of $G(q)$ can be found in Fig. 7.4. Because $G(q)$ can pick most main resonance modes of $G_0(q)$, $G_0(q)$ has been estimated reasonably well for filtering purposes.

The filtered input signal $x_f(t)$ and the observed error microphone signal $y(t)$ sampled at 2.56kHz were used to estimate a low (4th) order IIR model $F_f(q,\theta)$ to create the basis function $V_k(q)$ in (7.1) for the generalized FIR filter parametrization of the feedforward controller. During the estimation of the low order model $\hat{F}(q)$ also an estimate of the expected time delay n_k in (7.2) was performed and was found to be $n_k = 16$. The identification results of the 4th order IIR model $F_f(q,\theta)$ is shown in Fig. 7.5. From Fig. 7.5 it can be observed that the 4th order model $F_f(q,\theta)$ picks two resonance modes of $\frac{H_0(q)}{G_0(q)}$. The reason only 4th order model $F_f(q,\theta)$ is estimated is that $F_f(q,\theta)$ is only used to create the basis function, and a high accurate model is not necessary.

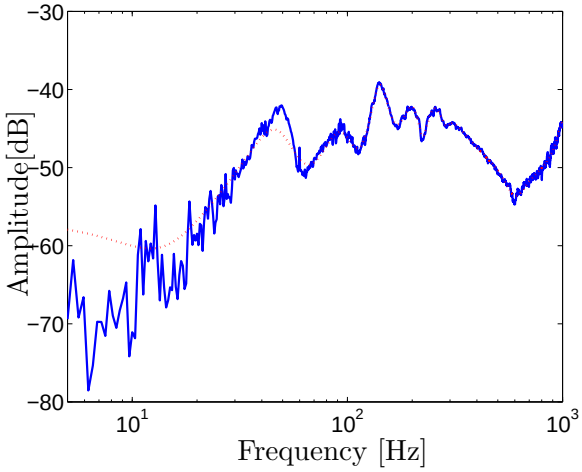

Figure 7.4. Amplitude plot of spectral estimate of $G_0(q)$(solid) and 21th order parametric model $G(q)$ (dotted)

7.4.2 Implementation of feedforward ANC

After initialization, the information of the filter $G(q)$, the basis function $V_k(q)$ and the time delay n_k was used to perform a recursive estimation of the generalized FIR filter based feedforward compensator $F(q)$. To illustrate the effectiveness of the recursive generalized FIR feedforward compensator, data has been generated over 1.5 seconds, where a sound disturbances is generated into the air-duct during the first half second and the last half seconds, and is turned off in between. For the generalized FIR filter only $N = 5$ parameters $\theta_i,\ i = 1, \ldots, 5$ in (7.8) were estimated for the construction of the feedforward compensator. With a 4th order basis function $V_k(q)$, each parameter $\theta_i \in R^{1\times 4}$ and this amounts to IIR feedforward compensator of order 20.

The performance of the generalized FIR filter is confirmed by the estimates of the spectral contents of the microphone error signal $e(t)$ plotted in Fig. 7.6. The spectral content of the error microphone signal has been reduced significantly by the generalized FIR filters in the frequency range from 40 till 400Hz.

To illustrating the stability and convergence properties of the recursive least

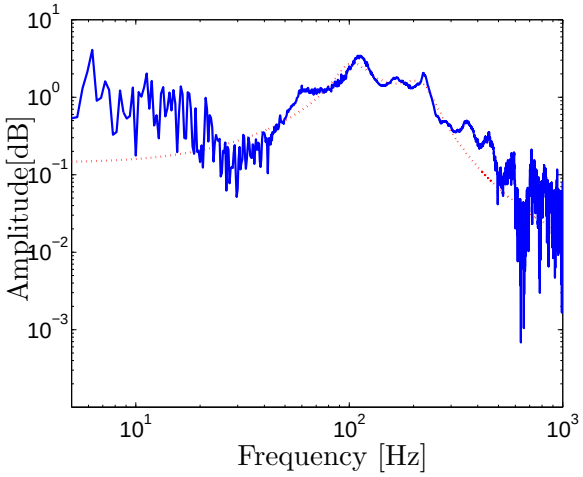

Figure 7.5. Amplitude of spectral estimate of $-\frac{H_0(q)}{G_0(q)}$ (solid) and 4th order parametric model $F_f(q,\theta)$ (dotted)

square (RLS) estimation, the norm of parameters $\|\theta_i\|$ for $i = 1,\ldots,5$ is shown in Fig. 7.7. Since each parameter θ_i in (7.8) is of dimension $R^{1\times 4}$, only $\|\theta_i\|$ for $i = 1, ..., 5$ is plotted to provide 5 lines for each multidimensional parameter. From Fig. 7.7, it can be observed that the parameters $\|\theta_i\|$ converge to a steady state very quickly which validates an important property for the recursive least square (RLS) algorithm. Moreover, the parameter values remain constant in the presence of lack of excitation at the middle part of the experiment.

The final conformation of the performance of the ANC has been depicted in Fig. 7.8. From Fig. 7.8 it can be observed that, even though the sound disturbance excitation drastically reduces from $t = 0.5$ and $t = 1$ seconds during the experiment, the error microphone signal is not identically zero because of the measurement error of the inlet and outlet microphones. Furthermore, the estimation of the parameters θ_i do not diverge during this time interval due to the robust property of the RLS algorithm. The significant reduction of the error microphone signal observed in the time traces and the norm of the signals displayed on the right part of Fig. 7.8 indicates the effectiveness of the generalized FIR filter for

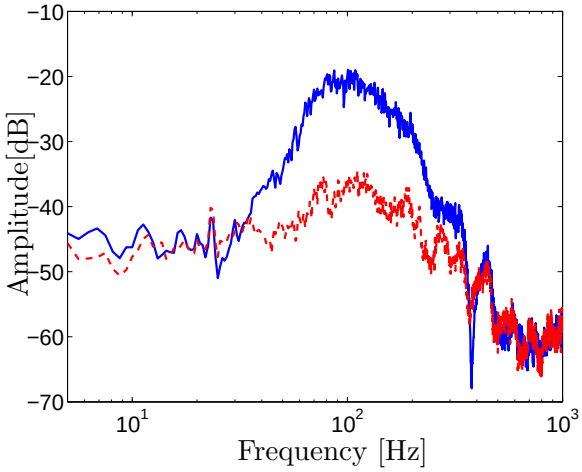

Figure 7.6. Estimate of spectral contents of error microphone signal $e(t)$ without ANC (solid) and with ANC using 20th order generalized FIR filter (dotted)

feedforward sound compensation.

7.5 Conclusions

In this chapter, a new methodology has been proposed for the active noise control in an airduct using a feedforward compensation that is parametrized with a generalized FIR filter. The feedforward filter with the linear parametrization is an IIR filter that can be estimated via filtered recursive least squares (RLS) techniques with variable forgetting factor. The design is evaluated on the basis of an experimental active noise cancellation experiment and shows significant sound reduction. The RLS is robust with respect to lack of disturbance excitation by the adaptation of the forgetting factor in the recursive estimation.

Acknowledgements

The text of Chapter 7, is a reprint of the material as it appears in the 42nd IEEE Conference on Decision and Control. The dissertation author was the primary

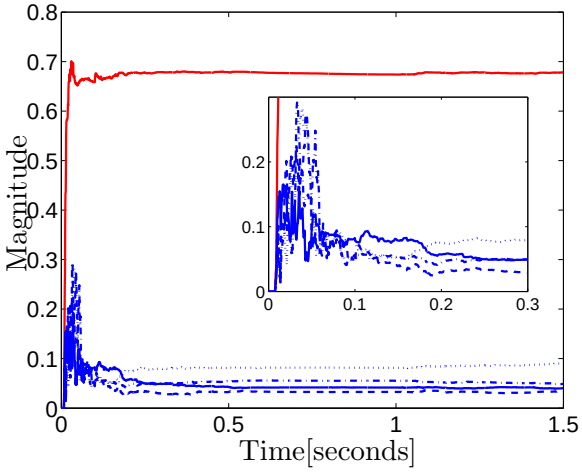

Figure 7.7. Norm $\|\theta_i\|$ for $i = 1, ..., 5$ where θ_i is given in (7.8): θ_1(red); θ_2(solid); θ_3(dotted); θ_4(dashdot); θ_5(dashed)

researcher and author in these works and the co-author listed in these publications directed and supervised the research which forms the basis for this chapter.

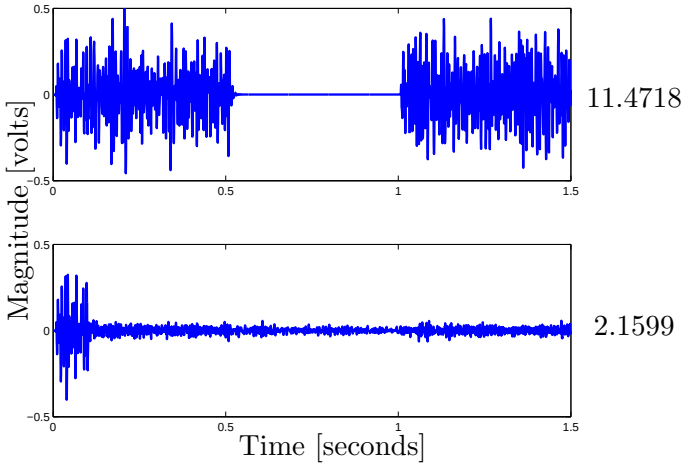

Figure 7.8. Evaluation of error microphone signal before ANC (top) and with ANC using 20th order generalized FIR filter (bottom)

Chapter 8

Application of Dual-Youla Parametrization in ANC System

In Section 6.4, some methods have been presented to compensate the effect of acoustic coupling in an ANC system. Even though somehow these methods maybe helpful to cancel the negative effect of acoustic coupling, the performance of the feedforward ANC is not guaranteed in practice. This chapter presents a framework to recursively estimate a feedforward filter in the presence of acoustic coupling, addressing both stability and performance of the active feedforward noise cancellation algorithm. The framework is based on fractional model representations in which a feedforward filter is parametrized by coprime factorization which is described in Section 3.4. Conditions on the parametrization of the coprime factorization formulated by the existence of a stable perturbation enables stability in the presence of acoustic coupling. In addition, this chapter shows how the stable perturbation can be estimated on-line via a recursive least square estimation of a generalized FIR filter to improve the performance of the feedfoward filter for active noise cancellation.

8.1 Dual-Youla parametrization

Referring the block diagram of a feedforward ANC system that includes the acoustic coupling has been shown in Fig. 8.1.

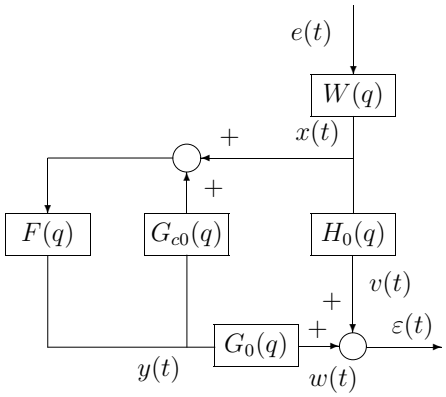

Figure 8.1. Block diagram of feedforward ANC system with acoustic coupling

The error microphone signal $\varepsilon(t)$ can be described by

$$\begin{aligned} \varepsilon(t) &= \left[H_0(q) + \frac{G_0(q)F(q)}{1 - G_{c0}(q)F(q)}\right] x(t) \\ &= H_0(q)x(t) + \frac{F(q)}{1 - G_{c0}(q)F(q)} \cdot G_0(q)x(t) \end{aligned} \tag{8.1}$$

and definition of the signals

$$v(t) := H_0(q)x(t),\ x_f(t) := G_0(q)x(t) \tag{8.2}$$

leads to

$$\begin{aligned} \varepsilon(t) &= v(t) + \frac{F(q)}{1 - G_{c0}(q)F(q)} x_f(t) \\ &= v(t) + L(q)x_f(t) \quad L(q) := \frac{F(q)}{1 - G_{c0}(q)F(q)} \end{aligned} \tag{8.3}$$

From (8.3) it can be seen that the acoustic coupling $G_{c0}(q)$ creates a positive feedback loop with the feedforward filter $F(q)$. The presence of the acoustic coupling $G_{c0}(q)$ might lead to an undesirable or unstable feedforward compensation if $G_{c0}(q)$ is not taken into account in the design of the feedforward filter $F(q)$ for

active noise cancellation [42]. To address the issues of stability it can be noted that certain signals can be used for estimation purposes of the dynamics of the various transfer functions in the ANC system. In case the signals $v(t)$ can be measured and the signal $x_f(t)$ can be created by filtering the measured signal $x(t)$ through a filter that models the dynamics of the acoustic control path $G_0(q)$, the estimation of the feedforward filter $F(q)$ can be considered as a closed loop identification problem, where the error $\varepsilon(t,\theta)$

$$\varepsilon(t,\theta) = v(t) + L(q,\theta)x_f(t)$$

is minimized according to

$$\hat{\theta} = \min_{\theta} \|\varepsilon(t,\theta)\|_2 \tag{8.4}$$

Minimization of $\|\varepsilon(t,\theta)\|_2$ in (8.4) is an output error based identification problem [59]. In this chapter, the presence of acoustic coupling G_{c0} during the estimation of $F(q)$ is taken into account by using a model G_c of the acoustic coupling G_{c0}. Using a model G_c, the estimation and computation of F can be done based on a so-called dual-Youla parametrization described in Section 3.4, which opens a possibility to guarantee the internal stability of $\mathcal{T}(\hat{F}, G_c)$ by constructing a feedforward filter $\hat{F}$ via estimation of a stable dual-Youla transfer function. Dual-Youla parametrization presented in Section 3.4 is built in the case that the closed loop system is a negative feedback closed loop system. However, the feedback connection of feedforward control F and acoustic coupling G_c in ANC system is positive feedback system. Therefore, we have to make a modification about the dual-Youla parametrization algorithm in order to use this algorithm in feedforward ANC application.

Based on the definitions described in Section 3.4, a characterization of the set of feedforward filters $F(q) = N(q)D(q)^{-1} = \tilde{D}(q)^{-1}\tilde{N}(q)$ that yields an internally stable feedback connection $\mathcal{T}(F(q), G_c(q))$ of the feedforward filter $F(q)$ and the model for the acoustic coupling $G_c(q)$ can be expressed via a dual-Youla parametrization Section 3.4 and is given in the following.

Lemma 8.1. *Let (N_x, D_x) be a rcf of an auxiliary feedforward filter $F_x = N_x D_x^{-1}$ over $\mathcal{RH}_\infty$, and (N_c, D_c) be a rcf of the model G_c of the acoustic coupling G_{c0} with $G_c = N_c D_c^{-1}$ such that $\mathcal{T}(F_x, G_c) \in \mathcal{RH}_\infty$, then a feedforward filter F with a $rcf(N, D)$ satisfies $\mathcal{T}(F, G_c) \in \mathcal{RH}_\infty$ if and only if there exists $R_0 \in \mathcal{RH}_\infty$ such that*

$$\begin{aligned} N &= N_x + D_c R_0 \\ D &= D_x + N_c R_0 \end{aligned} \tag{8.5}$$

Proof: For a proof, one is referred to Section 3.4. □

From (8.5) it is obtained that R_0 can vary over all possible transfer functions in $\mathcal{RH}_\infty$ such that $\{D_x + D_c R_0\}$ is well defined, which characterizes a set of filters F that are internally stabilized by G_c. For the interpretation of the result in Lemma 8.1, consider the following prior information to estimate the optimal feedforward filter F.

Firstly, assume the availability of an initial (not optimal) feedforward controller F_x that is used only to create a stable feedback connection $\mathcal{T}(F_x, G_c)$ in the presence of the acoustic coupling G_c. Secondly, if a model $G_c = N_c D_c^{-1}$ for the acoustic coupling G_{c0} is available, then a set of feedforward filters can be parameterized that is known to be stabilized by the model G_c of the acoustic coupling. With this prior information, the optimal feedforward filter F to minimize $\|\varepsilon(t, \theta)\|_2$ in (8.4) can be constructed by means of the nominal filter F_x plus a possible perturbation R_0 given by (8.5). Because R_0 is the only unknown parameter, the estimation of a stable model $\hat{R}$ of R_0 will yield an estimate $(\hat{N}, \hat{D})$ of a rcf of feedforward filter $\hat{F}$ described by

$$\begin{aligned} \hat{N} &:= N_x + D_c \hat{R} \\ \hat{D} &:= D_x + N_c \hat{R} \end{aligned} \tag{8.6}$$

If the estimate $\hat{R}$ is stable, then the model $\hat{F} = \hat{N}\hat{D}^{-1}$ estimated in (8.6) is guaranteed to create a stable acoustic feedback with the model G_c of the acoustic coupling and instabilities of the feedforward ANC can be avoided in the presence of acoustic coupling.

From equation (8.5), we know that the set of feedforward filters in Fig. 8.1 can be replaced by the combination of (N_x, D_x), (N_c, D_c) and stable transfer function R_0, The representation of $\mathcal{T}(F, G_{c0})$ in Fig. 8.1 can be found in Fig. 8.2 with the knowledge of G_{c0} represented by the model G_c.

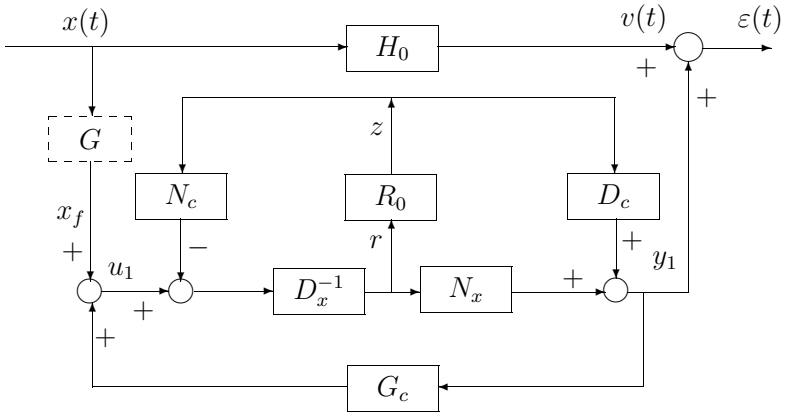

Figure 8.2. Block diagram of rcf representation of the feedback connection $\mathcal{T}(G_c, F)$

In order to estimate the dual-Youla transfer function R_0 using a standard open loop identification algorithm, the following signals are required. The reference signal $x_f(t)$ in Fig. 8.1 is a filtered version of the input microphone noise measurement

$$x_f(t) := G(q)x(t) \tag{8.7}$$

where $G(q)$ is the model of the secondary path G_0. Such a filtering is commonly used in filtered LMS algorithms to avoid bias of the estimate of the feedforward filter [33]. Subsequently, the output signal $y_1(t)$ is defined as

$$y_1(t) := -v(t) = -\varepsilon(t) \text{ for } F(q) \equiv 0 \tag{8.8}$$

where $v(t) = \varepsilon(t)$ is simply the measurement of the error microphone signal in the absence of a feedforward controller for noise cancellation. Finally, the input signal $u_1(t)$ is defined as

$$u_1(t) := x_f(t) + G_c(q)y_1(t) \tag{8.9}$$

where G_c is the model of the acoustic feedback path G_{c0}. The use of this filtered (closed-loop) input signal is needed to address stability of the feedforward compensation in the presence of acoustic coupling. The use of the filtered input signal $u_1(t)$ is in addition to the filtering in (8.8) used in filtered LMS estimation of feedforward filters. With the definition of these signals, the open-loop estimate problem of the dual-Youla transfer function R_0 can be formalized as follows.

Lemma 8.2. *Let (N_x, D_x) be a rcf of an auxiliary feedforward filter $F_x = N_x D_x^{-1}$ and (N_c, D_c) be a rcf of the model $G_c = N_c D_c^{-1}$ of the acoustic coupling G_{c0} such that $\mathcal{T}(F_x, G_c) \in \mathcal{RH}_\infty$. Then the intermediate signals $x(t)$ and $z(t)$ are related by*

$$z(t) = R_0(q)r(t) \tag{8.10}$$

where the intermediate input signal x is defined by the filter operation

$$r := (D_x - G_c N_x)^{-1} \begin{bmatrix} -G_c & I \end{bmatrix} \begin{bmatrix} y_1 \\ u_1 \end{bmatrix} \tag{8.11}$$

and dual-Youla signal z is defined by the filter operation

$$z := (D_c - F_x N_c)^{-1} \begin{bmatrix} I & -F_x \end{bmatrix} \begin{bmatrix} y_1 \\ u_1 \end{bmatrix} \tag{8.12}$$

where the signals r, y_1 and u_1 are defined respectively in (8.7), (8.8) and (8.9).

Proof: For a proof, one is referred to Section 3.4. □

From (8.10) it can be seen that the estimation of a stable model $\hat{R} = R(q, \hat{\theta})$ can be obtained via a standard output-error (OE) minimization by

$$\hat{\theta} = \min_{\theta} \|z(t) - R(q, \theta)r(t)\|_2 \tag{8.13}$$

Although the (8.10) and the proof of Lemma 8.2 indicate a noise free open-loop identification problem, the OE minimization in (8.13) is robust in the presence of possible measurement noise $e_n(t)$ on the error microphone signal $e(t)$. Under the

viable assumption that additional measurement noise $e_n(t)$ on $e(t)$ is uncorrelated with the signal $x(t)$ from the input microphone, it is easy to verify that the reference $x_f(t)$ in (8.7) in uncorrelated with $e_n(t)$. With

$$u_1(t) - G_c(q)y_1(t) = x_f(t) = G(q)x(t)$$

it can be seen that the intermediate input signal $x(t)$ in (8.11) is uncorrelated with $e_m(t)$, making (8.13) a standard open-loop identification problem even in the presence of additional measurement noise $e_n(t)$ on the error microphone signal $e(t)$. Once a stable model $\hat{R}$ is found, the optimal feedforward filter $\hat{F} = F(q, \hat{\theta})$ can be obtained from (8.6) with $\hat{F} = \hat{N}\hat{D}^{-1}$ which is guaranteed to be stabilized by the model G_c of the acoustic coupling G_{c0}.

8.1.1 Robustness against modeling errors

From Lemma 8.1, it is shown that if the estimate $\hat{R}$ is stable, then the model $\hat{F} = \hat{N}\hat{D}^{-1}$ estimated in (8.6) is guaranteed to stabilize the model G_c of the acoustic coupling G_{c0}. If the model G_c is an accurate approximate of the acoustic coupling G_c, i.e, the modeling error $G_c - G_{c0}$ is very small and can be neglected, then the model $\hat{F} = \hat{N}\hat{D}^{-1}$ is guaranteed to create a stable positive feedback with acoustic coupling G_{c0} and the instabilities can be avoided with the acoustic coupling. However, if sometimes a perfect model G_c of acoustic coupling G_{c0} can not be easily obtained, the robust stability against the modeling error needs to be analyzed in order to design a good feedforward filter which can robust stabilize the acoustic coupling G_{c0}.

For simplicity, we only use coprime factor uncertainty to describe the modeling uncertainty of acoustic coupling G_{c0}. The robust stability analysis with other model uncertainty such as additive uncertainty and multiplicative uncertainty is similar to the analysis in this section. Suppose $(\bar{N}_c, \bar{D}_c)$ be a rcf of acoustic coupling G_{c0}, (N_c, D_c) be a rcf of model G_c and (N_x, D_x) be a rcf of initial feedforward filter F_x, then similar to Lemma 8.1, the uncertain acoustic coupling $G_{c0} = \bar{N}_c\bar{D}_c^{-1}$ can

be expressed with

$$\begin{aligned} \bar{N}_c &:= N_c + D_x\Delta_0 \\ \bar{D}_c &:= D_c + N_x\Delta_0 \end{aligned} \tag{8.14}$$

where the uncertainty $\Delta_0 \in \mathcal{RH}_\infty$. The perturbed closed loop system is illustrated in Fig. 8.3. Using small gain theorem, the following lemma concerning the robust

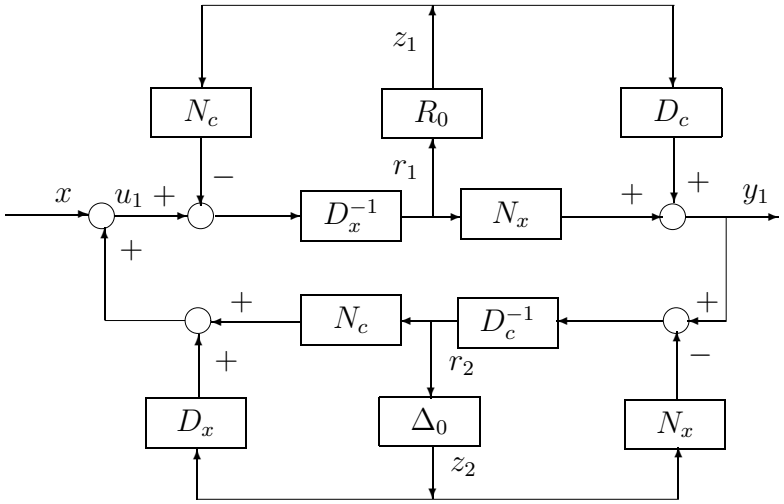

Figure 8.3. Block diagram of coprime factor perturbed closed loop system

stability against model uncertainty Δ_0 is obtained.

Lemma 8.3. *Suppose the uncertain acoustic coupling G_{c0} is given by*

$$G_{c0} = (N_c + D_x\Delta_0)(D_c + N_x\Delta_0)^{-1}$$

and feedforward filter is given as

$$\hat{F} = (N_x + D_cR_0)(D_x + N_cR_0)^{-1}$$

with $\Delta_0, R_0 \in \mathcal{RH}_\infty$. Then the closed loop system $\mathcal{T}(\hat{F}, G_{c0})$ is well posed and internally stable for all $\|\Delta_0 R_0\|_\infty < 1$.

Proof: Define $\bar{r} = [r_1, r_2]^T$ and $\bar{z} = [z_1, z_2]^T$. From Fig. 8.3, it is easy to write $\bar{r}$ as a function of $\bar{z}$ and $\bar{z}$ as a function of $\bar{r}$. Then one can get

$$\bar{r} = \begin{bmatrix} 0 & 1 \\ 1 & 0 \end{bmatrix} \bar{z} \tag{8.15}$$

and

$$\bar{z} = \begin{bmatrix} R_0 & 0 \\ 0 & \Delta_0 \end{bmatrix} \bar{r} \tag{8.16}$$

From (8.15) and (8.16), closed loop connection between r_2 and z_2 can be written as

$$\begin{aligned} z_2 &= \Delta_0 r_2 \\ r_2 &= z_1 = R_0 r_1 = R_0 z_2 \end{aligned} \tag{8.17}$$

By the small gain theory, the closed loop system is well posed and internal stable for all $\Delta_0 \in \mathcal{RH}_\infty$ if and only if

$$\|\Delta_0 R_0\|_\infty < 1 \tag{8.18}$$

Similarly, the closed loop connection between r_1 and z_1 can also be obtained with the same procedure, and the same result (8.18) can also obtained. □

From Lemma 8.3 it is obtained that if $\Delta_0 \neq 0$, then R_0 has constraint with $\|\Delta_0 R_0\|_\infty < 1$. If the model G_c is perfect, i.e, the uncertainty $\Delta_0 = 0$, then R_0 can be any stable rational transfer function which is actually estimated based on the choice of the initial feedforward controller F_x.

8.1.2 Summary of Feedforward Estimation

Since the intermediate signal $r(t)$ and the dual-Youla signal $z(t)$ can be created by (8.11) and (8.12), the estimation of the dual-Youla transfer function R_0 from (8.10) is an open loop identification problem that can be computed by standard system identification techniques [59]. For more information about the dual-Youla parametrization, one is referred to [29, 56, 11] for more details. As a result, the

estimation of the feedforward filter $F(q)$ using the dual-Youla parametrization can be summarized by the following steps.

1. A model G of the acoustic control path G_0 is needed for filtering purpose to create the reference signal $x_f(t)$. The model G can be estimated via a standard open-loop identification by performing an experiment using the controller speaker signal $y(t)$ as excitation signal and the error microphone signal signal $\varepsilon(t)$ as output signal. Such a filtering is commonly used in filtered LMS algorithms to avoid bias of the estimate of the feedforward filter [33].

2. A model G_c of the acoustic coupling G_{c0} is needed to design an initial nominal filter $F_x = N_x D_x^{-1}$ to stabilize the acoustic feedback loop. The model G_c along with the initially stabilizing F_x is used to parametrize the feedforward filter F according to Lemma 8.1. The model G_c can be estimated via a standard open-loop identification by performing an experiment using the controller speaker signal $y(t)$ as excitation signal and the input microphone signal $d(t)$ as output signal.

3. With the models G, G_c and the initial feedforward filter F_x, the reference signal $x_f(t)$, input signal u_1 and output signal y_1 can be created. With these signals, the optimal feedforward filter $\hat{F}$ can be estimated by minimizing $\|\varepsilon(t,\theta)\|_2$ in (8.4) using the dual-Youla parametrization of the filter $F(q,\theta)$.

Although both the acoustic coupling G_{c0} and the acoustic control path G_0 require an additional modeling effort for the implementation of the ANC, the use of the models G and G_c is beneficial for the ANC system. Since in most ANC systems both the acoustic coupling G_c and the acoustic control path G are fixed, adaptation of the feedforward filter F is not required to adjust for varying acoustics. As a result, the estimation of the feedforward filter can be seen as a self-tuning problem and this greatly simplifies the feedforward control algorithm.

Furthermore, using both models G and G_c for filtering purposes can be seen as a generalization of the filtering used in filtered LMS estimation of feedforward filters.

By adopting the theory of dual-Youla parametrization, the design of optimal feedforward controller F is transformed to the estimation of the perturbation R_0 from (8.10) using a standard open-loop output error (OE) identification technique [59]. It should be stated that the estimation of the perturbation R_0 is dependent on the initial feedforward filter F_x. In the unlikely event where the initial feedforward filter F_x equals the optimal filter $\hat{F}$, R_0 is equal to 0 and does not need to be updated. Since the initial feedforward filter F_x is chosen only to stabilize the acoustic system in the presence of acoustic coupling, further estimation of the perturbation R_0 will improve the feedforward filter to minimize the signal of the error microphone.

8.2 Perturbation estimation via generalized FIR filter

To facilitate the use of the generalized FIR filter described in Chapter 7, the basis functions $V_k(q)$ have to be selected. A low order model for the basis functions will suffice, as the generalized FIR model will be expanded on the basis of $V_k(q)$ to improve the accuracy of the feedforward compensator. For the initialization of the parametrization of the generalized FIR model, an initial low order IIR model $\bar{R}(q) = R(q, \bar{\theta})$ of the perturbation $R_0(q)$ can be estimated using an OE-minimization

$$\bar{\theta} = \min_{\theta} \|z(t) - R(q, \theta) r(t)\|_2 \tag{8.19}$$

with the intermediate signal r and the dual-Youla signal z available from (8.11) and (8.12). The initial low order IIR model $\bar{R}(q)$ can be used to generate the basis functions $V_k(q)$ of the generalized FIR filter. An input balanced state space realization of the low order model $\bar{R}(q)$ is used to construct the basis function

$V_k(q)$ in (7.1). With the basis function $V_k(q)$ in place, the linear parametrization of $R(q,\theta)$ is obtained.

$$R(q,\theta) = f_0 + \sum_{k=1}^{L-1} f_k V_k(q),\ \theta = [f_0 \quad f_1 \quad \cdots \quad f_{L-1}] \tag{8.20}$$

Since the parametrization of $R(q,\theta)$ is based on the generalized FIR model, the intermediate signal $r(t)$ is filtered by the tapped delay line of basis functions

$$\bar{x}_k(t) = V_k(q)r(t),\ k = 0,\ldots,L-1 \tag{8.21}$$

creating filtered intermediate signals $\bar{x}_k(t)$. With the generalized FIR filter expansion given in (8.20), the relation between the signal $z(t)$ in (8.12) and $\bar{x}_k(t)$ in (8.21) can be rewritten in a linear regression form

$$z(t) = \phi^T(t)\theta,\quad \theta = [f_0 \quad f_1 \quad \cdots \quad f_{L-1}]^T \tag{8.22}$$

where $\phi^T(t) = [\bar{x}_0^T(t)\ \cdots\ \bar{x}_{L-1}^T(t)]$ is the available input data vector and θ is the parameter vector of $R(q,\theta)$ in (8.20) to be estimated. The parameter vector θ can be estimated by RLS algorithm described in Section 7.2.2.

8.3 Application of feedforward ANC

8.3.1 Modeling of ANC system dynamics

For the experimental verification of the proposed feedforward noise cancellation, the ACTA silencer depicted in Fig. 7.3 was used. The system is an open-ended airduct located at the System Identification and Control Laboratory at UCSD. Experimental data and real time digital control is implemented at a sampling frequency of 2.56kHz and experimental data of the error and input microphone were gathered for the initialization of the feedforward filter.

Once the mechanical and geometrical properties of the ANC system in Fig. 7.3 are fixed, then the acoustic control path G_0 and the acoustic coupling G_{c0} both

are fixed. For initialization and calibration of ANC algorithm, the models of the acoustic control path G_0 and the acoustic coupling G_{c0} can be identified off-line. Estimation of a model G can be done by performing an experiment using the controller speaker signal $y(t)$ as excitation signal and the error microphone signal $\varepsilon(t)$ as output signal. The same experiment can also be used to measure the input microphone signal $x(t)$ as an additional output to estimate the model of the acoustic coupling G_{c0}. Because these models G and G_c will be used to design nominal feedforward filter F_x and feedforward filter $\hat{F}$, the order of these models should be controlled. In order to estimate a low order feedforward filter $\hat{F}$, a 20th order ARX model G was estimated for filtering purpose and a 17th order ARX model of G_c was estimated for feedforward filter design purposes. The identification results of G and G_c can be found in Fig. 8.4 and Fig. 8.5, respectively.

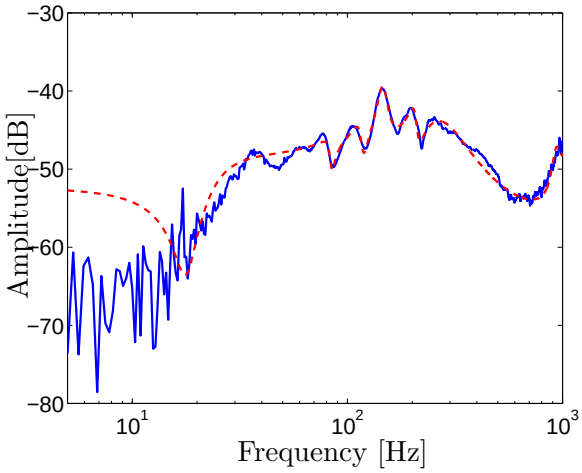

Figure 8.4. Amplitude Bode plot of spectral estimate of acoustic control path G_0 (solid) and 20th order parametric model G (dashed)

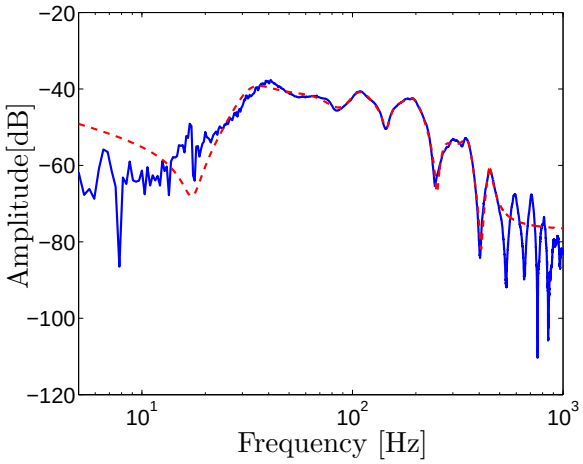

Figure 8.5. Amplitude Bode plot of spectral estimate of acoustic coupling G_{c0} (solid) and 17th order parametric model G_c (dashed)

8.3.2 Estimation of basis function for dual-Youla transfer function

A low order model $\hat{R}$ is estimated to compute the basis functions $V_k(q)$ for the parametrization and estimation of the dual-Youla transfer function R_0. On the basis of the model G_c a simple 2nd order nominal feedforward filter F_x is pre-computed that internally stabilize the positive feedback loop connection $\mathcal{T}(F_x, G_c)$. The initial feedforward controller is given by the discrete time transfer function

$$F_x(q) = \frac{-1.577q + 1.611}{q^2 - 1.99q + 0.9913} \tag{8.23}$$

and is lightly damped 2nd order system with one step time delay and a resonance mode at approximately 100 rad/s.

Given the experimental data and the prior information, consisting of the model G of the acoustic control path G_0 and the model G_c of acoustic coupling G_{c0}, the filtered signals $r(t)$, $y_1(t)$ and $u_1(t)$ can be created respectively via (8.7), (8.8) and (8.9). With the computation of a normalized right comprime factorization (N_x, D_x) and (N_c, D_c) of the initial filter F_x and the model G_c, the signals r and

z can be created obtained using (8.11) and (8.12). With the intermediate input signal r and the dual-Youla signal z a spectral estimate of the dual-Youla transfer function R_0 can be computed. The spectral estimate is plotted in Fig. 8.6 and compared with a simple 6th order OE model estimate $\bar{R}$. The 6th order OE model estimate $\bar{R}$ is found by (8.19) using standard open loop identification technique [59] and will be used to generate the basis functions $V_k(q)$ in (7.1) for the generalized FIR parametrization of $R(q,\theta)$ in (8.20).

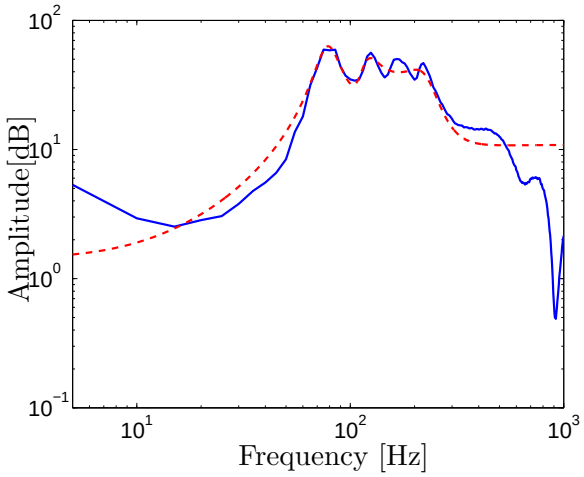

Figure 8.6. Amplitude Bode plot of spectral estimate of dual-Youla transfer function R_0 (solid) and 6th order parametric model $\bar{R}$ (dashed) used for basis function generation

From Fig. 8.6, it can be observed that the simple 6th order model $\bar{R}$ does not capture the spectral estimate of the dual-Youla transfer function R_0 very well. However, the model $\bar{R}$ will be used only to create the basis functions $V_k(q)$ in (7.1) for the orthonormal FIR expansion of the dual-Youla transfer function. The generalized FIR parametrization of $R(q,\theta)$ in (8.20) will then allow for a recursive estimation and self-tuning of the feedforward filter.

8.3.3 Application of feedforward ANC

The prior information reflected in the models G of the acoustic control path G_0, G_c of the acoustic coupling G_{c0}, the initial filter $F_x(q)$ and the basis functions $V_k(q)$ generated by the low order model $\bar{R}(q)$ all serve as an initialization for the recursive estimation of the feedforward controller in the presence of acoustic coupling.

For the recursive least squares estimation of generalized FIR filter in (8.20) only $N = 3$ parameters $\theta_i,\ i = 0, \ldots, 3$ were estimated. Since no feedthrough term was expected in the feedforward filter, the feedthrough term f_0 in (8.22) was set to $f_0 = 0$. With a 6th order basis functions $V_k(q), k = 0, \ldots, 3$ generated by the low order model $\bar{R}$, each parameter $\theta_i \in R^{1\times 6}$. As a result a generalized FIR filter $R(q, \theta)$ of order 24 is estimated by minimizing the error signal $e(t)$ using a recursive least squares estimation. The recursive estimation is implemented on a Pentium II based personal computer system using a 12 AD/DA Quanser card a sampling time of 2.56KHz.

From Fig. 8.4 and Fig. 8.5 it can be observed that the acoustic coupling G_{c0} in the ANC system is relatively large compared to the acoustic control path G_0. As a result, a straightforward implementation of a filtered LMS algorithm for the computation of a 24th order FIR filter leads to an unstable feedforward ANC system, where harmonic oscillation are observed due to destabilizing effects of the acoustic feedback path.

The performance of the feedforward compensator $\hat{F}$ that is estimated recursively using a dual-Youla parametrization with generalized FIR filters is confirmed by the estimate of the spectral content of the microphone error signal $\varepsilon(t)$ plotted in Fig. 8.7. The spectral content of the error microphone signal has been reduced significantly by the feedforward compensator $\hat{F}$ which is estimated by the recursive least square dual-Youla parametrization in the frequency range from 40 till 400Hz.

A final confirmation of the performance of the ANC has been depicted in Fig. 8.8. The significant reduction of the error microphone signal observed in the time domain traces and the norm of the signal displayed on the right part of

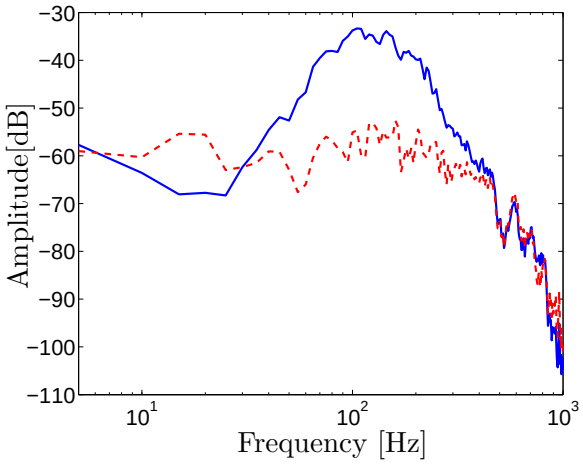

Figure 8.7. Spectral estimate of error microphone signal $\varepsilon(t)$ without ANC (solid) and with ANC (dashed) using feedforward filter $\hat{F}$ estimated via recursive least square dual-Youla parametrization

Fig. 8.8 indicates the effectiveness of the feedforward filter $\hat{F}$ estimated via recursive least square dual-Youla parametrization for feedforward sound compensation.

8.4 Conclusions

In this chapter a new methodology has been proposed for the active feedforward noise control using a dual-Youla parametrization with recursive least square (RLS) estimation in the presence of acoustic coupling. In this new approach the dual-Youla parametrization is used to incorporate the acoustic coupling to avoid instabilities of the feedforward ANC. Moreover, generalized FIR filters based on orthonormal basis function expansions can be used to efficiently parametrize and estimate the dual-Youla transfer function. The linear parametrization obtained by generalized FIR filters also facilitates the online RLS implementation using a variable forgetting factor.

The algorithm presented in this chapter combines the dual-Youla parametrization to guarantee stability in the presence of acoustic coupling with the generalized

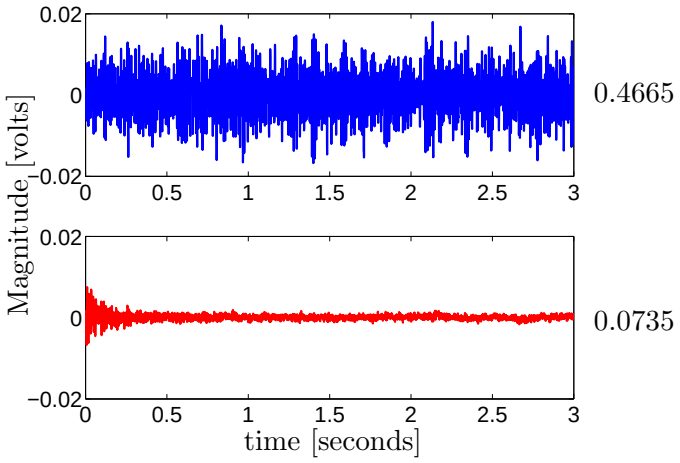

Figure 8.8. Time trace of reduction of error microphone signal $\varepsilon(t)$ without ANC (top) and with ANC turned on at $t = 0$ (bottom) using feedforward filter $\hat{F}$ estimated via recursive least square dual-Youla parametrization

FIR filter for online recursive least square (RLS) implementation. The algorithm does require prior information that include models of acoustic control path and the acoustic coupling, but this information is a generalization of the filtering used in filtered LMS estimation of feedforward filters. The prior information is also used to initialize the recursive estimation and separate adaptation from self-tuning.

The practical results of the algorithm are illustrated by an implementation on a commercial silencer for an air ventilation system. Using relative simple 6th order model for initialization of the recursive estimation along with relatively accurate models for the acoustic control and acoustic coupling path, excellent noise cancellation properties were obtained at a broad low frequency spectrum.

Acknowledgements

The text of Chapter 8, is a reprint of the material as it appears in the 42nd IEEE Conference on Decision and Control, in part, it has been submitted for publication in Journal of Sound and Vibration. The dissertation author was the primary

researcher and author in these works and the co-author listed in these publications directed and supervised the research which forms the basis for this chapter.

Chapter 9

Conclusions

9.1 Main conclusions of this dissertation

In model based control algorithms, the modeling of a dynamical system becomes very essential in order to obtain a good performance of its control system. In the literature, there are many methods can be chosen to approximately estimate the system dynamics such as direct method, indirect method, two stage method, coprime factorization and so on. However, all these methods only focused on the estimation of the deterministic system dynamics. The estimation of approximate model for disturbance dynamics is neglected which is important to design optimal controllers for disturbance rejection such as active noise control (ANC). Even though some methods can be used for disturbance model estimation, the estimated disturbance model is complicated and not good for lower order controller design. The extended two stage method described in this dissertation can be used to estimate the system dynamics and disturbance dynamics simultaneously. With the use of extended two stage method, the orders of both system model and disturbance model can be controlled based on the requirement of the frequency range the customer desired. This addresses the problem 1 which is formulated in Section 2.3.

Using the approximated models of system dynamics and noise/disturbance dy-

namics, an initial application to a H_2 / H_∞ model matching problem based on the orthonormal basis functions is developed in this dissertation. The advantage of using orthonormal basis in a orthonormal finite impulse filter lies in the possibility of including the prior knowledge of system dynamics into the tapped delay line of the filter. Therefore, it will largely improve the accuracy of the approximated modeling and converge rate during the adaptation process. Analytic solutions for H_2 / H_∞ model matching problem have been given in this dissertation and can be used for filter design in active noise control application.

In the application of active noise control, a feedforward filter parametrized with generalized (orthonormal) FIR filter with the use of orthonormal basis is designed for adaptive noise cancellation. The generalized FIR filter combines the linear parameter structure of FIR filter and the properties of orthonormal basis function. Therefore, the generalized FIR filter are not only suitable for adaptive control and approximation process, but also provide much better performance comparing with FIR filter, and which solves the problem 2 in Section 2.3.

During the feedforward filter design for acoustic active noise control application, acoustic coupling is an intricate problem which may cause the instability of system. In this dissertation, a dual-Youla parametrization is implemented to overcome acoustic coupling problem. The framework is based on fractional model representations in which a feedforward filter is parameterized by coprime factorization. With this method, the estimate of feedforward filter is recasted to the estimation of the stable perturbation, and the stable perturbation can be estimated by adaptive generalized FIR filter developed in this dissertation. The advantage of using this method is that the feedforward controller designed is guaranteed to be stabilized by the acoustic coupling. This accounts for the problem 3 in Section 2.3.

9.2 Summary on applications

The techniques developed in this dissertation have been illustrated for various applications. The low order model estimation of deterministic system dynamics and noise/disturbance dynamics using an extended two stage method has been illustrated on the experimental closed loop data obtained from a hard disk drive. The low order models of deterministic system dynamics and noise/disturbance dynamics estimated by the extended two stage method can capture the most essential dynamics in hard disk drive which is necessary to be used to design optimal controller for disturbance rejection. The generalized FIR filter parametrized with the orthonormal basis expansion has been successfully applied on the application of active noise control in air duct, the experiment results shows that the feedforward filter designed with generalized FIR filter can provide much better performance than FIR filter during the adaptation process in ANC application. Dual-youla parametrization method provides an alterative way to overcome the intricate acoustic coupling problem which mostly can not be neglected during the adaptation process of ANC. Applying dual-youla parametrization to ANC application in air duct in the presence of acoustic coupling, the robust stability of ANC system can be enforced, and the performance of ANC can also be maintained.

Bibliography

[1] N. Abe and H Ichihara. An iterative design of closed-loop identification and control using IMC structure for time delay systems. *Transactions of the Society of Instrument and Control Engineers*, 36(7):563–568, 2000.

[2] S. Adachi, M. Ogawa, A. Takahashi, and H. Sano. Feedback active noise control system based on H_∞ control. *Acoustical Science and Technology*, 22(6):437–438, 2001.

[3] K. J. Åström. Matching criteria for control and identification. In *European Control Conference*, pages 248–251. Groningen, the Netherlands, 1993.

[4] K. J. Åström and B. Wittenmark. Computer-controlled system: Theory and design, 1990.

[5] M. R. Bai and H. H. Lin. Comparison of active noise control structures in the presence of acoustical feedback by using the H_∞ synthesis technique. *Journal of Sound and Vibration*, 206(4):453–471, 1997.

[6] L. L. Beranek and I. L. Ver. *Noise and Vibration Control Engineering : Principles and Applications*. Wiley, New York, 1992.

[7] M. Bouchard and S. Quednau. Multichannel recursive-least-squares algorithms and fast-transversal-filter algorithms for active noise control and sound reproduction systems. *IEEE Trans. Speech Audio Processing*, 8:348–358, 1997.

[8] C. K. Chui and G. Chen. *Kalman Filtering with Real -Time Applications*. Springer, Berlin, Germany, 1999.

[9] J. M. Cioffi and T. Kailath. Fast, recursive-least-squares transversal filters for adaptive filtering. *IEEE Trans. Acoust., Speech, Signal Processing*, ASSP-32:304–337, 1984.

[10] D. H. Cradford and R. W. Stewart. Adaptive IIR filtered-v algorithms for active noise control. *J. Acoust. Soc. Amer.*, 101(4):2097–2103, 1997.

[11] R. A. de Callafon. *Feedback Oriented Identification for Enhanced and Robust Control*. PhD thesis, Delft University of Technology, Delft, the Netherlands, 1998.

[12] R. A. de Callafon, P. M. J. Van Den Hof, and D. K. de Veris. Identification and control of a compact disc mechanism using fractional representations. In *Prodeedings 10th IFAC Symposium SYSID'94*, pages 121–126, 1994.

[13] T. J. de Hoog, Z. Szabó, P. S. C. Heuberger, P. M. J. Van Den Hof, and J. Bokor. Minimal partial realization from generalized orthonormal basis function expansions. *Automatica*, 38:655–669, 2002.

[14] D. K. de Vries and P. M. J. Van Den Hof. Frequency domain identification with generalized orthonormal basis functions. *IEEE Transactions on Automatic Control*, 43(5):656–669, 1998.

[15] C. A. Desoer, R. W. Liu, J. Murray, and R. Saeks. Feedback system design: The fractional representation approach. *IEEE Trans. Autom. Control*, AC-25:399–412, 1980.

[16] P. S. R. Diniz. *Adaptive Filtering: Algorithms and Practical Implementation*. Kluwer academic publishers, Boston, 2002.

[17] K. H. Eghtesadi and H. G. Leventhall. Active attenuation of noise: The chelsea dipole. *Journal of Sound and Vibration*, 75(1):127–134, 1981.

[18] S. J. Elliot and P. A. Nelson. The application of adaptive filtering to the active control of sound and vibration. Technical Report 136, ISVR Technical Report, 1985.

[19] S. J. Elliott and P. A. Nelson. Active noise control. *IEEE Signal Processing Mag.*, 10:12–35, 1993.

[20] L. J. Eriksson, M. C. Allie, and R. A. Greiner. The selection and application of an IIR adaptive filter for use in active sound attenuation. *IEEE Trans. Acoust., Speech, Signal Processing.*, ASSP-35:433–437, 1987.

[21] E. Esmailzadeh, A. Alasty, and A. R. Ohadi. Hybrid active noise control of a one-dimensional acoustic duct. *ASME Journal of Vibration and Acoustics*, 124:10–18, 2002.

[22] P. L. Feintuch. An adaptive recursive LMS filter. *Proc. IEEE*, 64:1622–1624, 1976.

[23] U. Forssell and L. Ljung. Closed-loop identification revisited. *Automatica*, 35:1215–1241, 1999.

[24] B. A. Francis. *A Course in* H_∞ *Control Theory.* Springer– Verlag, Berlin, Germany, 1987.

[25] M. Gevers. Towards a joint design of identification and control? In H.L Trentelman and J.C. Willems, editors, *Essays on Control, Perspectives in the Theory and Its Application*, Boston, USA, 1993. Birkhäuser.

[26] M Gevers and L. Ljung. Optimal experiment designs with respect to the intended model application. *Automatica*, 22(5):543–554, 1986.

[27] D. Guicking. Active noise control – achievements, problems and perspectives. In *In Proc. Int. Symp. Active Control of Sound Vib.*, pages 109–118, 1991.

[28] D. Guicking. Recent advances in active noise control. In *In Proc. 2nd Int. Cong. Recent Developments in Air- and Structure-Borne Sound Vib.*, pages 313–320, 1992.

[29] F. R. Hansen. *A Fractional Representation Approach to Closed Loop System Identification and Experiment Design.* PhD thesis, Stanford University, Stanford, USA, 1989.

[30] F. R. Hansen and G. F. Franklin. On a fractional representation approach to closed-loop experiment design. In *In Proc. Am. Control Conf.*, pages 1319–1320, Atlanda, GA, 1988.

[31] F. R. Hansen, G. F. Franklin, and R. Kosut. Closed-loop identification via the fractional representation: Experiment design. In *In Proc. Am. Control. Conf*, pages 1422–1427, Pittsburgh, PA, 1989.

[32] C.M. Harris. *Handbook of Acoustical Measurements and Noise Control.* McGraw-Hill, New York, 1991.

[33] S. Haykin. *Adaptive Filter Theory.* Prentice Hall, 2001.

[34] P. S. C. Heuberger. *On Approximate System Identification with System Based Orthonormal Functions.* PhD thesis, Delft University of Technology, The Netherlands, 1991.

[35] P. S. C. Heuberger, T. J. De Hoog, P. M. J. Van Den Hof, and B. Wahlberg. Orthonormal basis functions in time and frequency domain: Hambo transform theory. *SIAM Journal on Control & Optimization*, 42(4):1347–1373, 2003.

[36] P. S. C. Heuberger, P. M. J. Van Den Hof, and O. H. Bosgra. A generalized orthonormal basis for linear dynamical systems. *IEEE Transactions on Automatic Control*, 40(3):451–465, 1995.

[37] P. S. C. Heuberger, P. M. J. Van Den Hof, and B. Wahlberg. *Modelling and Identification with Rational Orthogonal Basis Functions*. Springer Verlag, New York, 2005.

[38] H. Hjalmarsson, M. Gevers, F. De Bruyne, and J. Leblond. Identification for control: Closing the loop gives more accurate controllers. In *Conference on Decision and Control*, pages 4150–4155, Lake Buena Vista, FL, USA, 1994.

[39] J. S. Hu and J. F. Lin. Feedforward active noise controller design in ducts without independent noise source measurements. *IEEE Transactions on Control System Technology*, 8(3):443–455, 2000.

[40] J. S. Hu, S. H. Yu, and C. S. Hsieh. Application of model-matching techniques to feedforward active noise controller design. *IEEE Transactions on Control Systems Technology*, 6(1):33–42, 1998.

[41] H. Ichichara and N Abe. Iterative identification and LQG control design for time delay systems. *Transactions of the Institute of Systems, Control & Information Engineers*, 15(4):159–166, 2002.

[42] C. A. Jacobson, C. R. Johnson, D. C. McCormick, and W. A. Sethares. Stability of active noise control algorithms. *IEEE Signal Processing Letters*, 8(3):74–76, 2001.

[43] M. J. M. Jessel and G. A. Mangiante. Active sound sbsorbers in an air duct. *Journal of Sound and Vibration*, 23:383–390, 1972.

[44] A. Karimi and I. D. Landau. Comparison of the closed-loop identification methods in terms of the bias distribution. *Systems & Control Letters*, 34:159–167, 1998.

[45] T. M. Kostek and M. A. Franchek. Hybrid noise control in ducts. *Journal of Sound and Vibration*, 237:81–100, 2000.

[46] S. M. Kuo and J. Luan. Cross-coupled filter-X LMS algorithm and lattice structure for active noise control systems. In *In Proc. 1993 IEEE Int. Symp. Circuits. Syst.*, pages 459–462, 1993.

[47] S. M. Kuo and D. R. Morgan. *Active Noise Control Systems - Algorithms and DSP Implementations*. John Wiley and Sons Inc, 1996.

[48] S. M. Kuo and D. R. Morgan. Active noise control: A tutorial review. *Proceedings of the IEEE*, 87(6):943–973, 1999.

[49] S. M. Kuo and M. Tahernezhadi. Frequency-domain periodic active noise control and equalization. *IEEE Trans. Speech Audio Processing*, 5:348–358, 1997.

[50] I. D. Landau. *System Identification and Control Design: Using P. I. M. Plus Software*. Prentice Hall, 1990.

[51] I.D. Landau and A. Karimi. An output error recursive algorithm for unbiased identification in closed loop. *Automatica*, 33:933–938, 1997.

[52] I.D. Landau and A. Karimi. Recursive algorithms for identification in closed loop: A unified approach and evaluation. *Automatica*, 33:1499–1523, 1997.

[53] I.D. Landau and A. Karimi. A recursive algoritnm for ARMAX model identification in closed loop. *IEEE Transactions Automatic Control*, 44:840–843, 1999.

[54] J. R. Larimore, J. R. Treichler, and C. R. Jr. Johnson. SHARF: An algorithm for adaptive IIR digital filters. *IEEE Transactions on Acoustics, Speech and Signal Processing*, ASSP-28:428–440, 1980.

[55] S. Laugesen. *Active Control of Acoustic Noise Using Adaptive Signal Processing*. PhD thesis, Technical University of Denmark, 1992.

[56] W. S. Lee, B. D. O. Anderson, R. L. Kosut, and I. M. Y. Mareels. A new approach to adaptive robust control. *Int. Journal of Adaptive Control and Signal Processing*, 7(3):183–211, 1993.

[57] W.S. Lee. *Iterative Identification and Control Design for Robust Performance*. PhD thesis, Australian National University, Canberra, 1994.

[58] W.S. Lee, B.D.O. Anderson, I.M.Y. Mareels, and R.L Kosut. On some key issues in the windsurfer approach to adaptive robust control. *Automatica*, 31(11):1619–1636, 1995.

[59] L. Ljung. *System Identification: Theory for the User*. Prentice Hall, 1999.

[60] P. Lueg. *Process of Silencing Sound Oscillations*. U.S. Patent 2,043,416, 1936.

[61] J. M. Maciejowski. *Multivariable Feedback Design*. Addison-Wesley, Wokingham, England, 1989.

[62] T. Meurers, S. M. Veres, and S. J. Elliot. Frequency selective feedback for active noise control. *Control Systems Magazine*, 22:32–41, 2002.

[63] D. R. Morgan. An analysis of multiple correlation cancellation loops with a filter in the auxiliary path. *IEEE Trans. Acoust., Speech, Signal Processing*, ASSP-28:454–467, 1980.

[64] B. Ninness, H. Hjalmarsson, and F. Gustafsson. The fundamental role of generalized orthonormal basis in system identification. *IEEE Transactions on Automatic Control*, 44(7):1384–1406, 1999.

[65] Brett Ninness and Fredrik Gustafsson. A unifying construction of orthonormal bases for system identification. *IEEE Transactions on Automatic Control*, 42(4):515–521, 1997. An extended version is available as Technical report EE9433, Department of Electrical and Computer Engineering, University of Newcastle, Australia, 1994.

[66] S. Ochs and S Engell. Application of an iterative identification for control scheme to a neutralization process. In H-F. Chen, D-Z. Cheng, and J-F. Zhang, editors, *Proceedings of the 14th World Congress. International Federation of Automatic Control*, pages 55–60, Kidlington, UK, 1999.

[67] Y. C. Park and S. D. Sommerfeldt. A fast adaptive noise control algorithm based on lattice structure. *Appl. Acoust.*, 47(1):1–25, 1996.

[68] J. H.B. Poole and H. G. Leventhall. An experimental study of swinbanks' method of active attenuation of sound in ducts. *Journal of Sound and Vibration*, 49:257–266, 1976.

[69] K. M. Reichard and D. C. Swanson. Frequency domain implementation of the filtered-X algorithm with on-line system identification. In *In Proc. Recent Advances in Active Control of Sound Vib*, pages 562–573, 1993.

[70] W. Ren and P. R. Kumar. Stochastic parallel model adaptation: Theory and applications to active noise canceling, feedforward control, IIR filtering, and identification. *IEEE Transactions on Automatic Control*, 37(5):566–578, 1992.

[71] A. Roure. Self-adaptive broadband active sound control system. *Journal of Sound and Vibration*, 101:429–441, 1985.

[72] R. J. P. Schrama. An open loop solution to the approximate closed loop identification problem. In *Proc. 9th IFAC/IFORS Symp. On Identification and System Parameter Estimation*, pages 1602–1607, Budapest, Hungary, 1991.

[73] R. J. P. Schrama. *Approximate Identification and Control Design with Application to a Mechanical System.* PhD thesis, Delft University of Technology, Delft, the Netherlands, 1992.

[74] Q. Shen and A. Spanias. Time and frequency domain X-block LMS algorithms for signal channel active noise control. In *In Proc. 2nd Int. Cong. Recent Developments in Air- and Structure- Borne Sound Vib*, pages 353–360, 1992.

[75] Q. Shen and A. Spanias. Frequency-domain adaptive algorithms for multi-channel active sound control. In *In Proc. Recent Advances in Active Control of Sound Vib*, pages 755–766, 1993.

[76] C. F. So, S. C. Ng, and S. H. Leung. Gradient based variable forgetting factor RLS algorithm. *Signal Processing*, 83:1163–1175, 2003.

[77] M. M. Sondhi and D. A. Berkeley. Silencing echoes on the telephone network. *Proceedings of the IEEE*, 68:948–963, 1980.

[78] D. C. Swanson. Lattice filter embedding techniques for active noise control. In *In Proc. Inter-Noise*, pages 165–168, 1991.

[79] M. A. Swinbanks. The active control of sound propagation in long ducts. *Journal of Sound and Vibration*, 27:411–436, 1973.

[80] Z. Szabó, P. S. C. Heuberger, J. Bokor, and P. M. J. Van Den Hof. Extended ho-kalman algorithm for systems represented in generalized orthonormal bases. *Automatica*, 36:1809–1818, 2000.

[81] P. M. J. Van Den Hof and R. J. P. Schrama. An indirect method for transfer function estimation from closed loop data. *Automatica*, 29:1523–1527, 1993.

[82] P. M. J. Van Den Hof, R. J. P. Schrama, R. A. de Callafon, and O. H. Bosgra. Identification of normalized coprime plant factors from closed-loop experimental data. *European Journal of Control*, 1(1):62–74, 1995.

[83] P. M.J Van Den Hof and R. J. P. Schrama. Identification and control–closed-loop issues. *Automatica*, 31:1751–1770, 1995.

[84] E. T. Van Donkelaar and P. M. J. Van Den Hof. Analysis of closed-loop identification with a tailor-made parametrization. *Selected Topics in Identification, Modelling and Control*, 9:17–24, 1996.

[85] B. Wahlberg. System identification using laguerre models. *IEEE Transactions on Automatic Control*, AC-36:551–562, 1991.

[86] B. Wahlberg. System identification using kautz models. *IEEE Transactions on Automatic Control*, AC-39:1276–1282, 1994.

[87] G. E. Warnaka. Active attenuation of noise– the state of the art. *Noise Control Eng. J.*, 18:100–110, 1982.

[88] G. E. Warnaka, L. A. Poole, and J. Tichy. Active acoustic attenuators. Technical Report U.S. Patent 4,473,906, 1984.

[89] B. Widrow, D. Shur, and S. Shaffer. On adaptive inverse control. In *Fifteenth Asilomar Conference on Circuits, Systems and Computers. IEEE*, pages 185–189, New York, NY, USA, 1982.

[90] S. Q. Yuan and L. H. Xie. H_∞ feedback active noise control in acoustic duct system. In *Proceedings of the IASTED International Conference Modelling, Identification, and Control.*, pages 269–274, Anaheim, CA, USA, 2001. ACTA Press. 2001.

[91] Z. Zang, R.R. Bitmead, and M. Gevers. Iterative weighted least-squares identification and weighted LQG control design. *Automatica*, 31(11):1577–1594, 1995.

[92] J. Zeng and R. A. de Callafon. Feedforward noise cancellation in an airduct using generalized FIR filter estimation. In *Proc. 42nd IEEE Conference on Decision and Control*, pages 6392–6397, Maui, Hawaii, USA, 2003.

[93] K. Zhou and J. C. Doyle. *Essentials of Robust Control*. Prentice-Hall, 1998.

[94] W. H. Zhuang. RLS algorithm with variable forgetting factor for decision feedback equalizer over time-variant fading channels. *Wireless Personal Communicatrions*, 8:15–29, 1998.